INFORMATION TO USERS

This manuscript has been reproduced from the microfilm master. UMI films the text directly from the original or copy submitted. Thus, some thesis and dissertation copies are in typewriter face, while others may be from any type of computer printer.

The quality of this reproduction is dependent upon the quality of the copy submitted. Broken or indistinct print, colored or poor quality illustrations and photographs, print bleedthrough, substandard margins, and improper alignment can adversely affect reproduction.

In the unlikely event that the author did not send UMI a complete manuscript and there are missing pages, these will be noted. Also, if unauthorized copyright material had to be removed, a note will indicate the deletion.

Oversize materials (e.g., maps, drawings, charts) are reproduced by sectioning the original, beginning at the upper left-hand corner and continuing from left to right in equal sections with small overlaps.

Photographs included in the original manuscript have been reproduced xerographically in this copy. Higher quality 6" x 9" black and white photographic prints are available for any photographs or illustrations appearing in this copy for an additional charge. Contact UMI directly to order.

Bell & Howell Information and Learning
300 North Zeeb Road, Ann Arbor, MI 48106-1346 USA

UMI®
800-521-0600

THE USE OF DEEP-SEA CORALS AS PALEOCEANOGRAPHIC MONITORS

By
JODIE SMITH

A thesis
Submitted to the School of Graduate Studies
in Partial Fulfilment of the Requirements
for the Degree
Doctor of Philosophy

McMaster University

The Use of Deep-Sea Corals as Paleoceanographic Monitors

DOCTOR OF PHILOSOPHY (1997) McMaster University
(Geology) Hamilton, Ontario

TITLE: The Use of Deep-Sea Corals as Paleoceanographic Monitors

AUTHOR: Jodie Smith, H.BSc (McMaster University)

SUPERVISOR: Dr. Henry P. Schwarcz

NUMBER OF PAGES: xx, 155

ABSTRACT

The study of past ocean processes is essential to the understanding of current oceanography and climate systems, and to the prediction of future global change. The study of paleoceanography requires proxies: to date many studies have used foraminifera and reef corals. Each of these tools, however, has its limitations. The time resolution of paleoceanographic reconstruction using forams can be very poor, while reef corals can only give information about shallow, tropical processes. Azooxanthellate corals, in contrast, are suitable for highly precise and accurate radiogenic dating and are found everywhere in the world oceans, at all depths. The few attempts to use this taxon for paleoceanographic work have been, for the most part, unsuccessful. This is because the techniques for decoding the environmental information stored within azooxanthellate skeleton had not yet been developed. This thesis represents the first attempt to extract paleoceanographic information from 'deep-sea' corals and is presented in five sections, each a published or publishable manuscript.

Part 1 describes an investigation of corals from Orphan Knoll (*Desmophyllum cristagalli* from 1600 m depth), in the northwest Atlantic. They were dated by the $^{230}Th/^{234}U$ method using thermal ionization mass spectrometry (TIMS) and found to have grown around the time of the Younger Dryas cooling event (13,000 to 11,700 calendar years BP). The origin of this cooling recently been attributed to a reduction or cessation of deep-water production in the North Atlantic and a concurrent lessening of the heat flux from low latitudes. The $\delta^{18}O$ in the coral skeletons shift markedly, coincident with the initiation of the Younger Dryas, suggesting that profound changes in intermediate water circulation may have occurred.

Part 2 describes a study of skeletogenesis in deep-sea corals in order to develop a suitable isotopic sampling scheme for 'time-series' analyses. Numerous scanning electron micrographs of *D. cristagalli* have shown that this organism has skeletal banding analogous to that in reef corals. A long term record will be difficult to collect from *D. cristagalli* since lamellae are less than 10 μm thick, band position is unpredictable and degree of band dissolution is difficult to assess.

Part 3 attempted to ascertain if portions of the coral skeletons displayed minimal isotopic disequilibria. A specimen of *D. cristagalli* was intensively sampled on all interior and exterior coeval surfaces. Even though the coral grew at an almost-constant temperature, $\delta^{18}O$ varied by almost 3‰ and was up to 3.25‰ depleted with respect to aragonite-seawater oxygen isotope equilibrium. Portions of the skeleton approached equilibrium, the location of those areas were unpredictable and were not associated with any readily-identifiable characteristics.

Part 4 describes the study of thirty-five azooxanthellate corals belonging to 18 species, collected at sites ranging from the Norwegian Sea to the Antarctic and of depths ranging from 10 to 5220 m. All specimens showed distinct, well-defined linear correlations between carbonate oxygen and carbon isotopic composition, with slopes ranging from 0.23 to 0.67 (mean 0.45 ± 0.9) and linear correlation r^2 values which averaged 0.89. These pronounced isotopic disequilibria are what have rendered azooxanthellate corals unsuitable for use in paleothermometry to date. Despite the disequilibria, a reliable method for obtaining paleotemperature data was obtained. It was found that, if a $\delta^{13}O$ vs $\delta^{13}C$ regression line from an individual coral could be generated, the $\delta^{18}O_{arag}$ value corresponding to $\delta^{13}C_{arag} = \delta^{13}C_{water}$ and corrected for $\delta^{18}O_{water}$ was a linear function of temperature: δ^{8} O= -0.25 T(°C) + 4.97.

Part 5 describes a study of trace-element and stable-isotope analyses which was performed on two sets of azooxanthellate corals from the North Atlantic: one

set from Orphan Knoll and the other from the Mid-Atlantic-Ridge. The Mid-Atlantic-Ridge corals had episodic pulses of Fe, Mn, Cu, Ni and Zn contained within their skeletons. We believe these metals originated in a hydrothermal discharge zone associated with the Mid-Atlantic spreading centre. With sufficient specimens of known ages, it may be possible to reconstruct the history of a particular segment of a spreading centre.

ACKNOWLEDGEMENTS

It is no longer possible to do science by one's self. We truly stand on the shoulders of the giants, mesomorphs and pygmies who have gone before us, and are supported and nurtured by our colleagues and co-workers. The number of people whose support I would like to acknowledge is very long, and my debt very great. The order in which I discuss them is not to be taken as a ranking of their importance.

Throughout my research, my supervisor, Dr. Henry Schwarcz, has been a constant source of support, ideas, critical thinking and encouragement. Dr. Ted McConnaughey helped out with calculations of equilibrium isotope values, shed light on this complex thing called Kinetic Isotope effects, and was a great house guest and ski partner. But he should learn not to split kindling in the living room at 6:00 a.m. Dr. Natalia Keller very generously provided the critically important coral collection to which we now refer as the Keller Collection. It was specimens in this collection that allowed us to calibrate the deepwater coral record with sea water temperature. Dr. Uwe Brand facilitated the heavy metal analyses for the Mid-Atlantic-Ridge paper, and contributed discussion as to interpretation of those data.

One could argue that the assistance of persons with "Dr." before their names is all well and good, but real support also comes from others. Everyone who has used the Isotope Lab at McMaster over the past few decades had quickly come to realise how critical is Martin Knyf to its workings. He is always helpful, always inventive, always good company. In addition to Martin, we also were fortunate to be able to secure the services of Ines Guerrero. Ines works entirely too hard, but

at least some of the work was done for me, and I am deeply grateful. Ian Campbell, a fellow PhD student at Brock, generously donated a lot of time to help me run the AAS.

The key Orphan Knoll collection was brought to our attention 6 years ago, by Shelley Thibaudeau, then at the Bedford Institute. She has also provided data on the site, and depositional conditions in the area. Dr. Peta Mudie has also assisted in interpretation of benthic conditions in the area of Orphan Knoll. The behaviour of senior staff at the Geological Survey of Canada, Dr. David Prior and Dr. Richard Howarth, gave new meaning to the term cooperation.

Key coral samples were also loaned or donated to me by the National Museum of Canada, Dr. Andre Freiwald, Dr. Michael Schleyer and Dr. Barbara Hecker. Given the demonstrated importance of the deep-water climatic record, and the enormous expense of acquiring samples, it becomes very clear that my work depended on the cooperation of persons with specimens already in their possession.

Dr. Stephen Cairns, of the Smithsonian Institution, Washington, D.C. and Dr. Helmut Zibrowius, Station Marine d'Endoume, Université d'Aix-Marseille (two of the three world's experts on deep-sea coral - the third is Natalia Keller) graciously and freely provided advice and information

My fellow students and friends were a constant source of assistance, good humour, and frustration. I would like to thank Mark Epp, Hilary Stuart-Williams, Evan Edinger, Jeff Heikoop, Richard McLaughlin, Trevor Bohay, Cam Tsujita, Tucker, Beowulf and Freya (O.K. - the last three are my dogs, but they were very supportive). I would also like to thank José Carriquiry, Tonny Bachtiar, Tom Tomascik and Mike Risk for a variety of enriching near-death experiences.

I would also like to acknowledge my parents and my sister for their unwavering support and encouragement, even though, I suspect, they thought I was

a bit crazy when I started back at university nine years ago claiming that I was intending to get a PhD.

The last person I wish to thank should actually be at the top of the list. Michael Risk, my spouse and friend, has been a constant source of ideas, support, advice and excuses to raid the wine cellar. He has shared the frustrations, battles, triumphs, negotiations, travels and tribulations of this thesis. Michael helped me to gather samples and held his breath 'til he turned blue getting some corals from inside an underwater cave in Kenya. With his conversation, jokes, songs, poems, rants, raves and pepitas, he has kept me entertained through thick, thin and thesis. On to the next phase in our lives!

Funding for this reseach came from National Sciences and Engineering Reseach Council (NSERC) Research Grants to Henry Schwarcz and Michael Risk, a NSERC Collaborative Grant to Michael Risk (principal investigator) and Henry Schwarcz, and a Research Subvention from Fisheries and Oceans to M.Risk. NSERC also provided me with graduate student support; awards were also presented by the Planetary Society and the Canadian Federation of University Women.

TABLE OF CONTENTS

ABSTRACT....iii
ACKNOWLEDGEMENTS....vi
TABLE OF CONTENTS....ix
PREFACE....x
LIST OF FIGURES....xvi
LIST OF TABLES....xix
CHAPTER 1: INTRODUCTION....1
1.1 Background....1
1.2 Overview of Thesis....5
1.3 References....9
CHAPTER 2: RAPID CLIMATE CHANGE IN THE NORTH ATLANTIC DURING THE YOUNGER DRYAS RECORDED BY DEEP-SEA CORALS....12
2.1 Abstract....12
2.2 Introduction....13
2.3 Methods....14
2.4 Results....15
2.5 Discussion....20
2.6 Acknowledgements....22
2.7 References....23
CHAPTER 3: THE SKELETAL STRUCTURE OF DESMOPHYLLUM CRISTAGALLI: THE USE OF DEEP-WATER CORALS IN SCLEROCHRONOLOGY....27
3.1 Abstract....27

3.2 Introduction....28
3.3 Methods....31
3.4 Results....32
3.4.1 Desmophyllum cristagalli....32
3.4.2 Septum....35
3.4.3 Theca....35
3.4.4 Epitheca....36
3.5 Discussion....48
3.5.1 Ontogeny / Skeletal Development....48
3.5.2 Banding....54
3.6 Conclusions....57
3.7 Acknowledgements....61
3.8 References....61
CHAPTER 4: PATTERNS OF ISOTOPIC DISEQUILIBRIA IN AZOOXANTHELLATE CORAL SKELETONS....65
4.1 Abstract....65
4.2 Introduction....65
4.3 Methods....73
4.4 Results....74
4.5 Discussion....79
4.6 Conclusions....83
4.7 Acknowledgements....83
4.8 References....83
CHAPTER 5: PALEOTEMPERATURES FROM DEEP-SEA CORALS: OVERCOMING 'VITAL EFFECTS'....86
5.1 Abstract....86
5.2 Introduction....87

5.3 Methods and Materials....89
5.4 Results....93
5.5 Discussion....98
5.5.1 Temperature / oxygen isotope relationships....98
5.5.2 Minimum number of points required....105
5.5.3 Using $\delta^{18}O$ value as paleotemperature indicator....106
5.5.4 Slopes....107
5.5.5 Species dependence....107
5.5.6 Carbon isotope data and the respired CO_2 effect....108
5.6 Conclusions....112
5.7 Acknowledgements....113
5.8 References....113
CHAPTER 6: MID-ATLANTIC-RIDGE HYDROTHERMAL EVENTS RECORDED BY DEEP-SEA CORALS....118
6.1 Abstract....118
6.2 Introduction....118
6.3 Methods....120
6.4 Results....125
6.5 Discussion....141
6.5.1 Origin of metals....141
6.5.2 Timing of hydrothermal events....144
6.5.3 Stable isotopes....145
6.5.4 Concentration of trace metals in seawater....146
6.6 Conclusions....147
6.7 Acknowledgements....147
6.8 References....148
CHAPTER 7: CONCLUSION....151

PREFACE

Chapters 2-6 of this thesis are presented in publication format. The following descriptions document my contribution to each paper.

Chapter 2:

Title: Rapid climate change in the North Atlantic during the Younger Dryas recorded by deep-sea corals..

Authorship: Smith, J.E.; Risk, M.J.; Schwarcz, H.P. and McConnaughey, T.A.

Status: published in *Nature* **386**, pp. 818-820 (1997)

Contribution: The preliminary work for this paper constituted my bachelor's thesis. MJR borrowed the corals from the Atlantic Geoscience Centre and had the idea to sample for stable isotopes. Cherylyn Heikoop and Jim Rubenstone (Lamont Doherty) did the uranium-series dating. I subsampled the corals, did the laboratory analyses, data manipulation and wrote the paper. MJR and HPS provided advice and editorial comments. TAM helped with problems involving kinetic isotope effects. MJR displayed great valour in battle.

Chapter 3

Title: The skeletal structure of *Desmophyllum cristagalli*: the use of deep-water corals in sclerochronology.

Authorship: Lazier, A.V., Smith, J.E. , Risk, M.J. and Schwarcz, H.P.

Status: to be submitted to Lethaia

Contribution: AVL was hired as an undergraduate summer student to help with this project. I gave her some of my Baltimore Canyon corals and directed her work. AVL sliced the corals, took the SEMs, constructed the photomosaics and wrote the descriptions of the sections. I interpreted her work with regards to time-series sampling schemes and ontogeny and wrote the remaining portions of the paper. MJR provided reef coral expertise, and both he and HPS provided useful comments and editorial input.

Chapter 4:

Title: Patterns of isotopic disequilibria in azooxanthellate coral skeletons

Authorship: Smith, J.E.; Risk, M.J.; Schwarcz, H.P. and McConnaughey, T.A.

Status: to be submitted to Palaeogeograpy, Palaeoclimatology, Palaeoecology

Contribution: I subsampled the coral, performed laboratory analyses and did data manupulation. Branko Gosjic made the contour maps for me, using 'Surfer' software. HPS, MJR and TAM all made useful comments and provided editorial assistance.

Chapter 5:

Title: Deep-sea corals as paleotemperature indicators: Overcoming 'vital effects'

Authorship: Smith, J.E., Schwarcz, H.P., Risk, M.J., McConnaughey, T.A. and Keller, N.B.

Status: Presented before a professional audience (American Geophysical Union Spring Meeting, 1996)
Reviewed and revision for *Geochimica et Cosmochimica Acta.*

Contribution: This manuscript gave me many grey hairs. I was determined that I could somehow get a temperature signal from the deep-sea corals, so I did analysis after analysis until I finally figured out a way to do it. Most of the corals were provided by NBK. I did all the subsampling and laboratory analyses and data manipulation. HPS was a great deal of help on this paper, spending much time thinking about the problem. TAM provided information on metabolic CO_2 in coral skeletons and editorial

assistance. MJR gave useful advice and displayed his editorial prowess.

Chapter 6:

Title: Mid-Atlantic-Ridge hydrothermal events recorded by deep-sea corals.

Authorship: Smith, J.E., Brand, U., Risk, M.J. and Schwarcz, H.P.

Status: Presented to a professional audience (Geological Society of America, Fall Meeting, New Orleans, 1995)
To be submitted to *Geology*

Contribution: This manuscript was derived from a project done as part of a course on carbonate diagenesis. UB supervised the work and operated the AAS. Ian Campbell helped with machine operation. I did subsampling, sample preparation, data manipulation and wrote the manuscript. UB, MJR and HPS gave advice and editorial comments. Mark Epp gave me a crash course on hydrothermal vent systems.

LIST OF FIGURES

Chapter 2

Figure

1 (Top) Scatter plot of $\delta^{18}O$ vs $\delta^{13}C$ values for four Orphan Knoll corals.....19

(Bottom) Regression lines for data from each coral.....19

Chapter 3

Figure

1 A typical specimen of *Desmophyllum cristagalli*.....33

2 Composite of *D. cristagalli* showing location of Figures 3-13.....34

3 Longitudinal cross-section of the trabecular plane.....37

4 Exterior of a septum.....38

5 Longitudinal cross-section of a septum.....39

6 Longitudinal section of lamellar bands.....40

7 Transverse section of the theca.....41

8 Transverse section of the trabecular plane.....42

9 Transverse section of the theca.....43

10 Stereome crystals.....44

11 Longitudinal section of the epitheca.....45

12 Exterior of the epitheca.....46

13 Exterior of the epitheca.....47

14 Ontogeny of *D. cristagalli* - parts a-c.....50

14 Ontogeny of *D. cristagalli* - part d.....51

14 Ontogeny of *D. cristagalli* - parts e-f.....52

14 Ontogeny of D. *cristagalli* - parts g-h....53
15 Cross section of septum or theca....58
16 Cross section showing possible transects....59
17 Longitudinal section of epithelium....60

Chapter 4

Figure

1a Cross section of thecal wall or septum....70
1b Layer-by-layer growth of thecal wall or septum....71
2 Position of coral tissue at various stages of growth....72
3 A typical specimen of *Desmophyllum cristagalli*....75
4 Pattern of subsamples removed from a single specimen....76
5 Isotopic contour map of coral surfaces....78
6 SEM photograph of coral surface....81
7 $\delta^{13}C$ vs $\delta^{18}O$ for contoured coral....82

Chapter 5

Figure

1 A typical deep-sea coral....91
2 The $\delta^{13}C$ vs $\delta^{18}O$ values for six of the coral specimens....97
3 $\delta^{18}O_{arag}$ - $\delta^{18}O_{water}$ when $\delta^{13}C_{arag} = \delta^{13}C_{water}$ for each regression line....103
4 $\delta^{18}O_{arag}$ when $\delta^{13}C_{arag} = 0$ for each regression line....104
5 Plot of $\delta^{13}C$ vs $\delta^{18}O$ for Specimens 16, 17a and 17b....111

Chapter 6

Figure

1 Location of Orphan Knoll and Mid-Atlantic-Ridge sampling sites.....122

2 Bathymetry of Mid-Atlantic-Ridge site and coral dredging location.....123

3 Sampling scheme on D. cristagalli.....124

4 $\delta^{13}C$ vs $\delta^{18}O$ for OK1 and MAR1.....128

5 Metal concentrations for MAR1 plotted against height on coral.....134

6 Metal concentrations for MAR2 plotted against height on coral.....135

7 Metal concentrations for MAR3 plotted against height on coral.....136

8 Metal concentrations for OK1 plotted against height on coral.....137

9 Metal concentrations for OK2 plotted against height on coral.....138

10 Metal concentrations for OK3 plotted against height on coral.....139

LIST OF TABLES

Chapter 2

Table

1 Comparison of available intermediate-depth foraminiferal isotopic values at different times, compared with the Orphan Knoll deep-sea coral results....21

Chapter 4

Table

1 Oxygen isotopic results for each subsample....77

Chapter 5

Table

1 List of coral specimens used for isotopic analyses with environmental information....92

2 $\delta^{18}O$ and $\delta^{13}C$ values for each of the deep-sea corals....94, 95, 96

3 Regression data for each of the 35 deep-sea coral data sets....102

Chapter 6

Table

1 Stable isotope data for all six corals....127

2 Copper data for all six corals....129

3 Zinc data for all six corals.....130
4 Manganese data for all six corals.....131
5 Nickel data for all six corals.....132
6 Iron data for all six corals.....133
7 Statistical summary for MAR vs OK corals for each metal.....140

CHAPTER 1

Introduction

1.1 Background

The chapters in this thesis have been chosen from a larger body of work in press or in manuscript, intended to demonstrate the utility of azooxanthellate (deep-sea) corals in paleoenvironmental reconstructions. The sustained intellectual thread connecting these chapters is the development of the techniques required to understand the message encoded in the coral skeletons, and some of the intriguing results obtained so far.

For more than a century, the philosophical lodestone that has guided geological research has been the Principle of Uniformitarianism. This basically holds that *the present is the key to the past*, that phenomena preserved in the rocks, or in the fossil record, may be interpreted by observing processes at work in the modern world. This has served us well since the days of Hutton, Lyell and Darwin, all of whom were, by some definitions, paleoceanographers. With the waning of the 20th century, however, it seems as though we are entering a new era of geological research. We now have to understand that human activities have begun to modify the Earth itself. With this understanding comes a reinterpretation of Uniformitarianism. We now realise that *the past is the key to the present.* It is only by understanding rates and mechanisms of previous episodes of climate change, for example, that we can understand how we may be proximal agents of

changing the rate and nature of future modifications to the climate of the globe on which we live.

The study of past ocean processes accelerated greatly with the discovery that foraminifera in deep-sea sediment cores recorded unbroken sequences of oceanic history extending back several millennia. Of particular note was the discovery by Emiliani (1955) that the Northern Hemisphere had experienced not only the four great glacial episodes which had been known about for decades, but also more than 20 other glacial / interglacial transitions during the Pleistocene alone. As reliable a tool for paleoenvironmental reconstructions as forams are, however, they do present some limitations. One of the most critical of these is the degree of time resolution of which they are capable: at best, this is probably ± 1,000 years or so (CLIMAP, 1984). The poor resolution may be due to bioturbation, a churning of the uppermost layers of sediment by benthic organisms. The inability to date forams beyond the range of ^{14}C contributes to the problem, as much dating involves interpolation between layers of known ages: fluctuating sedimentation rates exacerbates the problem.

Recently, many paleoceaonographic reconstructions have been made using reef corals, with records sometimes extending 400 years (Hudson *et al.*, 1976). The presence of annual banding, and suitability of corals for uranium-series dating allows precise estimates of age which are not dependent on sedimentation rates. The growth rate variation of reef corals can be used to document past changes in light levels, allowing long-term reconstructions of paleoecological patterns (e.g., Goreau, 1959). Oxygen isotopic analyses of coral bands have been used to produce estimates of paleotemperature: Carriquiry *et al.* (1988) used oxygen isotopes to establish the magnitude, duration and timing of the 1982-1983 El Niño warming event. In so doing, they have also suggested a means whereby similar occurrences may be recognized in the geologic record. Stable carbon isotopes

have been used to recount the recent history of fossil fuel CO_2 uptake by the ocean. Nozaki *et al.* (1978) produced a 200-year record of atmospheric variations in carbon isotopes using a continuous core from a large, colonial reef coral.

Although difficult to separate from temperature effects, the isotopic composition of corals varies with salinity changes. It is possible, therefore, to identify corals subjected to fresh- or meltwater fluxes or which grew in areas of excessive evaporation (Rye and Sommer, 1980). Aharon (1991) demonstrated that shifts in the $\delta^{18}O$ values in corals from the Great Barrier Reef coincided with the local rainfall record and suggested that corals could be used as 'paleo-rain gauges'. Isdale (1984) showed that fluorometric analysis of banding in corals could be used to estimate the magnitude of terrestrial runoff into the coastal environment.

Reef corals, because of their light and wave-energy requirements, are limited in vertical distribution by the concurrent sea level. Fairbanks (1989) used this phenomenon to recontruct a paleo-sea level curve extending back over several millennia. Certain trace elements substitute readily for calcium in carbonate skeletons; trace element histories in corals, then, can offer a record of an element's concentration in seawater and thus of specific environmental processes. Cadmium, for example, has been found to be a sensitive tracer of historic upwellings and industrial fallout (Shen *et al.*, 1987)

Reef corals, then, have proven themselves as tools for paleoceanographic reconstructions *par excellence*. There are, however, limitations: reef corals have algal symbionts (zooxanthellae), which restrict these taxa to shallow, tropical waters. Data from reef corals give information about equatorial processes only. Azooxanthellate corals, in contrast, attain much wider distributions: they are in all major oceans, from 0 - 6200 m depth, -1 to 29 C and from the Norwegian Sea (70 N) to the Ross Sea, Antarctica (78 24'S)(Stanley and Cairns, 1988). Data from 'deep sea' corals could conceivably allow global paleoenvironmental

reconstructions.

Throughout the geological column, it appears that most successful reef builders have had a symbiotic relationship with algae (Cowen, 1983). The fossil record from the early Mesozoic shows little evidence of shallow-water coral-reef development. The algal symbiosis necessary for reef building is thought to have evolved in the late Triassic, thereby initiating the ecologic differentiation of the two groups of corals (Stanley, 1981). Benton (1966) suggested that the impetus for this change was a profound mass-extinction event: certainly the fossils of the Jurassic and succeeding geological periods reveal ahermayptic (non-reef building) coral communities as distinctly separate from the hermatypic taxa (Wells, 1956). This is usually explained in terms of competition - when zooxanthellate species are excluded from an environment due to restrictive conditions, azooxanthellates often can flourish. In less-than-optimum, non-reef settings, azooxanthellates can coexist with zooxanthellates, however, they are generally outcompeted and relegated to cryptic habitats on shallow-water reefs.

Azooxanthellates comprise a significant fraction of Holocene scleractinia - 90 of the 190 genera and about 560 of the 1500 species belong to this group. Character may be ecologically influenced, however, as some species can exist in either condition (apozooxanthellate). Factors essential to ahermatypic coral establishment appear to include hard substrates accompanied by sufficient submarine topography and vigourous currents carrying an abundance of nutrients (Stanley and Cairns, 1988).

Although reef corals have been shown to be excellent recorders of oceanographic data, at the time this thesis was begun very little work had been performed on azooxanthellate corals. Most studies concentrated on taxonomy or biogeography (e.g., Cairns, 1982; Zibrowius and Gili, 1990; Keller, 1989). Attempts to use azooxanthellate corals as environmental monitors had been unsuccessful

(e.g., Emiliani et al., 1978; Mikkelson, et al., 1982). McConnaughey (1989) demonstrated why this was so: he showed that the isotopic ratios in a single subsample from an azooxanthellate coral could have values several per mil different than a second subsample a few millimetres away. This enormous degree of biological fractionation (often termed 'the vital effect') appeared to overwhelm any environmental signal preserved within the coral. McConnaughey also showed that the skeletal $\delta^{18}O$ and $\delta^{13}C$ showed a strong positive correlation and that the regression line extended from a point near aragonite/seawater equilibrium to a point depleted in both ^{18}O and ^{13}C. Although the isotopic ratios of the coral skeletons showed considerable disequilibria, they were not random: the $\delta^{13}C$ vs $\delta^{18}O$ regression lines had a predictable relationship with respect to aragonite/seawater equilibrium. Perhaps, then, the lines themselves could be used to reveal information about the oceanographic conditions under which the corals lived.

1.2 Overview of Thesis

Chapter 2, "Rapid climate change in the North Atlantic during the Younger Dryas recorded by deep-sea corals" is the product of a chance conversation five years ago between Dr. M. Risk and Ms. Shelley Thibaudeau, then working as a technician at the Bedford Institute of Oceanography, as to whether some useful information might be garnered from the study of a collection of deepwater corals (*Desmophyllum cristagalli*) taken from Orphan Knoll. The preliminary work on the corals in this collection formed the subject of my bachelor's thesis. Several corals were dated, using the uranium-series method, and were found to originate from the time of the last deglaciation. We were very lucky to find a large specimen whose lifetime spanned the beginning of the Younger Dryas - a sudden, brief return to glacial conditions midway through deglaciation. We found that the glacial and non-

glacial $\delta^{13}C$ vs $\delta^{8}O$ regression lines for the different corals occupied entirely different regions of ($\delta^{13}C$, $\delta^{18}O$) space, allowing unequivocal differentiation of the two subsets. Furthermore, the 'heaviest' ends of the regression lines (theoretically closest to the equilibrium point) were in agreement with previously-published data from coeval foraminifera from sediment cores.

It seemed that, although the coral skeleton contained large 'vital effects', they still retained an environmental signal within them. What we needed, however, was a key to unlock the puzzle of the intermixture of biological and oceanographic signals. How should the corals be sampled for a sequential record? Were coeval parts of the skeleton alike in their isotope values? Did the $\delta^{13}C$ vs $\delta^{18}O$ regression lines have a reliable relationship with the aragonite/seawater equilibrium point? If not, how could the equilibrium point be identified? Did the pattern of trace element inclusion into the skeletons give information of oceanic conditions?

Chapter 3, "The skeletal structure of Desmophyllum cristagalli: the use of deep-water corals in sclerochronology" is a 'road map', a plan of how the coral skeleton is developed. This sort of work has greatly aided interpretation of the record of shallow-water corals. This study of coral growth (running title: "They start small and grow big", or TSSGB, after a quote from Dr. Helmut Zibrowius) allowed the development of a suitable sampling scheme for gathering isotopic or trace element data over the course of the coral's lifetime. Dr. M. Risk hired Amy Lazier, an undergraduate summer employee, to help work on this problem. Over the course of an entire summer, Amy took hundreds of SEM micrographs of coral surfaces and sections, and the group was able finally to build up a picture of skeletal development in *D. cristagalli*. We discovered that growth recessions are common along some transects, as are missing parts of the record. The central trabecular plane in the theca and septa provides the only guaranteed continuous surface. The isotopic record in this plane has been shown to be close to aragonite/seawater

equilibrium and would thus be the best for paleoceanographic sampling. The trabecular plane, however, is narrow and weaves unpredictably back and forth within the septa or theca. Sampling the epitheca gives an approximate sequential surface, accurate enough for many applications. It was also possible to identify coeval regions of the skeleton.

Chapter 4, "Patterns of isotopic disequilibria within the skeletons of deep-sea corals" looked at a coeval surface (i.e., regions experiencing the same ambient conditions) to examine if and how the isotopic ratios varied. One such area of simultaneously skeletal deposition is the entire surface of the inside of the coral and at least the top portion of the exterior, and perhaps all of it. Numerous subsamples for isotopic analyses were removed from all interior and exterior surfaces in a systematic manner. It was found that the isotopic results varied by up to 3‰ and were up to 3.5‰ from equilibrium. Furthermore, when I drew contour lines of $\delta^{18}O$ values as they appear on the corals, no pattern was seen and, seemingly, no way in which to identify areas close to equilibrium. There are no annual changes, no secular shifts. This is extremely bad news for potential interpretation of oceanographic change, and fascinating from the point of view of skeletogenesis in marine organisms. This is an area of research that requires further work.

Chapter 5, "Deep-sea corals as paleotemperature indicators: overcoming 'vital effects'" represents, I believe, the greatest contribution of this thesis to paleoceanography. Through our collaboration with Dr. Natalia Keller, of the Russian Academy of Sciences, we were able to obtain a collection of deepwater corals from locations all over the globe. These were taken years ago, using the *Mir* submersible vessels, and put into the care of Dr. Keller. We have termed these corals the Keller Collection, and without this collection we would not be where we are now in our understanding. In Chapter 5, we report findings that I feel go a long way towards allowing an understanding of kinetic isotopic overprints of climatic data in these

organisms, and perhaps others.

On analysing many of the Keller Collection corals, we found that graphs of $\delta^{18}O$ against $\delta^{13}C$ formed a family of lines, separated according to temperature. A plot of $\delta^{18}O_{arag} - \delta^{18}O_{water}$ where $\delta^{13}C_{arag} = \delta^{13}C_{water}$ yielded a linear relationship with a r^2 value of 0.95. This relationship allowed a means to estimate aragonite/seawater equilibrium, and thus water temperature in Holocene corals. This was an extremely exciting discovery, because it allowed me to calibrate the coral isotopic record with sea water temperature, virtually independent of biological effects.

Chapter 6: "Mid-Atlantic Ridge hydrothermal events recorded by deep-sea corals" is the final chapter in the thesis, describing some work we did with deepwater corals that did not employ isotope stratigraphy. I took a graduate course in Geochemistry from Dr. Uwe Brand, at Brock, and as part of the course we were all required to undertake a series of AAS measurements. For my course work, I chose a series of corals that had been collected on the Mid-Atlantic Ridge (MAR), that we were able to borrow from the National Museum of Canada. The corals from the MAR record metal profiles very different from the Orphan Knoll corals, which come from a tectonically quiescent setting. The MAR corals seem to be recording pulses of hydrothermal activity on the spreading centre, lasting a few decades. This is the first time such activity has been indirectly measured.

In summary, this thesis embodies work that has demonstrated that deepwater corals are a New Archive of oceanographic information. Although specimens are small and rare, and acquiring new material will be very expensive, they have some unparalleled advantages over traditional data archives:

- the coral record is never obscured by bioturbation
- it is possible to obtain time resolution on a scale previously undreamt of. Annual resolution is not difficult, and shorter time scales may be obtainable.

- 'deepwater' corals may better be termed Ubiquitous Corals. Azooxanthellate corals occurs almost everywhere in the world ocean, at all depths if suitable conditions are available. This allows relative comparison of geochemical change in the oceans.

1.3 References

Aharon, P. (1991) Recorders of reef environment histories: Stable isotopes in corals, giant clams and calcareous algae. *Coral Reefs* **10**, pp. 71-90.

Benton, M.J. (1986) More than one event in the late Triassic mass extinction. *Nature* **321**, pp. 857-861.

Cairns, S.D. (1982) Antarctic and Subantarctic Scleractinina. *Antarctic Research Series* **34** (1), pp. 1-74.

Carriquiry, J.D., Risk, M.J. and Schwarcz, H.P. (1988) Timing and temperature record from stable isotopes of the 1982-1983 El Niño warming event in eastern Pacific corals. *Palaios* **3**, pp. 359-364.

CLIMAP (1984) The last interglacial ocean. *Quaternary Research* **21**, pp. 123-224.

Cowen, R. (1983) Algal symbiosis and its recognition in the fossil record. In: Tevesz, M.J.S. and McCall, P. (eds) *Biotic Interactions in Recent and Fossil Benthic Communities*, Plenum Press, New York, pp. 431-478.

Emiliani, C. (1955) Pleistocene temperatures. *J. Geol.* **63**, pp. 538-578.

Emiliani, C., Hudson, J.H., Shinn, E.A. and George, R.Y. (1978) Oxygen and carbon isotopic growth records in a reef coral from Florida Keys and a deep-sea coral from Blake Plateau. *Science* **202**, pp. 627-629.

Fairbanks, R.G. (1989) A 17,000-year glacio-eustatic sea level record: Influence of glacial melting rate on the Younger Dryas event and deep-ocean circulation. *Nature* **342**, pp. 637-642.

Goreau, T.F. (1959) The physiology of skeleton formation in corals. 1. A method for measuring the rate of calcium deposition by corals. *Biological Bulletin* **117**, pp. 239-250.

Hudson, J.H., Shinn, E.A., Halley, R.B. and Lidz, B. (1976) Sclerochronology: A tool for interpreting past environments. *Geology* **4**, pp. 361-364.

Isdale, P. (1984) Fluorescent bands in massive corals record centuries of coastal rainfall. *Nature* **310**, pp. 578-579.

Keller, N.B. (1989) The comparative characteristics of the coral associations at Atlantic near-continental and mid-oceanic submarine mountains. *Trudy Instituta Okeanologii* **123**, pp. 69-69.

McConnaughey, T.A. (1989) ^{13}C and ^{18}O isotopic disequilibrium in biological carbonates: 1. Patterns. *Geochimica et Cosmochimica Acta* **53**, pp. 151-162.

Mikkelson,N., Erlenkeuser, H., Killingley, J.S. and Berger, W.S. (1982) Norwegian corals: radiocarbon and stable isotopes in *Lophelia pertusa*. *Boreas* **11**, pp. 163-17

Nozaki, Y., Rye, D.M., Turkian, K.K. and Dodge, R.E. (1978) A 200 year record of carbon-13 and carbon-14 variations in a Bermuda coral. *Geophysics Research Letters* **5**, pp. 825-828.

Rye, D.M. and Sommer, M.A. (1980) Reconstructing paleotemperature and paleosalinity regimes with oxygen isotopes. In: Rhodes, D.C. and Lutz, R.H. (eds) *Skeletal Growth of Aquatic Organisms*, Plenum Press, New York, pp. 169-202.

Shen, G.T., Boyle, E.A. and Lea, D.W. (1987) Cadmium in corals as a tracer of historical upwelling and industrial fallout. *Nature* **328**, pp. 794 - 796.

Stanley, G.D. (1981) Early history of scleractinian corals and its geological consequences. *Geology* **9**, pp. 507-518.

Stanley, G.D. and Cairns, S.D. (1988) Constructional azooxanthellate coral communities: An overview with implications to the fossil record. Palaios **3**, pp. 233 - 242.

Wells, J.W. (1956) Scleractinia. In: Moore, R.C. (ed) *Treatise on Invertebrate Paleontology*. Part F, Coelenterata. University of Kansas Press, Lawrence, Kansas, pp. F328-F344.

Zibrowius, H. and Gili, J.M. (1990) Deep-water Scleractinia from Namibia, South Africa and Walvis Ridge, southeastern Atlantic. *Scientia Marina* **54**, pp. 19-46.

CHAPTER TWO

Rapid climate change in the North Atlantic during the Younger Dryas recorded by deep-sea corals

2.1 Abstract

Global climate-change research has increasingly focussed on century- and decadal scale changes. One much-studied such climatic shift, the Younger Dryas cooling event, took place 13,000 to 11,700 calendar years BP[1]. Greenland ice cores and high-resolution sediment cores from the North Atlantic region display high-frequency isotopic, chemical and faunal-abundance oscillations that imply significant shifts in temperature (>5°C), occurring within 50 to 100 years[2]. The origin of the Younger Dryas has recently been attributed to a reduction or cessation of deep-water production in the North Atlantic and a concurrent lessening of the heat flux from low latitudes[3,4]. The role of intermediate water is less certain, however, because climatic proxies for this reservoir are rare and ambiguous. Here we report on the use of a new archive: deep-sea corals from Orphan Knoll (1600 m depth), in the northwest Atlantic. The $\delta^{18}O$ in the coral skeletons shift markedly, coincident with the initiation of the Younger Dryas, suggesting profound changes in intermediate water circulation. The oxygen-isotope record from the Orphan Knoll corals is dated by the $^{230}Th/^{234}U$ method using thermal ionization mass spectrometry (TIMS), making it one of the most accurately- and precisely-dated deeper-water records of deglacial climate.

2.2 Introduction

Evidence concerning past oceanographic conditions is derived largely from isotopic analyses of foraminiferal and coral carbonates. Temperature affects the partitioning of oxygen isotopes between seawater and precipitating carbonates, while ocean circulation patterns and other climatically-important factors affect both the oxygen and carbon isotopic compositions of seawater. Carbonates from foraminifera and reef corals have been especially useful sources of isotopic data; forams are, however, difficult to date accurately and reef corals only live in shallow tropical waters. Non-reef-building, non-photosynthetic corals potentially offer the advantages of both groups: widespread distribution (from surface to abyssal depths, and from polar to equatorial latitudes[5]), suitability for ^{230}Th- U disequilibrium dating, and more-or-less continuous skeletal deposition over periods of decades to centuries.

Attempts to use deep-sea corals as recorders of ambient oceanographic conditions have so far yielded ambiguous results[6-8]. The major problem is that the skeletons of deep-sea corals usually do not precipitate in isotopic equilibrium with seawater, and the extent of the disequilibrium varies widely within a particular individual. Multiple isotopic analyses of individual modern deep-sea corals collected live from waters of known temperature and isotopic composition show strong positive $\delta^{18}O$ / $\delta^{13}C$ correlations[8,9]. Regression lines extend from a point at or near ^{18}O equilibrium with seawater but a few per mil depleted (re equilibrium) in ^{13}C, to a point up to 4 ‰ depleted in ^{18}O and up to 12 ‰ depleted in ^{13}C. These features have been explained as a superposition of "kinetic" and "metabolic" isotope effects[10]. Slower CO_2 hydration and hydroxylation reactions by molecules bearing the heavy isotopes ^{13}C and ^{18}O cause the kinetic effects. Partial re-equilibration accounts for the strong positive correlations between skeletal $\delta^{18}O$ and

$\delta^{13}C$. Skeletal incorporation of ^{13}C-depleted respired CO_2 causes the metabolic effects: these effects are probably small in deep-sea corals, however, as respired CO_2 contributes little to their skeletal makeup[11].

Even though considerable isotopic disequilibria were observed, the regression lines for the data from individual corals (plotted in $\delta^{18}O$, $\delta^{13}C$ space) were offset from each other as a function of temperature[9]. In each case, the heaviest isotopic ratios approach or reach oxygen equilibirum with seawater; the carbon-isotope data were always depleted with respect to equilibrium by varying amounts.The heaviest $\delta^{18}O$ values for each coral were plotted against temperature, resulting in a trend parallel to the biogenic aragonite equilibrium curve[12]. This demonstrates that, although the isotopic signals from each individual coral represent a superposition of kinetic components on equilibrium values, the environmentally-controlled portion (reflecting the ambient temperature and isotopic composition of the water) should be extractable from fossil corals, and may be used to reconstruct paleoceanographic conditions.

2.3 Methods

In 1978, the Atlantic Geoscience Centre (Geological Survey of Canada) recovered dredge samples from the top of Orphan Knoll, at the edge of the continental rise 550 km northeast of Newfoundland (50° 25.57' N, 46° 22.05' W)[13]. Several well-preserved, dead specimens of *Desmophyllum cristagalli* Milne Edwards and Haime, 1848, were recovered. The corals were stored for several years at the AGC; unfortunately, much of the collection was discarded at some point because of space problems. This robust species of deep-sea coral[14] attaches to suitable hard substrates, often vertical to sub-vertical rock walls. Several of the fossil Orphan Knoll specimens were dated at McMaster and at Lamont-Doherty by

the TIMS uranium-series method and were found to range in age from 77 to 4 ky[15]. We chose to use uranium series rather than radiocarbon dating, because $^{14}C/^{12}C$ ratios in fossil deep-sea corals may be influenced not only by radioactive decay and atmospheric variations, but also by the ventilation history of the deep ocean[16]. The calculated initial $^{238}U/^{234}U$ ratios in the coral skeletons were only slightly less than the seawater activity ratio, indicating a closed system. Since the amount ^{232}Th in the corals was negligible, a detrital thorium correction was not required. Various parts of the coral were isotopically analyzed, but the data presented here derive only from the outer theca of the pedicels from above the base to below the calices. These parts of the skeleton displayed the strongest linear correlations between $\delta^{18}O$ and $\delta^{13}C$.

2.4 Results

Among the dated specimens, four corals were of particular interest because their dates spanned much of the last deglaciation. The stable-isotope data are shown in Figure 1; each set of isotopic ratios and matched regression line represents the data retrieved from one dated specimen. Complete data are given in appendix. Dates are given with 2σ uncertainties. The oldest coral discussed here (Coral #14 at 15,140 ± 104 y BP) grew during the middle of the Bölling chronozone, when the North Atlantic still retained much of its glacial character. The heaviest $\delta^{18}O$ value of the set, which presumably approaches the oxygen-equilibrium value, is 4.51 per mil. By 14,143 ± 86 y BP (Coral #23), the highest skeletal value had dropped to 4.34 ‰, presumably reflecting climatic warming during deglaciation. The base of Coral #1 was dated at 13,636 ± 103 y BP, and the top at 13,322 ± 98 y BP: from the base to about two-thirds the way up Coral #1 (to

approximately the 13,400 y BP mark) the highest skeletal oxygen-isotope value was 2.73 per mil. This total drop of 1.78 ‰ comprises signals both from the warming of the ambient seawater plus changes in the $\delta^{18}O$ of the seawater attributable to the addition of meltwater to the North Atlantic. Following this mid-Alleröd low, the $\delta^{18}O$ vs $\delta^{13}C$ plot for the same specimen, Coral #1, changed abruptly, from one sampling location on the same coral to the next three millimetres away, to give a non-overlapping data set with a significantly different slope (t-test, $p < 0.001$) dated at 13,322 ± 98 y BP. Its highest $\delta^{18}O$ value is 4.05‰, implying a sudden return to glacial-like conditions at this intermediate-depth site. We interpret this shift, an increase of 1.32‰, as representing the initiation of the Younger Dryas event, which has been widely documented in ice cores, ocean sediment cores, terrestrial pollen, insect records and other climate proxies from various parts of the world, including the circum-Atlantic region[17,18,19].

None of the other deep-sea corals analysed, including corals of similar size, but with ages lying outside the Younger Dryas, show such abrupt shifts in $\delta^{18}O$ ratios. Equally important, the isotopic shift at the apparent onset of the Younger Dryas occurred between two seemingly-identical subsamples within 3 mm of skeletal growth. There is no evidence of any growth hiatus, or change in texture or morphology of the coral at the transistion. If we assume that this fossil coral had growth rates comparable to those of modern representatives and that the $^{230}Th/^{234}U$ dates are accurate, the abrupt shift in the isotopic values along Coral #1 suggests that the initiation of the Younger Dryas may have taken place over as few as 5 years. This rate of change in deeper-ocean chemistry is one of the most rapid such recorded events in the marine record.

The isotopic record of the youngest coral (Coral #27 at 4093 ± 44 y BP), with a maximum $\delta^{18}O$ value of 2.54 per mil, reflects modern interglacial ocean conditions and is only slightly lower than $\delta^{18}O$ of the base of Coral #1. As with the suite of

modern corals[11], the changes in $\delta^{13}C$ are difficult to explain; clearly, a 5 ‰ shift in the carbon-isotope composition of seawater is improbable. This is an area in which further research is required.

Figure 1

Top: Scatter plot of $\delta^{18}O$ vs $\delta^{13}C$ values for four Orphan Knoll corals. The squares (■) represent isotopic values from coral #14, dated at 15,140 ± 104 absolute (calendar) years before present while the triangles (▲) are data from coral #23 at 14,143 ± 86 y BP. The upside-down triangles (▼) are from the lower part of coral #1 from skeleton growing at approximately 13,400 y BP, and circles (●) denote subsamples taken from the upper part of coral #1, dated at 13,322 ± 98 y BP. Hourglass symbols represent isotopic values from a submodern specimen (#27 at 4,093 ± 44 y BP). Note that there is no relationship between position of data points on the plot and position on the corals.

Bottom: Regression lines for data from each coral (numbers 14, 23 and 27) and the two sections (lower - earlier and upper - later) of coral #1). The two glacial-aged corals (coral #14 and #23) closely resemble each other and the Younger Dryas-aged coral (the upper portion of coral #1). The coral skeleton growing just before the onset of the Younger Dryas (the lower portion of coral #1) is similar to the submodern specimen (#27). Note the regression llines indicate analyses from a single specimen (coral #1) show that the shift from one data set to the other occurred between subsamples spaced < 3 mm apart. Symbols at the "northeast" end of each regression line indicate the maximum $\delta^{18}O$ value for each coral: these values approach or reach oxygen equilibrium with seawater; some of these values are displayed in Table 1.

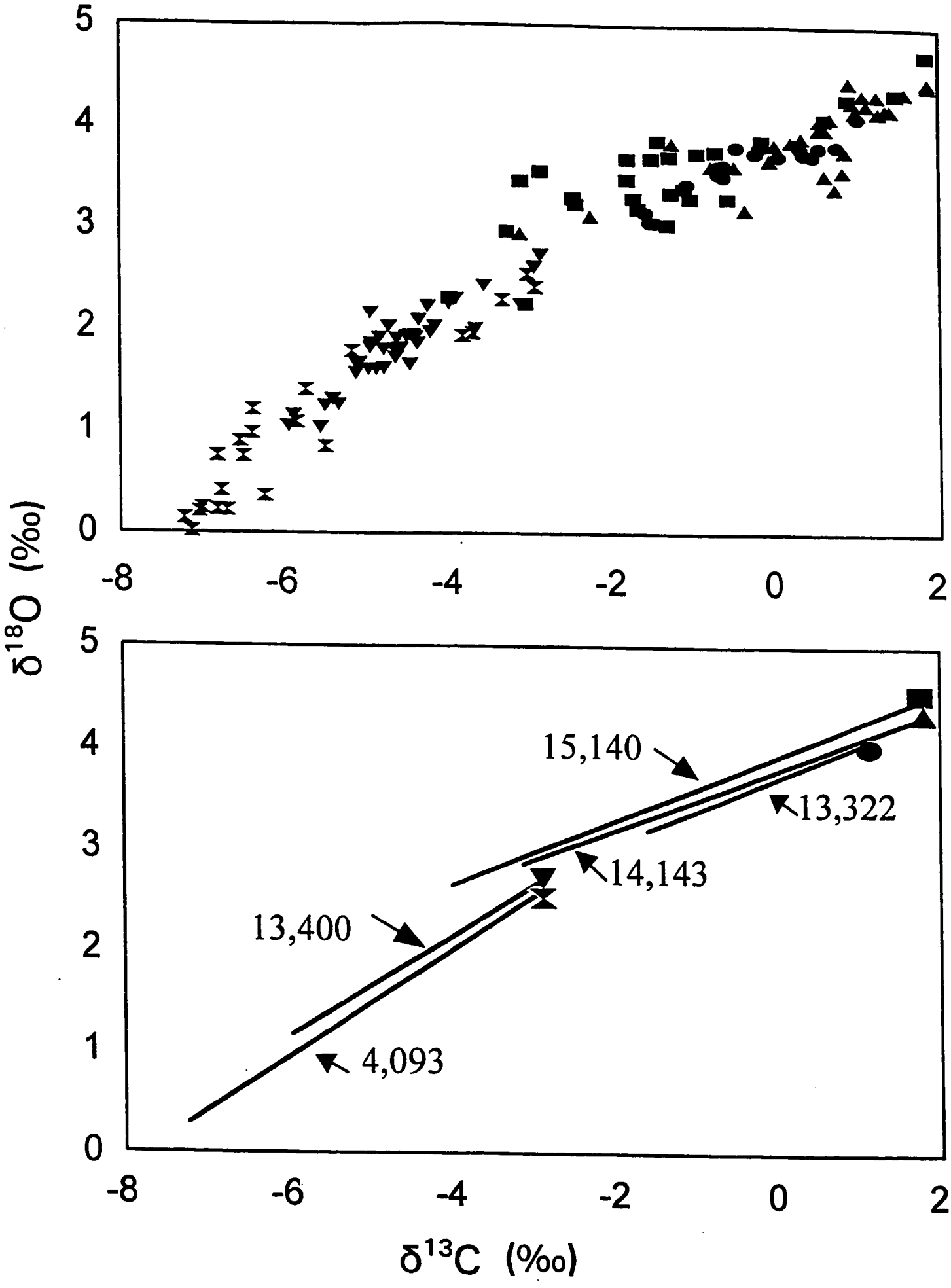
5
4
3
2
1
0
-8
-6
-4
-2
0
2
δ18O (‰)
15,140
13,322
14,143
13,400
4,093
δ13C (‰)

2.5 Discussion

North Atlantic Deep Water (NADW) production releases approximately 1 petaWatt of heat (10^{15} joules per second) to the atmosphere[20]. A shutdown of this overturning cell (the so-called heat 'conveyor') has been implicated in past studies of the Last Glacial Maximum (LGM) and Younger Dryas climatic intervals[3,4]. Recent studies[21-23], however, have shown that while the deepest portions of the North Atlantic did not seem to feel the presence of NADW during the LGM and the Younger Dryas, other proxies implied the conveyor was still in operation. It has been suggested that the conveyor shoaled, i.e., decreased the penetration depth of NADW, rather than shut down. Intermediate waters (1000 - 2000 m depth) were then formed at the expense of the densest components of the NADW. If this is true, the midwater should show distinct changes in temperature and isotopic composition as the North Atlantic shifted from one circulation mode to another. We interpret our data as lending support to this hypothesis: the two glacial-aged corals show that the ambient water had significantly different characteristics than the midwaters of early deglaciation. The coral which grew during that time (13.6 to 13.4 ky BP) recorded similar conditions to those experienced by the submodern (4.1 ky BP) specimen. During the Younger Dryas, however, the intermediate waters appear to resemble closely those of the last glacial period and imply a similar provenance.

Records of changes in the isotopic composition of benthic foraminifera from mid-depth North Atlantic sites[24,25] are virtually identical in magnitude to our isotopic results for the deep-sea corals (Table 1).

Table 1: Comparisons of available intermediate-depth (1000-2000 m) foraminiferal isotopic values at different times, compared with the Orphan Knoll deep-sea coral results.

	Oppo and Lehman[25]	Labeyrie et al.[24]	This Study
Glacial	3.77-4.60 ‰	4.1-4.8 ‰	4.51 ‰
Younger Dryas		3.1-3.9 ‰	4.05 ‰
Modern	2.29-2.77 ‰	2.0-3.0‰	2.54 ‰
$\Delta\ \delta^{18}O$ (Glac-YD)		0.2-1.7‰	0.46‰
$\Delta\ \delta^{18}O$ (Glac-Mod)	1.0-1.31 ‰	1.1-2.8 ‰	1.97 ‰

The $\delta^{18}O$ record from the Orphan Knoll corals, however, is a much more accurately-and precisely-dated record of the last deglaciation. Average 2-sigma uncertainty of the seven $^{230}Th/^{234}U$ dates is 87 years, whereas bioturbation, uncertainties in the radiocarbon calibration and in the ^{14}C reservoir age bring the typical age uncertainty in foraminiferal or other microfaunal analyses to thousands of years[26]. Errors in the ice-core record[27] are also too large to determine accurately the phase relationship between ice-core accumulation or $\delta^{18}O$ stratigraphy and the Orphan Knoll $\delta^{18}O$ record. Accurate and precise dating is crucial in the investigation of chronozones as condensed as the Younger Dryas event, since subtle shifts in age assignments can significantly alter the interpretation of deep-ocean responses to climate change[28]. One record with comparable accuracy to ours is the $^{230}Th/^{234}U$-dated Barbados sea-level record.[28] Using this, along with data from other drowned reefs in the Caribbean-Atlantic province, Blanchon and Shaw[29] theorized that ocean-atmosphere reorganization

resulted from atmospheric changes induced by ice-sheet collapse, which in turn lead to a series of catastrophic sea level rises. One of our deep-sea corals (14,143 ± 43 y BP) originates at or very near the time of one of these proposed sea-level rises (14.2 ± 0.1 ky BP), but shows no evidence of a rapid oceanographic change. The change in ocean circulation suggested by the Orphan Knoll data at *ca.* 13.3 ky BP is not associated with a sea-level rise, lending support to Fairbanks' assertion[28] that the Younger Dryas occurred at a time of minimum ice-sheet melting.

Shallow-water corals are recognized as enviromental recorders without equal. Deep-water corals afford us the opportunity to access previously-unavailable records of climate change[30]. Their study may well lead to a new archive, a more complete understanding of the past and better prediction of the future.

2.6 Acknowledgements

We thank Richard G. Fairbanks for providing U-series dates and advice, and Tom Guilderson, Jim Rubenstone, Cherylyn Heikoop and Martin Knyf for help with analyses. Stephen Cairns identified the fossil corals. The paper benefitted from discussions with Shelley Thibaudeau, Peta Mudie, Helmut Zibrowius, Jess Adkins and the QOL group at McMaster. Special thanks to anonymous Reviewer #4. Funded by an Energy, Mines and Resources Research Subvention, an NSERC Canada Research Grant to MJR; NSERC postgraduate student support plus Planetary Society and Canadian Federation of University Women Fellowships to JES.

2.7 References

1. Fairbanks, R.G. (1990) The age and origin of the Younger Dryas event in Greenland ice cores. *Paleoceanography* **5**, pp. 937-948.

2. Johnsen, S.J. *et al.* (1992) Irregular glacial interstadials recorded in a new Greenland ice core. *Nature* **359**, pp. 311-313,

3. Broecker, W.S. and Denton, G.H. (1989) The role of ocean-atmosphere reorganization in glacial cycles. *Geochim. Cosmochim. Acta* **53**, 2465-2501.

4. Broecker, W.S., Peteet, D.M. and Rind, D. (1986) Does the ocean-atmosphere system have more than one stable mode of operation? *Nature* **315**, pp. 21-26.

5. Stanley, Jr., G.D. and Cairns, S.D. (1988) Constructional azooxanthellate coral communities: an overview with implications for the fossil record. *Palaios* **3,** pp. 233-242.

6. Druffel, E.R.M., King, L.L., Belastock, R.A. and Duesseler, K.O. (1990) Growth rate of a deep-sea coral using Pb-210 and other isotopes. *Geochim. Cosmoschim. Acta* **54**, pp. 1492-1500.

7. Mikkelson, N., Erlenkeuser, H., Killingley, J.S. and Berger, W.H. (1982) Norwegian corals: radiocarbon and stable isotopes in *Lophelia pertusa*. *Boreas* **11**, pp. 163-171

8. Emiliani, C., Hudson, J.H., Shinn, E.A. and George, R.Y. (1978) Oxygen and

carbon isotopic growth records in a reef coral from Florida Keys and a deep-sea coral from Blake Plateau. *Science* **202**, pp. 627-629.

9. Smith. J.E., Schwarcz, H.P., Risk, M.J., McConnaughey, T.A. and Keller, N.B. (1996) Isotopic analyses of deep-sea corals yield climatic information after compensating for kinetic isotope effects. Spring Meeting, American Geophysical Union, *EOS* **77**, April 23, 1996 Supplement, S160.

10. McConnaughey, T.A. (1989) C-13 and O-18 isotopic disequilibrium in biological carbonates I: Patterns. *Geochim. Cosmochim. Acta* **53**, pp. 51-163.

11. McConnaughey, T.A., Burdett, J., Whelan, J.F. and Paull, C.K. (1997) Respiration and photosynthesis: effects on the carbon-13 content of biological carbonates. *Geochim. Cosmochim. Acta* **61**, pp. 611-622.

12. Grossman, E and Ku, T.L. (1986) Oxygen and carbon fractionation in biogenic aragonite: temperature effects. *Chemical Geology* **59**, pp. 59-74.

13. Keen, C.E. (1978) *Cruise Report, C.S.S. Hudson 78-020.* Atlantic Geoscience Centre, Dartmouth, 15 pp.

14. Schumacher, H. and Zibrowius, H. (1985) What is hermatypic? A redefinition of ecological groups in corals and other organisms. *Coral Reefs* **4**, pp. 1-9.

15. Smith, J.E. (1994) Late Quaternary climate reconstruction using the deep-water coral *Desmophyllum cristagalli. Geol. Surv. Canada Open File* **2950**, Ottawa, 100 pp.

16. Broecker, W.S. *et al.* (1990) Radiocarbon age of waters in the deep Atlantic. *Global Biogeoch. Cycles* **4,** pp.103-117.

17. Lehman, S.J. and Keigwin, L.D. (1992) Sudden changes in North Atlantic circulation during the last deglaciation. *Nature* **356**, pp. 757-762.

18. Woillard, G.M. and Mode, W.D. (1982) C-14 dates at Grande Pile: correlation of land and sea chronologies. *Science* **215**, pp. 159-161.

19. Coope, G.R. (1977) Fossil coleopteran assemblages as sensitive indicators of climate change during Devensian (last) cold stage. *Phil. Trans. R. Soc. B* **280**, pp. 313-340.

20. Lehman, S.J., Wright, D.G. and Stocker, T.F. (1993) Ice in the climate system. In: *NATO ASI Series 1 "Global Climate Change"* **12**, pp. 187-209.

21. Boyle, E.A. (1988) Cadmium: chemical tracer of deepwater paleoceanography. *Paleoceanography* **3**, pp. 471-489.

22. Yu, E.-F., Francois, R. and Bacon, M.P. (1996) Similar rates of modern and last-glacial ocean thermohaline circulation inferred from radiochemical data. *Nature* **379,** pp. 689-694.

23. Samthein, M. et al. (1994) Changes in east Atlantic deepwater circulation over the last 30,000 years: eight time slice reconstructions. *Paleoceanography* **9**, pp. 209-267.

24. Labeyrie, L.D. et al. (1992) Changes in the vertical structure of the North Atlantic ocean between glacial and modern times. *Quaternary Science Reviews* **11**, pp. 301-413.

25.Oppo, D.W. and Lehman, S.J. (1992) Mid-depth circulation of the subpolar North Atlantic during the last glacial maximum. *Science* **259**, pp. 1148-1152.

26. CLIMAP (1984) The last interglacial ocean. *Quaternary Science* **21**, pp. 123-224.

27. Alley, R.B. (1993) Abrupt increase in Greenland snow accumulation at the end of the Younger Dryas. *Nature* **342**, pp. 527-529.

28. Fairbanks, R.G. (1989) A 17,000 year glacio-eustatic sea level record: influence of glacial melting rates on the Younger Dryas event and deep ocean circulation. *Nature* **342**, pp. 637-642.

29. Blanchon, P. and Shaw, J. (1995) Reef drowning during the last deglaciation: evidence for catastrophic sea-level rise and deep-ocean circulation. *Geology* **23**, pp. 4-8.

CHAPTER 3

The skeletal structure of Desmophyllum cristagalli: the use of deep-water corals in sclerochronology

3.1 Abstract

Skeletal banding has been found in the deep-water coral *Desmophyllum cristagalli*, an organism which has recently been shown to be important in studies of recent climate change. The detailed study of this banding pattern sheds light on the means of skeletogenesis in these organisms, and suggests means by which the record of climate change contained within their skeletons may be interpreted.

A central wall of trabeculae forms the interior of the septa and rings the theca. Lamellae form a sheath over the trabecular frame, showing continuity from epitheca to septum. Bands are added by the tissue layer, which overlaps and seals the internal coral and upper portion of the epitheca. Truncated inner bands on the epitheca indicate a pattern of skeletal deposition and dissolution dependent on the presence or absence of the live tissue layer. A long term record will be difficult to collect from *D. cristagalli* since lamellae are less than 10 μm thick, and band position is unpredictable. Density banding in shallow-water coral skeletons has been recognized as a valuable paleo-oceanographic tool. Before deep-water corals achieve the same status, there needs to be careful consideration of the pattern of skeletal growth.

3.2 Introduction

In recent years, reef-building (hermatypic) corals have been increasingly recognized as superb tools for paleoceanographic recontructions. Much of their utility in climatic research is based on the observation that their skeletons generally show a series of growth bands, with each band consisting of a dense/less dense couplet. Density bands appear to have annual periodicity. This was first demonstrated by the detection of radioactivity within dated bands in some of the coral specimens collected from regions where nuclear weapons testing had occurred (Knutson *et al.*, 1972). The annual nature of the growth bands suggests that banding is triggered by one or more aspects of the environment which also vary seasonally. Banding patterns have been shown to be consistent within a species in an area (Hudson, 1976), implying a common external trigger for the deposition of the regular cycle of dense and less dense bands. Various agents have been invoked to explain this phenomenon, including changing light levels (Baker and Weber, 1975; Highsmith, 1979); changes in water temperature (Weber *et al.*, 1975); and initiation of reproduction (Wellington and Glynn, 1983).

Whatever their provenance, it has been thought that study of the growth bands in a coral may reveal details of the past environment, much in the way terrestrial tree rings do. Within trees, the width of an individual band, i.e., the amount of growth during the season of deposition, varies predictably with temperature, light, etc., so can be used to reconstruct past climates. The controls on the width of coral growth bands, however, are far from clearcut and may have more to do with nutrient availability than with climatic signals (Edinger *et al.*, in review).

Stable-isotopic ratios within coral bands (typically $\delta^{18}O$ and $\delta^{13}C$) have been shown to be accurate recorders of past oceanographic conditions in reef corals

(e.g., Carriquiry *et al.*, 1988; Rye and Sommer, 1980). As corals build their skeleton, these stable isotopes fractionate in response to certain environmental conditions, thereby reflecting differences in seawater temperature, salinity, ambient productivity, light, etc. over time. Although an individual band may be secreted over a matter of months (Barnes and Lough, 1993), reducing the sharpness of the record, stable-isotopic analyses can still give a good interpretation of the changing conditions experienced by a reef coral throughout its life.

Most hermatypic corals, though, contain symbiotic algae (zooxanthellae) which limit their distribution to shallow, tropical waters. Consequently, paleoclimatic records based on reef corals only produce records of oceanographic changes in the low latitudes. There are corals, however, without symbionts (azooxanthellates) which experience no such restrictions: they are found from the Norwegian Sea to Antarctic coasts, from 0-6000 m depth and in waters from -1 to 28 C in temperature (Stanley and Cairns, 1988). Isotopic records from azooxanthellate corals (often termed deep-water corals) could allow paleoenvironmental reconstructions for the vast majority of the Earth's oceans.

Deep-water coral can be difficult to obtain, as many species occur at great depths and high latitudes. To date, most of the work on these creatures has been on taxonomic or biogeographic aspects (e.g., Cairns, 1982; Zibrowius and Gili, 1990; Keller, 1989). The few efforts to extract environmental information from deep-water corals have been hampered by the lack of unequivocal growth bands in these creatures (e.g., Emiliani *et al.*, 1978; Mikkelson *et al.*, 1982). The growth patterns of the corals were unknown and subsamples taken for isotopic analyses were not necessarily from the organisms' growth axes and therefore not a true 'time series'. Often, regions which appear to be banded (containing sections with slightly different colours or textures of aragonite) were actually areas of stereome deposition by the corals for strengthening or straightening themselves. The isotopic ratios in these

regions of secondary thickening probably reflect aspects of coral metabolism as well as environmental parameters (Smith *et al.*, in revision). Druffel *et al.* (1990) exploited what appeared to be definite growth bands on a deep-sea gorgonian, an organism relatied to scleractinian corals. Despite the apparent presence of banding, Druffel *et al.* (1990) concluded that the isotopic record probably did not accurately reflect the conditions experienced by the creature over its lifetime. They predicted, however, that deep-sea corals may be useful as recorders of paleoenvironmental information if the relationship between skeleton and environment could be unravelled.

It has been shown that isotopic analyses of several subsamples from a deep-water coral can accurately determine the average annual temperature of the seawater in which the coral grew (Smith *et al.*, 1996, 1997, in revision). To perform an isotopic time series, that is, to track changes in the ambient conditions experienced by a coral throughout its lifetime, a suitable sampling scheme would have to be developed. The central plane of crystalization is the part of the skeleton most likely to be in isotopic equilibrium with the ambient seawater and therefore is the most promising to yield accurate environmental information. As primary precipitation, it records the history of skeletal extension and, since it is protected from external conditions, it is less likely to be subject to chemical dissolution or isotopic alteration than are secondary layers. The isotopic chemistry of secondary precipitation may be more dependent on aspects of coral metabolism and the localization of ion transport properties by the skeletogenic tissues, meaning increased deviation from equilibrium. Thus, the efficient use of deep-water coral as paleoceanographic monitors, then, requires a detailed analysis of their skeletal structure and careful reconstruction of their probable growth habits.

The development of the skeletons of corals has been shown to consist of variations in four basic subunits: the basal plate, the septa, horizontal structures

known as dissepiments or tabulae, and the epitheca (Wells, 1956). The epitheca is a thin outer layer made up of fine crystals. All other structures made by Scleractinia are built up from fan-shaped subunits called trabeculae.

Most previous work on growth and form in corals, and development of the skeleton, has concentrated on reef corals. The growth banding referred to earlier is produced by variation in the production of skeletal elements, and by changes in the architecture (Barnes, 1972). Recent detailed studies of the production of growth bands in reef corals has greatly aided our ability to decipher climatic signals contained therein (Barnes and Lough, 1993). There has been almost no study of the microstructure of deep-water corals: although their skeletons are also constructed from the basic trabecular unit, the ordering and arrangement of these units must be understood in order to decipher the climatic record they contain. This paper describes the skeletal growth patterns of an azooxanthellate coral, and assesses the potential of these creatures for climatic reconstructions using sclerochronology.

3.3 Methods

Specimens of *Desmophyllum cristagalli* were collected from Baltimore Canyon by the submersible *Alvin*, during a canyon assessment project undertaken by Woods Hole Oceanographic Institute in 1984. The corals were collected alive from a depth of 1024 m. Baltimore Canyon is one of a number of such features located off the eastern coast of North America, near the Delaware estuary (Grow *et al.*, 1988). The corals were airdried, the tissue mechanically removed and were sliced with a small-kerf hand-held cutting disc: sections were chosen to examine various skeletal elements at several different angles. Samples were embedded in epoxy (Spurr's) resin, ground, polished, and etched in 10% HCl for 10 seconds,

stopped with a sodium bicarbonate bath. After drying in a dessicator overnight, samples were gold coated (Polaron SEM coating system) to a thickness of 5 -10 nm, and examined under a Scanning Electron Microscope (SEM). Hundreds of photographs, of average magnification of 120x, were pieced together to create several large photomosaics to examine various parts of the corals in minute detail. Detailed images of sections of interest were produced.

3.4 Results

3.4.1 *Desmophyllum cristagalli*

The genus *Desmophyllum* consists of fixed, solitary corals lacking pali and columella, with few, thin dissepiments. *D. cristagalli* has a variable form, ranging from cone-like to cylindrical. An average specimen has calicular diameters of 45 x 35 mm, and is 60 - 75 mm tall. One such typical organism is shown diagramatically in Figure 1. Septa are arranged in six systems and five cycles, creating a total of 96 septa in larger corals. In elongate forms, dissepiments are present in the deep fossa. The coral is common in the Atlantic, Pacific, Indian, and Antarctic Oceans (Hummelinck and van der Steen 1979). The specimens described in this paper had calical diameters of 20 - 30 mm, and heights of 40 - 55 mm. Figure 2 shows location of skeletal elements in Figures 3 to 13.

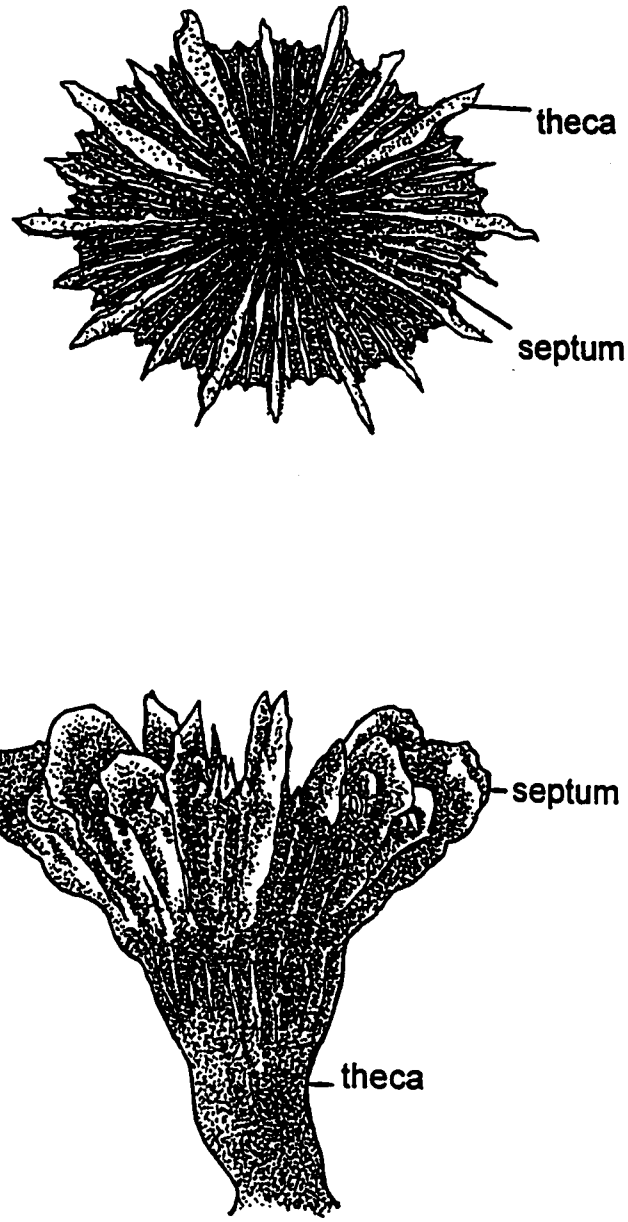

Figure 1: A typical specimen of *Desmophyllum cristagalli*. Drawn by Cameron Tsujita.

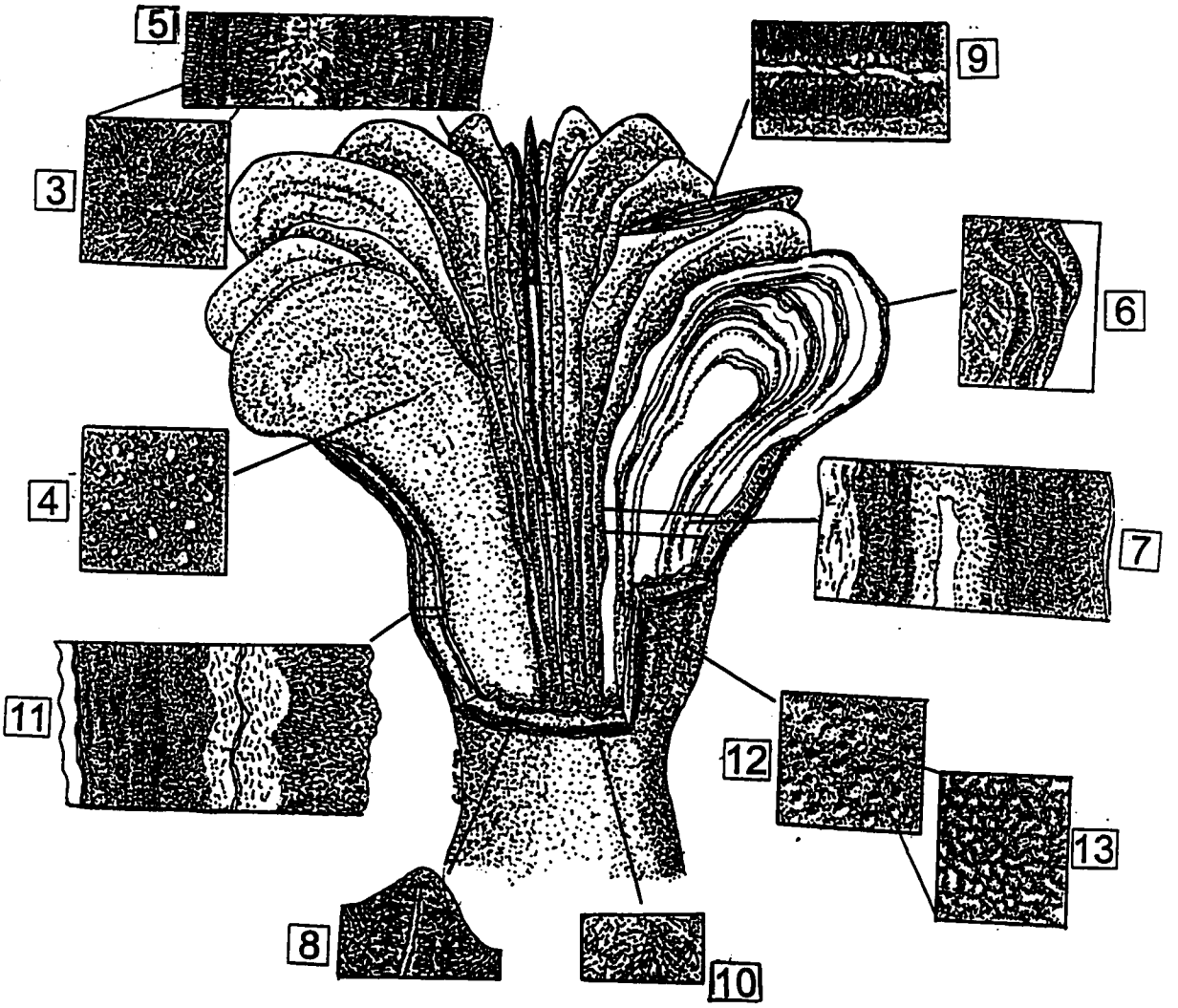

Figure 2: Composite of *D. cristagalli* showing the location of Figures 3-13. Drawn by Cameron Tsujita.

3.4.2 Septum

The mid-plane of each septum is a trabecular sheet. Trabecular units curve across the long horizontal axis of the septum in a convex upward orientation, giving the septum a rounded appearance. Trabecular units form a vertically stacked wall one unit wide (Figure 3). Along the outer faces of the septum, granulations line up along the trabeculae, making the curve of the these lines more visible externally (Figure 4). Acicular aragonite crystals fan out in small bundles perpendicular to the trabecular plane, terminating orthogonally to the septal face. At the septal edges, banding is apparent (Figure 5); thin lamellae are seen, with rod-like, stacked crystals arranged perpendicular to the septal edge (Figure 6). These bands form a sheath over the septum, curling over the trabecular plane at the top of the septum to form continuous layers on both sides. As new trabeculae are added vertically, subsequent bands form over the new upper edge of the septum (Figure 6). The growth of the septum is not precisely vertical; it can be seen in side view that the septum undulates from side to side in its growth. The trabecular plane weaves back and forth through the septum, likely contributing to this growth pattern. When the trabecular plane moves too far in one horizontal direction, the other side of the septum adds a region of stereome to compensate, serving to keep the septum sub-vertical (Figure 9).

3.4.3 Theca

The theca also possesses a central trabecular unit, which encircles the theca as a cylinder. This trabecular sheet branches to form the basis for septa (Figure 7). On either side of the plane and each septal branch is a field of crystals fanning out perpendicular to the trabecular sheet in clinogonal fashion (Figure 8). Immediately adjacent to this field, towards the outside of the theca, is a series of bands. As described for the septa, these bands are thin and lamellar, with stacked

crystals oriented horizontally towards the epitheca. Beyond these bands is a wide, thickened area. Consisting of unoriented clinogonal crystals, this area serves to widen substantially the theca (Figure 10). Beyond it, at the epitheca, lamellar banding reappears.

Between the quasi-cylindrical trabecular sheet and the centre of the coral lies another set of bands, each of which follows the line of the trabecular plane as it curves between septal branches (Figure 7). Successive bands are built towards the centre of the coral, making progressively tighter curves, and giving the bands a crescent shape. This material serves to fill in thicken the spaces between septa. These bands continue to envelop the septa, as described previously.

3.4.4 Epitheca

The epitheca consists of successive lamellar bands (Figure 11). These bands are continuous with those described for the inner theca and septum; each band curls over the top of the calice, marking a former growing edge of the coral skeleton. The epitheca is covered with small granulations (Figure 11, made up of interlocking crescent-shaped crystals (Figure 13). These differ from those found on septa in that they are smaller, and are randomly placed. Epithecal bands faithfully follow this topography, as the granulations can be traced back through numerous banding layers within the theca.

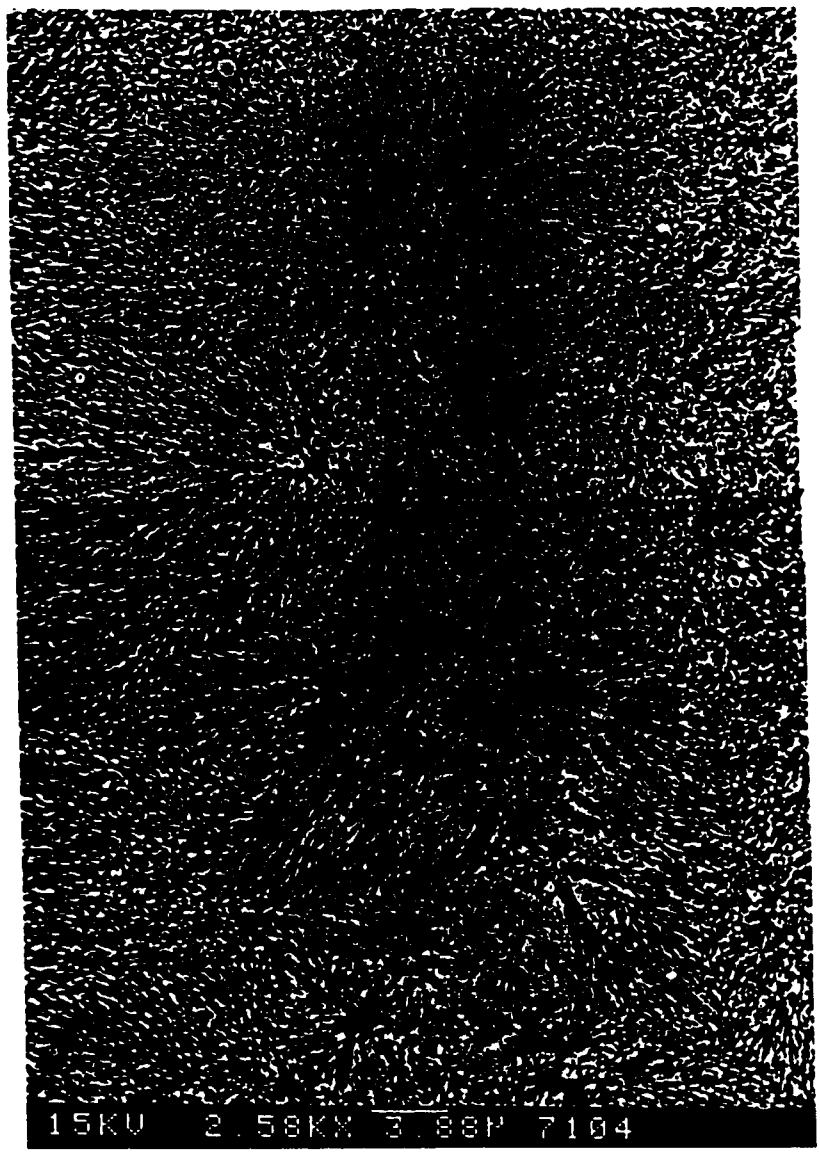

Figure 3: Longitudunal section of the trabecular plane. Trabecular nuclei (centres of calcification) appear as dark spots, surrounded by aragonite crystals fanning horizonatally away from the plane. The plane extends vertically in a wall one trabecula wide.

Figure 4: Exterior of a septum. Septal granulations line up across the curve of trabeculae.

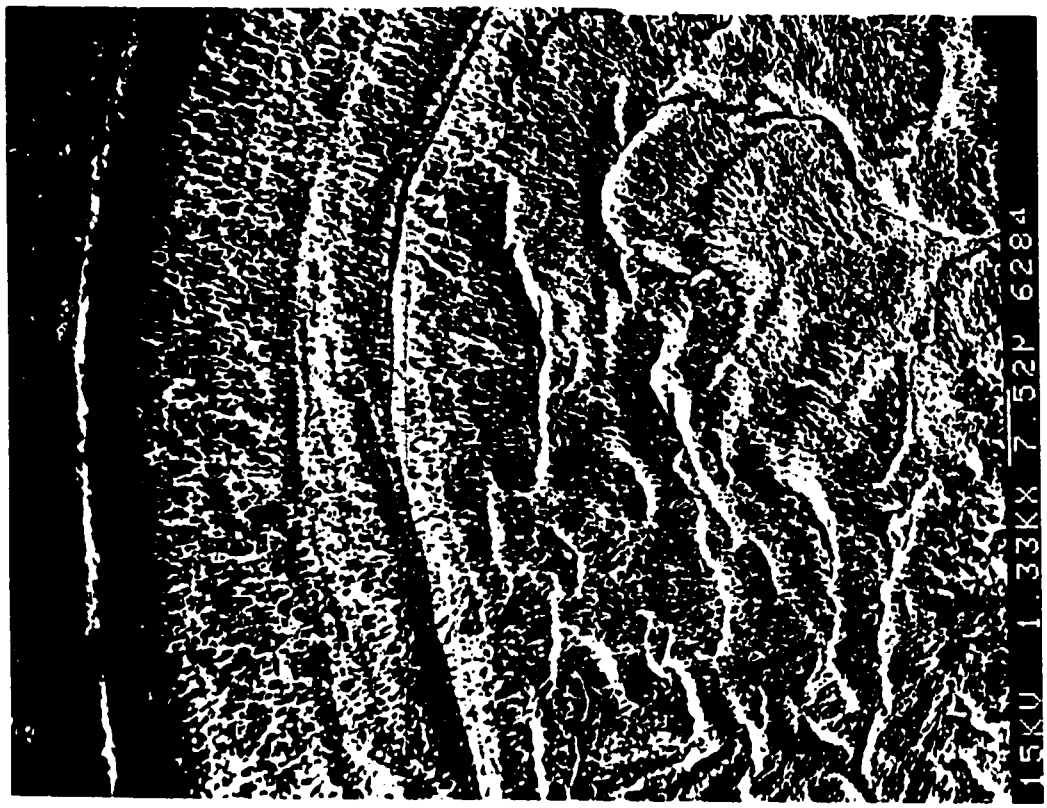

Figure 5: Longitudinal section of a septum. The central trabecular plane is surrounded by clinogonal crystals. At the edges of the septum, lamellar bands are formed.

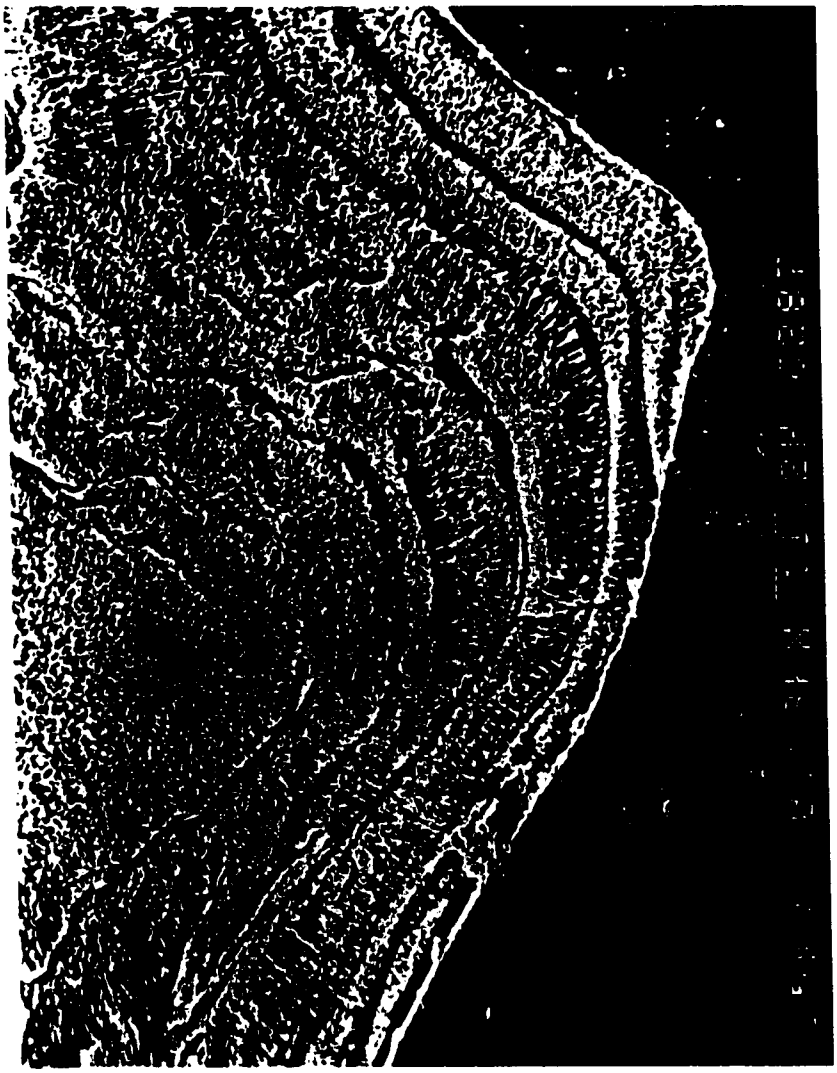

Figure 6: Longitudinal section of lamellar bands. Rod-shaped orthogonal crystals are stacked withinin each band.

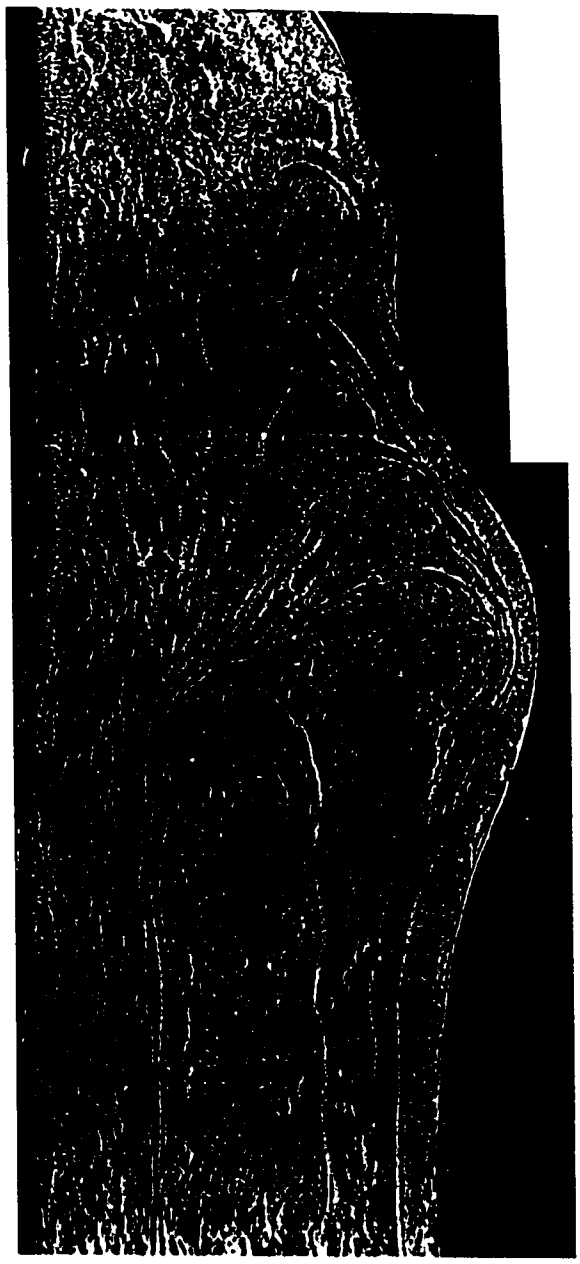

Figure 7: Transverse section of the theca. The trabecular plane, surrounded by a field of dark crystals, can be seen to branch to form a septum. Between septa, a crescent-shaped pattern of banding is seen to fill the inner theca.

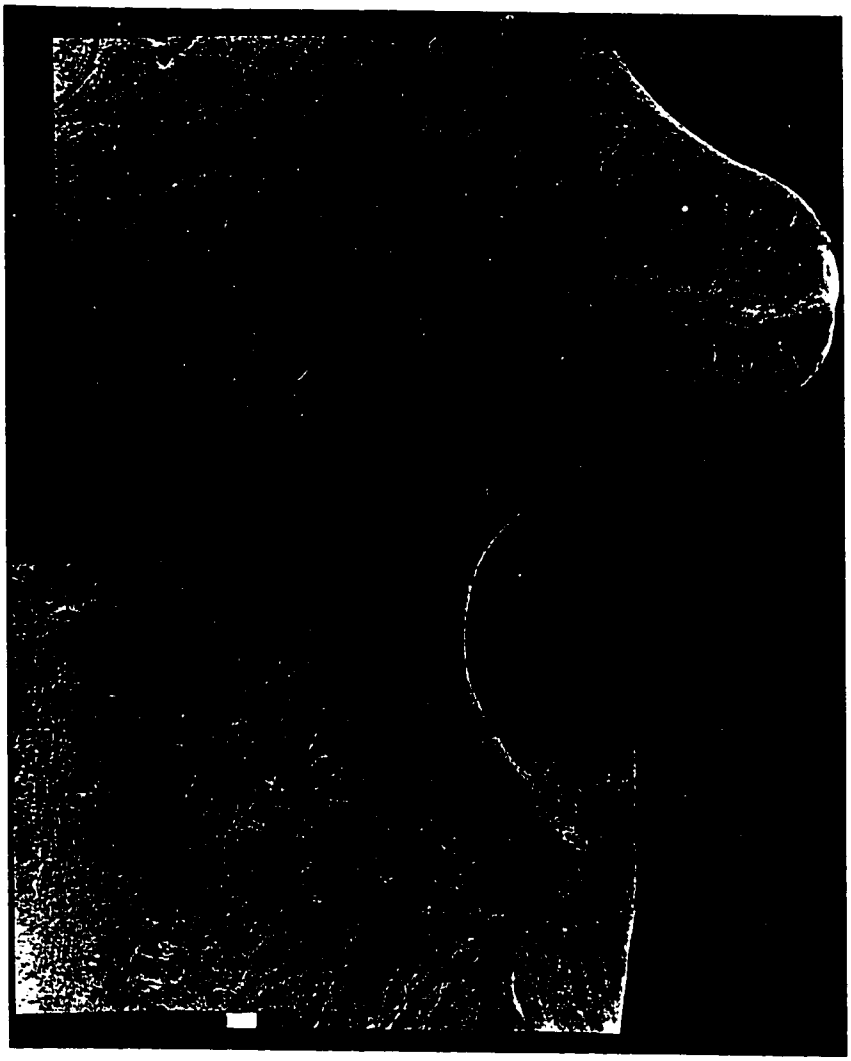

Figure 8: Transverse section of the trabecular plane. A field of tightly arranged clinogonal crystals form parallel bundles perpendicular to the line of the plane.

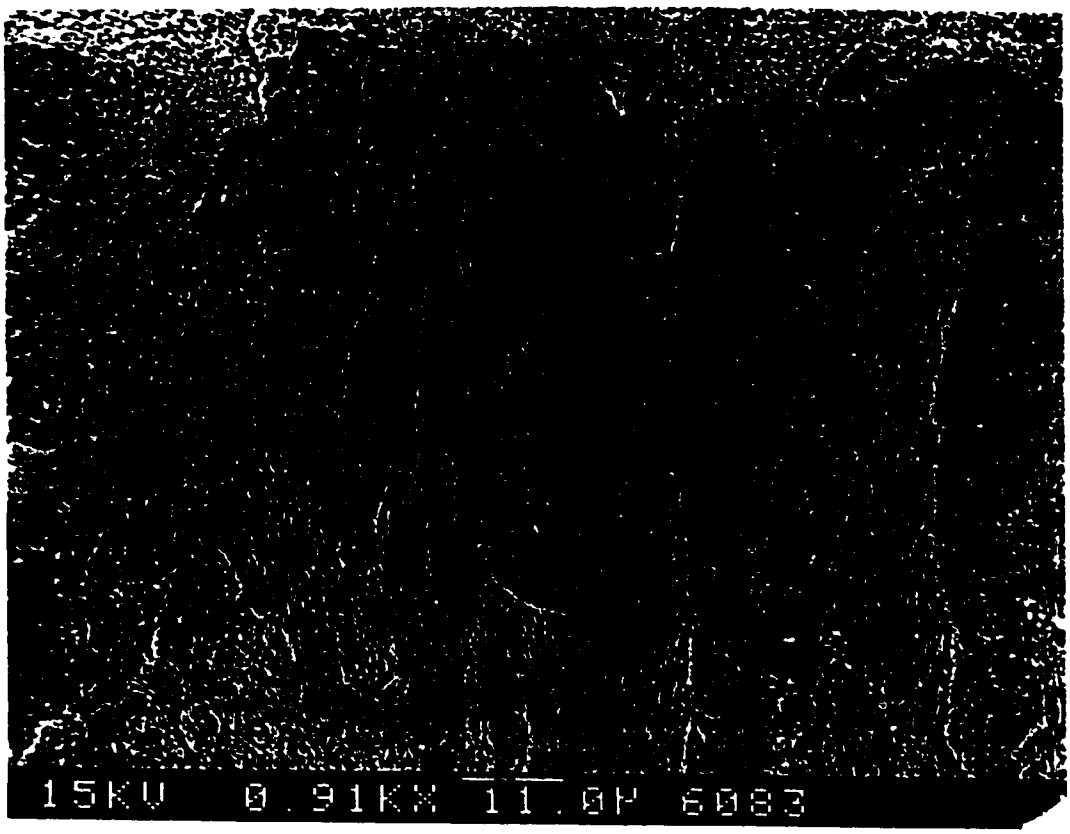

Figure 9: Transverse section of the theca. A large thickened area exists between the trabecular area and the epitheca. Randomly oriented clinogonal fans fill this area.

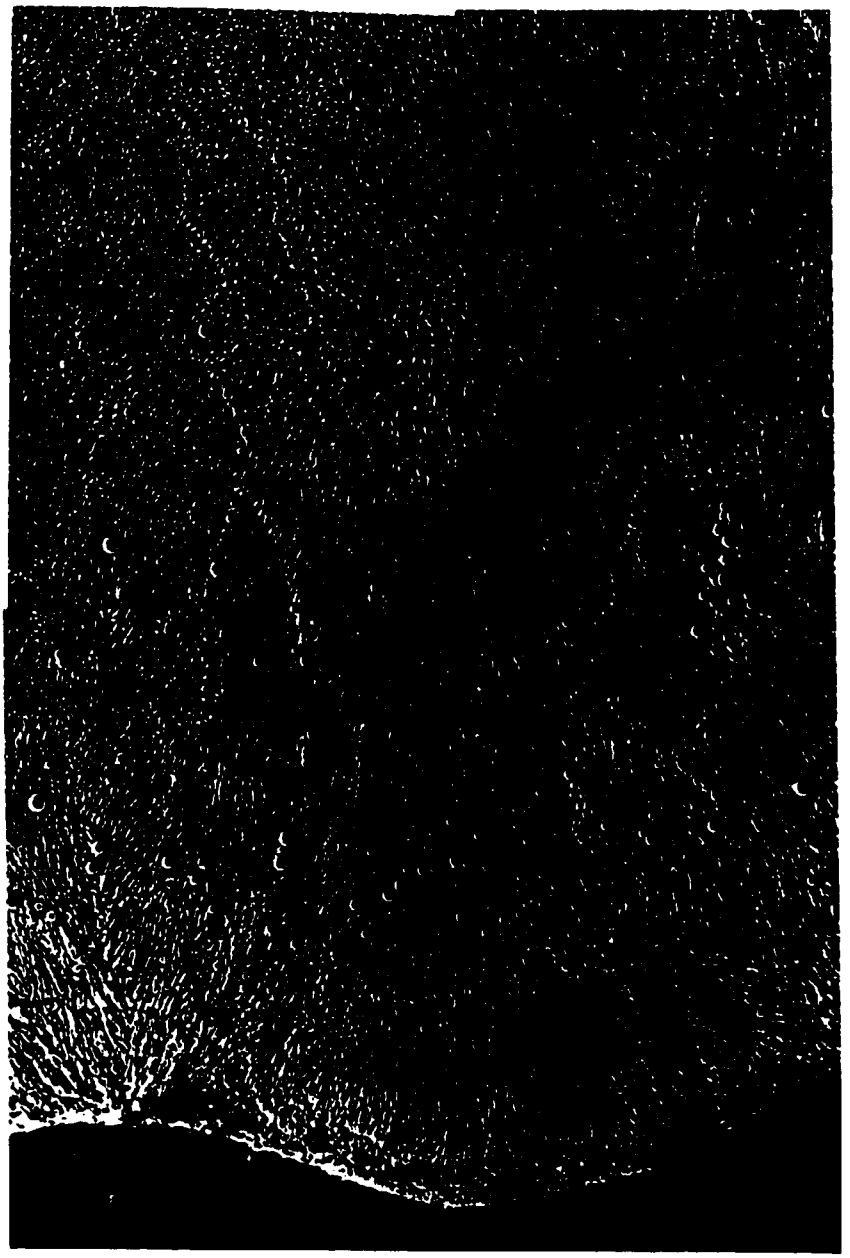

Figure 10: Randomly-oriented stereom crystals for strengthening the theca.

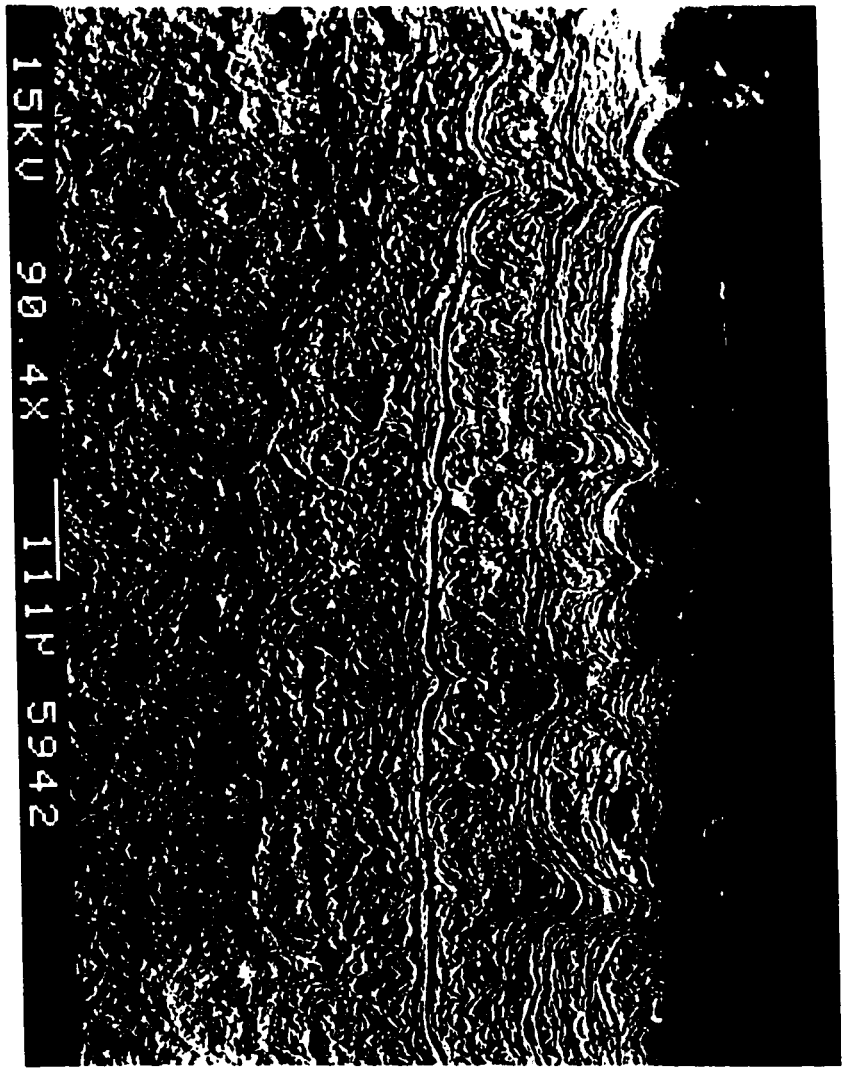

Figure 11: Longitudinal section of the epitheca. Lamellar bands follow the granulations present on the epitheca.

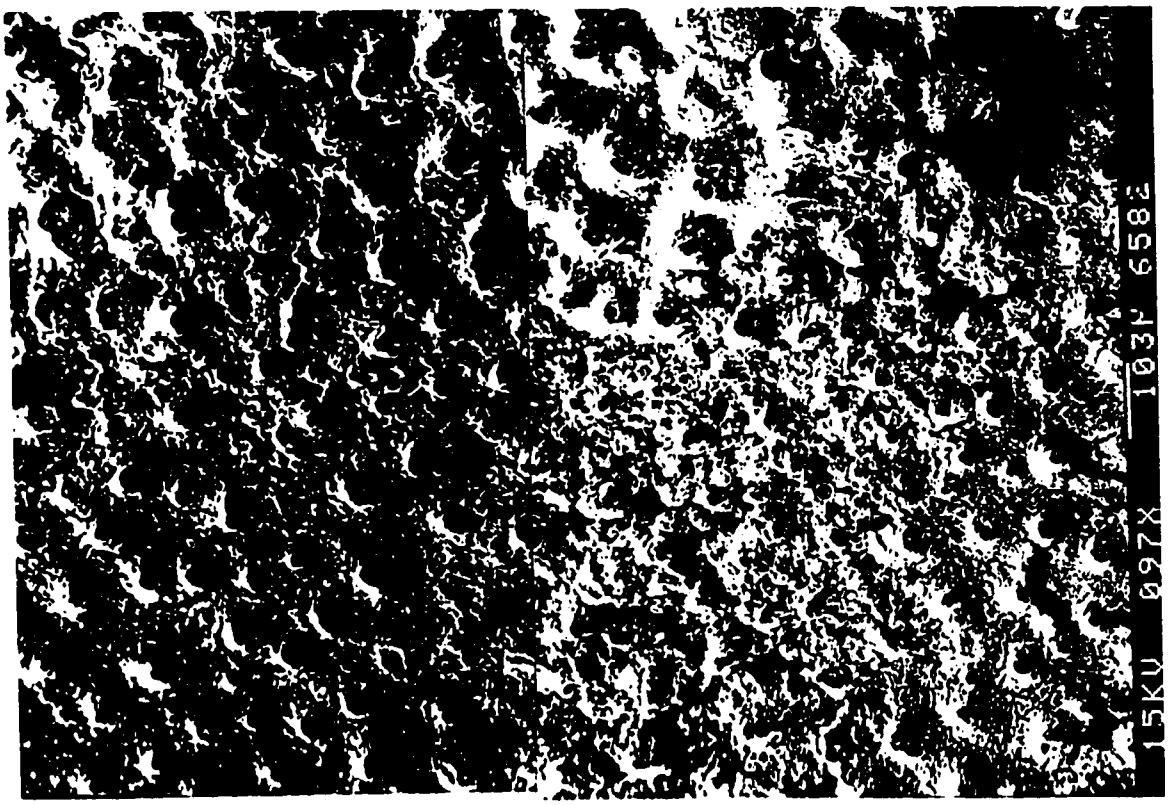

Figure 12: Exterior of the epitheca. Randomly placed granulations cover the surface of the epitheca.

Figure 13: Exterior of the epitheca. Close inspection shows that the crystals of the epitheca are crescent -shaped and interlocking.

3.5 Discussion

3.5.1 Ontogeny/Skeletal Development

The above observations allow a reconstruction of coral growth and skeletal development, observations that are highly relevant to the understanding and interpretation of the paleoclimatic signals encoded in the carbonate skeleton. Initial stages are similar to those of reef corals (Wells, 1956). The newly-settled planula larva makes a basal plate from separated seed crystallites (Figure 14a). After a short while, the basal plate has compacted enough to begin the first stages of upward trabecular growth at the location of the six protosepta (14b). Successive cycles of septa are added and the basal plate turns upwards at the rim (the beginning of the epitheca). Calicoblastic tissue covers all surfaces and precipitates skeletal material of unoriented aragonite crystals (stereome) to strengthen the structure and increase the diameter. At later stages, this lower portion of the pedicel becomes a solid piece of material. The trabeculae of the protosepta and upturned plate edge continue their upward and slightly outward growth, forming true septa and theca. The trabeculae of the septa are fused basally but are free at their upper ends (14c).

Thickening of the newly-formed septa and theca, on both sides, occurs by the precipitation of acicular aragonite crystals orthogonal to the trabecular plane. Stereome is deposited in regions where strengthening or straightening is required; this is especially common within the theca (14d). Skeletal precipitation can occur only beneath the tissue layer of the calicoblastic epithelium (14e) Polyps often contract into the corallum, causing a temporary hiatus in deposition over the outer surfaces. Reasons for these contractions, and their timing, are as yet unclear. As the coral stem grows, the lower edge of the tissue extended over the outside surfaces of the coral also rises, leaving the lowest portions now permanently

exposed (14f). At full height, the lower two-thirds or more of the skeleton may be without tissue cover, meaning that skeletal deposition cannot occur on much or all of the outside stem (14g). After this point, the inside surfaces may continue to thicken, while the calice continues to extend and thicken and generally develop outwards as the 'flower' on the coral 'stalk' (14h). It is not known if this later stage of growth continues in some manner until the animal's death or if, at some point, deposition ceases-although there is reason to believe that some skeletal deposition continues until death of the individual. Reef corals continue to accrete material under the calicoblastic epithelium all of their lives. In addition, relatively huge specimens of *D. cristagalli* (to lengths of 20 cm, suggesting individual ages of about 200 years) are occasionally found.

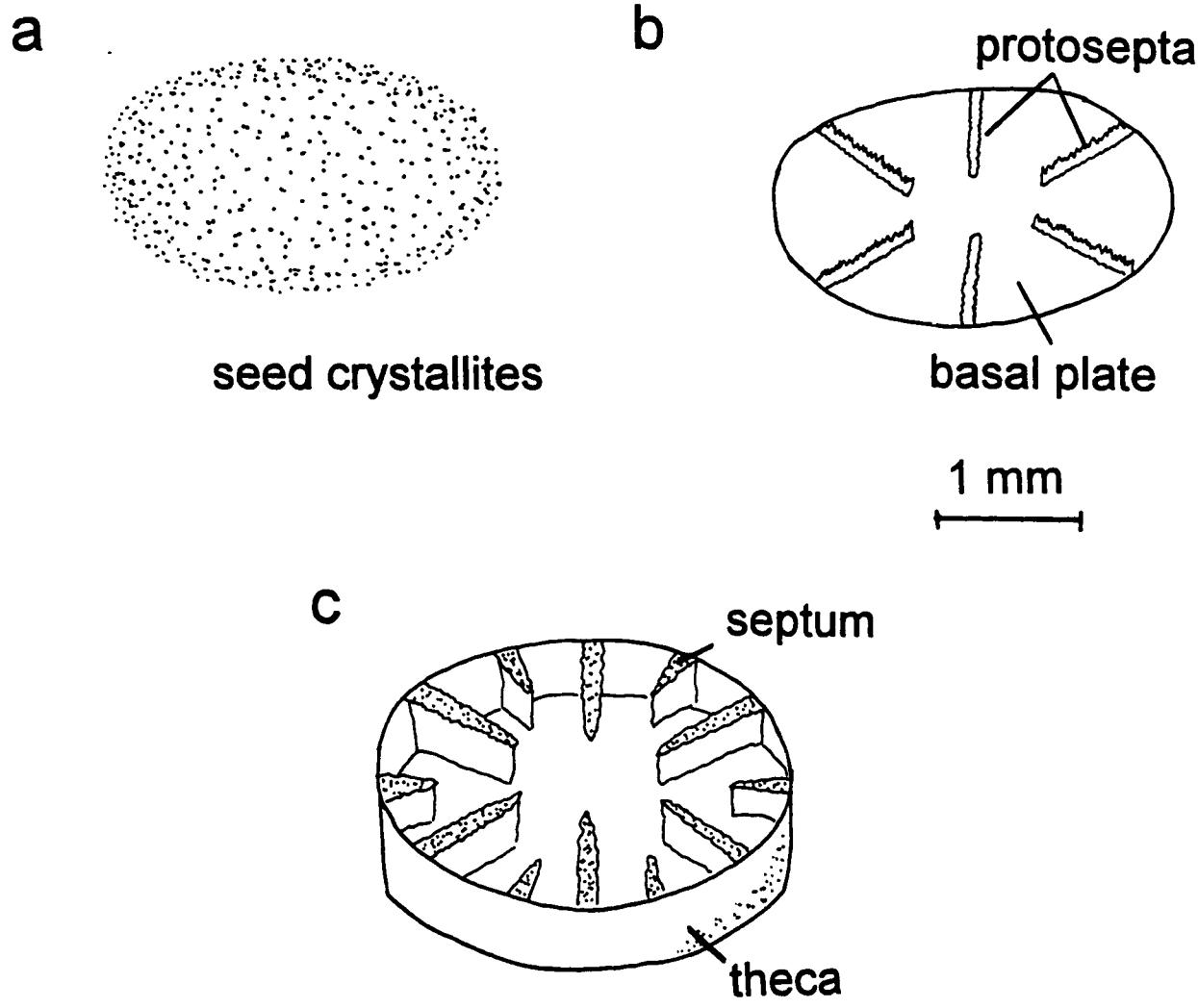

Figure 14: Ontogeny of *D. cristagalli*

a) basal plate forms from seed crystallites

b) the basal plate has compacted enough to begin the first stages of upward trabecular growth at the location of the six protosepta

c) successive cycles of septa are added; the trabeculae of the protosepta and upturned plate edge continue their upward and slightly outward growth, forming true septa and theca

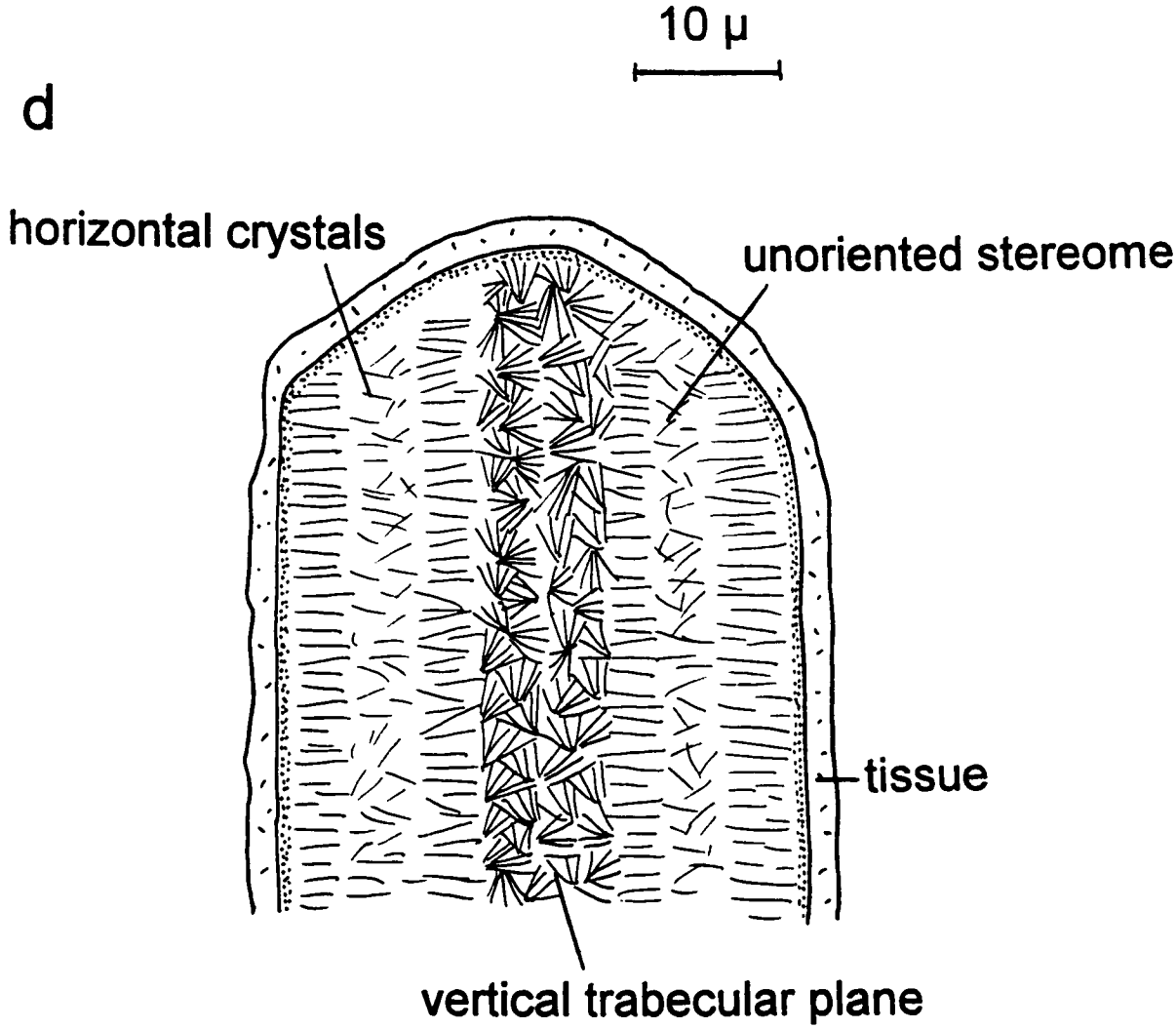

Figure 14: Ontogeny of *D. cristagalli* continued

d) cross-section of top edge of a septum, showing trabecular plane for vertical growth, horizontal crystals for horizontal growth and stereome for thickening

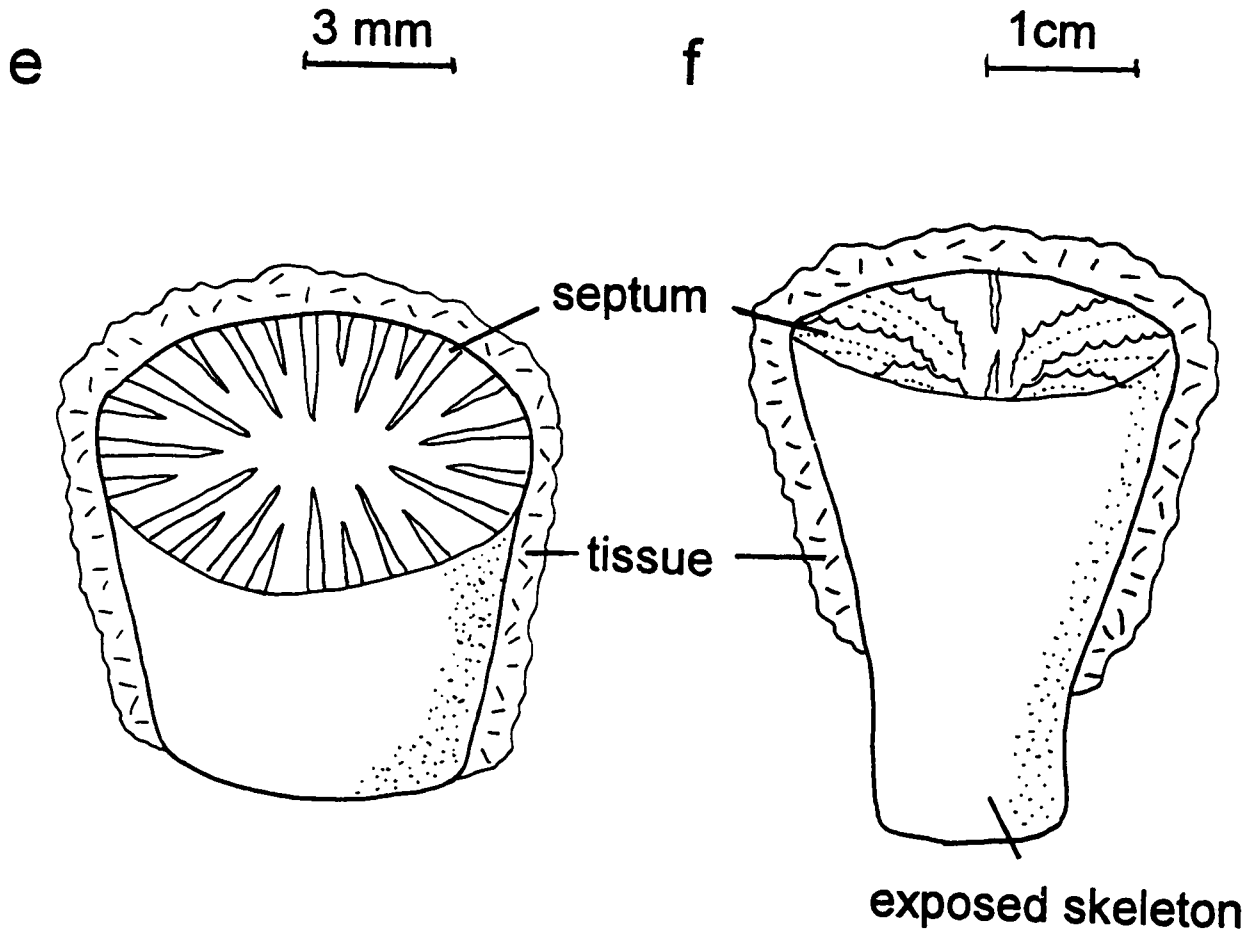

Figure 14: Ontogeny of *D. cristagalli* continued

e) young coral with tissue covering entire skeleton

f) in growth, the lower edge of the tissue extended over the outside surfaces of the coral also rises, leaving the lowest portions now permanently exposed

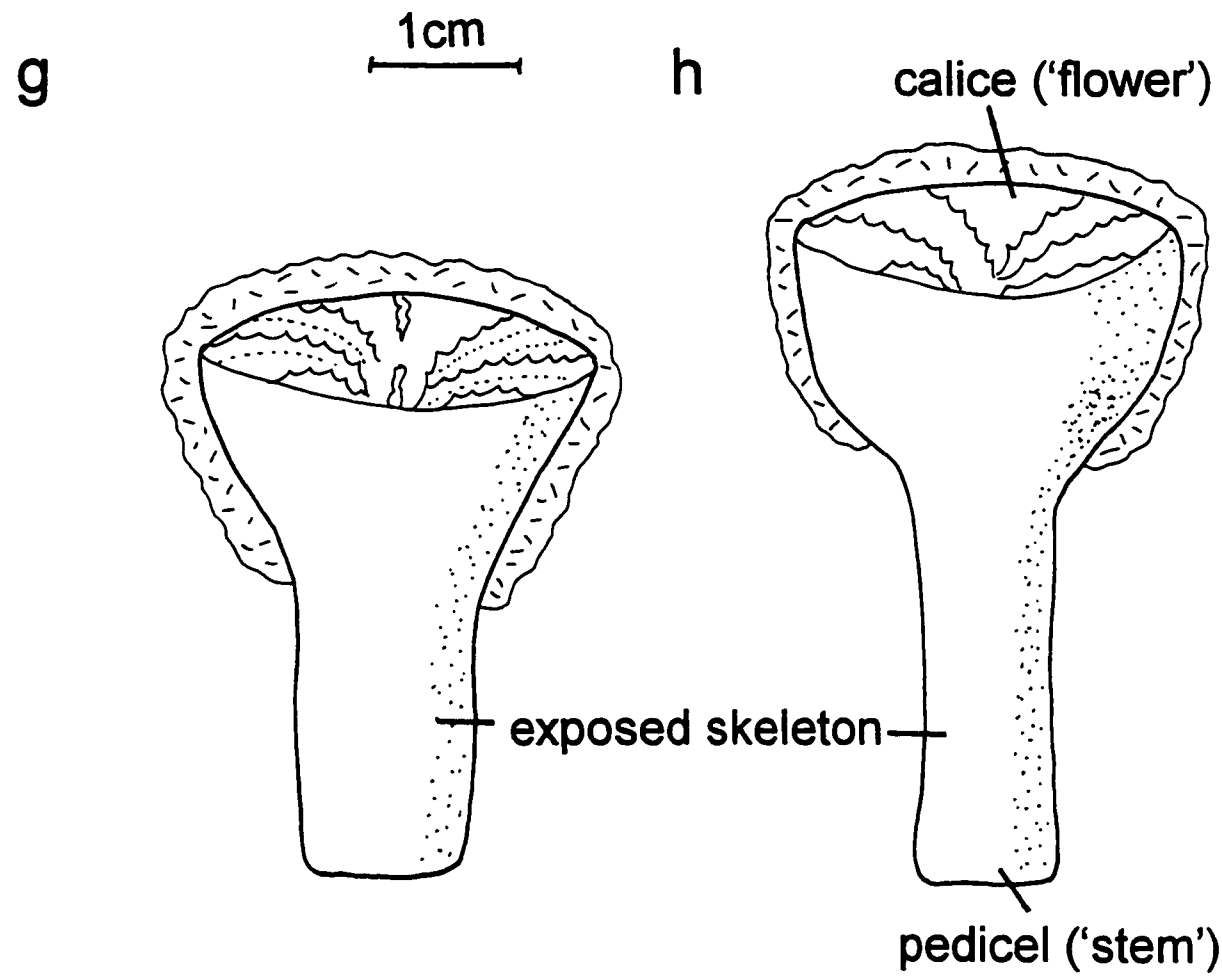

Figure 14: Ontogeny of *D. cristagalli* continued

g) at full height, the lower two-thirds or more of the skeleton may be without tissue cover, meaning that skeletal deposition cannot occur on much or all of the outside stem

h) the inside surfaces may continue to thicken, while the calice continues to extend and thicken and generally develop outwards as the 'flower' on the coral 'stem'

3.5.2 Banding

The skeletal structure of *D. cristagalli* shows that bands are added in successive lamellae to the outer parts of the skeleton. These sheets show continuity from the epitheca to the septa. Each band is added to by the tissue layer, as decribed by Barnes (1972), which seals the internal features of the coral, and overlaps and seals the upper portion of the epitheca. Figure 15 is a diagramatic cross section of a septal or thecal section showing the sequential upward and outward growth and the development of bands. Theoretically, there should be an effective way to sample portions of skeletal material that were sequentially deposited for isotopic analyses and year-by-year paleoceanographic reconstructions.

A transect taken from the epitheca into the central plane (outside surface to the centre), labelled A to A' on Figure 16 intersects bands which become progressively older towards the centre. In any one transect, though, not all available layers will be encountered. As banding can only occur beneath the calicobastic layer, which ascends as the coral grows, skeletal deposition ceases below the new tissue line. Newly-formed epithecal bands thin and lap down onto the older skeleton at the lower limit of the tissue layer (Figure 5). The lower regions therefore do not have an opportunity to have new bands deposited on them, and upper regions do not include the older bands.

This phenomenon, however, ensures that a transect taken on the outside surface of the coral, from base to top (B to B' on Figure 15) consists more-or-less of consecutively laid down skeletal elements. A source of error is the possible dissolution of previously laid-down bands. Within the central area of the coral, a microenvironment is maintained. The centre is sealed off by the tissue layer, and thus is independent of the conditions experienced by the exterior. The epitheca

that is not covered by the tissue layer is afforded no such protection; once the tissue layer retracts, the epitheca is exposed to the surrounding water. If the coral is growing below the lysocline, as the Baltimore Canyon corals were, dissolution can occur. Figure 17 shows a cross section of the epithecal bands. Inspection reveals that several inner bands have been truncated and overlain by new bands. This suggests that, after the bands were deposited, the tissue lappet retracted, and the exposed area underwent erosion or dissolution. At a later time, the tissue layer grew back, and new bands were deposited. The lysocline varies from ocean to ocean and has changed throughout time, but many deep-sea corals live below the depth of beginning skeletal dissolution.

Any growth record taken from the epitheca is potentially incomplete. This poses a problem for sampling, since bands may disappear abruptly within the skeleton. Fortunately, this problem can be circumvented. All bands within the coral are continuous, thus, one should be able to trace any band found on the outside of the coral to the inside (although not *vice-versa*). Since the inside of the coral is protected beneath the tissue layer, it should be immune from this type of destruction, and the record there should be complete. This is only true, however, while the coral is alive. Once the animal is dead and the tissue layer has decayed, dissolution can then occur in water undersaturated in aragonite. While the layers of the septa can be assumed to be continuous, it is not possible to say how many of the outer layers were lost before the collection of the specimen. Even if a complete record could be found, the lamellae are so thin (<10 μm thick) that sampling may be impossible using current technology.

A transect taken along the central trabecular plane (Figure 15 - C to C') should also comprise a complete series of sequentially deposited aragonite. Because this section has never been exposed to seawater, it is unlikely that any material has been lost to dissolution. Adkins and Boyle (1995) have demonstrated

that the central trabecular plane is in aragonite-seawater isotopic equilibrium, rendering it potentially valuable in the reconstruction of oceanic conditions. Ideally, a long-term record could be obtained from these corals. Before this occurs, two points must be addressed: how much time is represented in each growth band; and how can these lamellae be sampled? Most bands seen in *D. cristagalli* are less than 10 μm thick, and the central trabecular plane and hence, the associated bands, have been shown to wander back and forth across the septum. In many places, secondarily-precipitated stereome (which is probably not in aragonite-seawater isotopic equilibrium) is present immediately adjacent to the central trabecular plane. In order to recontruct oceanic conditions accurately over the course of a coral's lifetime, it would be essential to know what time interval is represented between each subsample analysed for stable isotope ratios. It would also be important to sample each growth band in succession and be able to ascertain whether any are missing. Any sampling technique, then, would have to consider these problematic aspects of growth.

The cause of banding in deep water corals remains unknown. As the corals studied lived at a depth of more than 1 kilometre, it can be inferred that neither light effects nor temperature changes directly trigger banding in these organisms. Whatever variable is causing these lamellae to form, it must be undergoing change at depth in the ocean, presumably on a regular basis. The amount of time represented by each lamella remains to be seen. In times of environmental stress (e.g., during low nutrient levels), these animals may reduce skeletal growth, and retract the tissue layer into the centre of the skeleton. In this situation, the epithecal record may be incomplete. Although the full record should be evident within the central part of the skeleton, the lamellae may be almost vanishingly small.

We have shown here, however, that precise intra-annual climatic records from these corals could be derived only via precise sampling of extremely small

internal structures. At the present state of development of sampling and analytical techniques, this would be a difficult task. The technique described by Smith *et al.* (1996, 1997, in revision) gives estimates of mean annual temperature, which allows some broad generalisations to be made. Determination of intraannual changes may come from a refinement of this technique.

3.6 Conclusions

1) *Desmophyllum cristagalli* grows by secreting growth bands in lamellae in successive layers between the tissue layer and the skeleton, over a central trabecular framework. The skeleton is thickened basally by the addition of stereome.

2) The central trabecular plane in the protected septa and inner theca provide the most complete record of the life of the coral, as the epitheca may be subject to chemical dissolution by the surrounding waters of the ocean.

3) The timing and causes of banding in deep-water corals remain, quite literally, in the dark.

4) The small thickness of the bands and their often-erratic patterns makes sampling this deep-water coral for year-by-year paleoclimatic information a difficult, if not impossible, task.

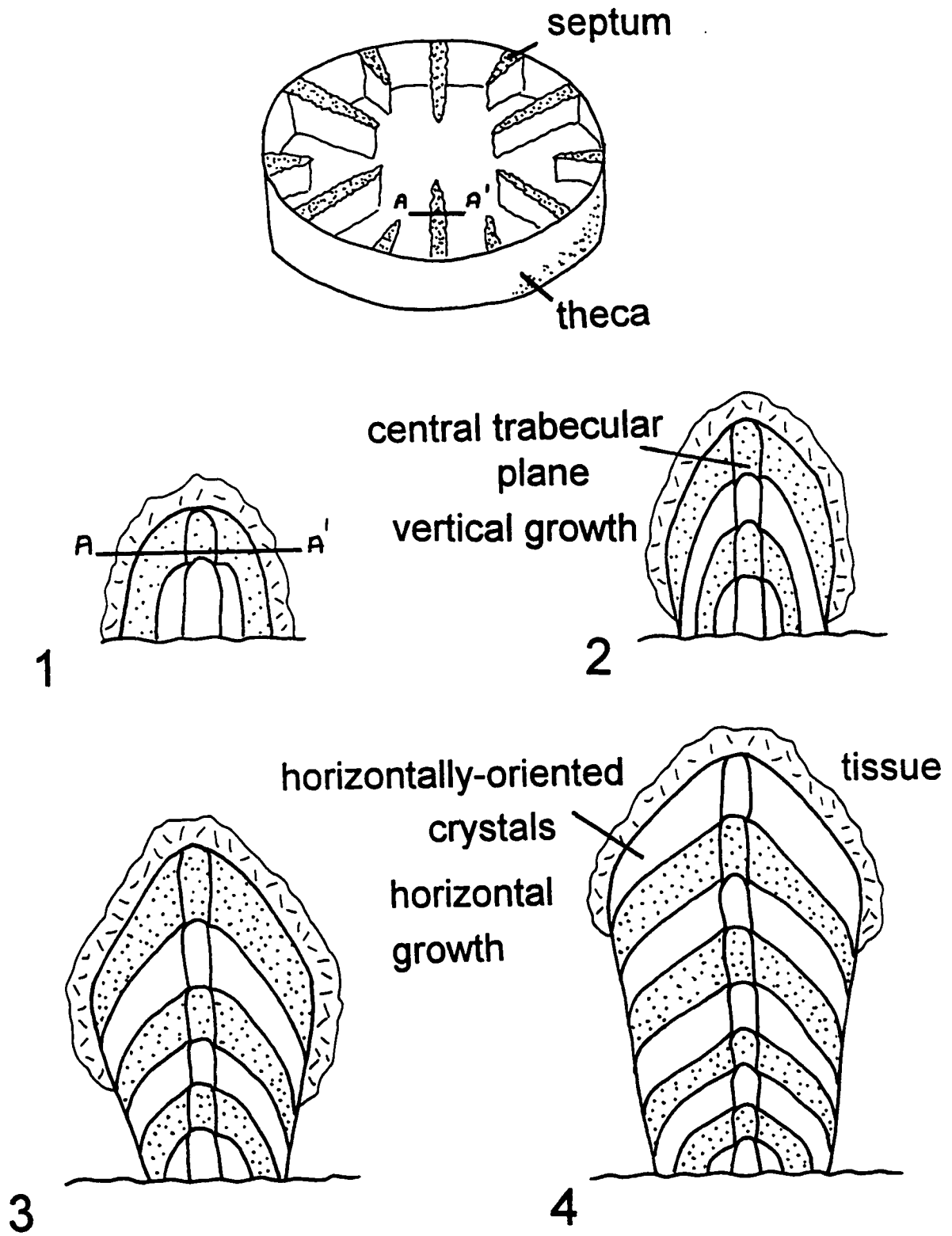

Figure 15: Diagramatic cross-section of septal or thecal section showing sequential upward and outward growth and development of bands.

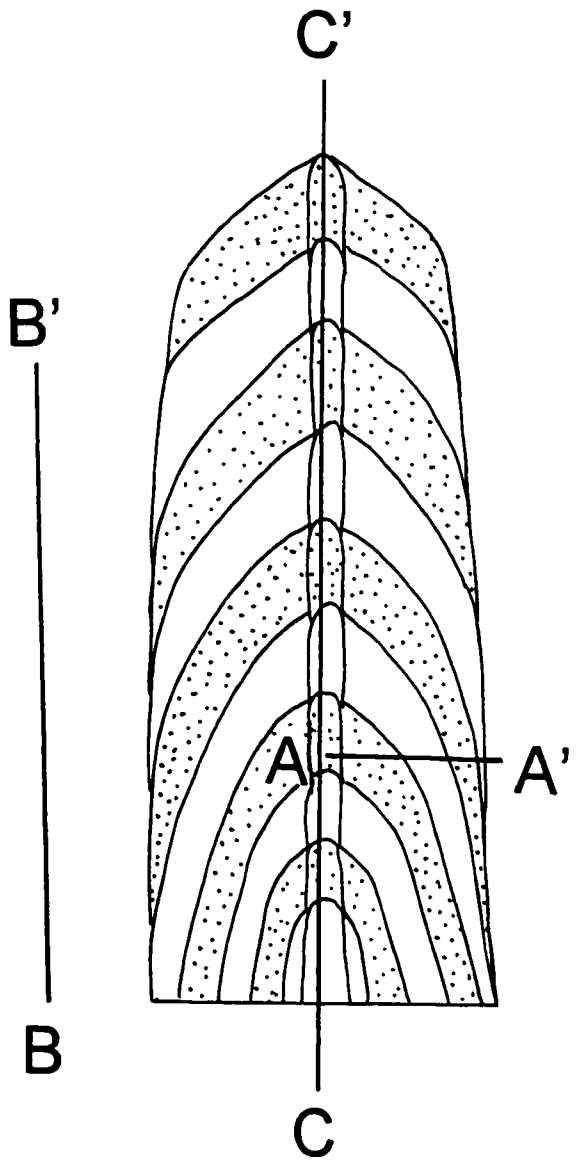

Figure 16: Cross-section showing possible transects for 'time series' analysis

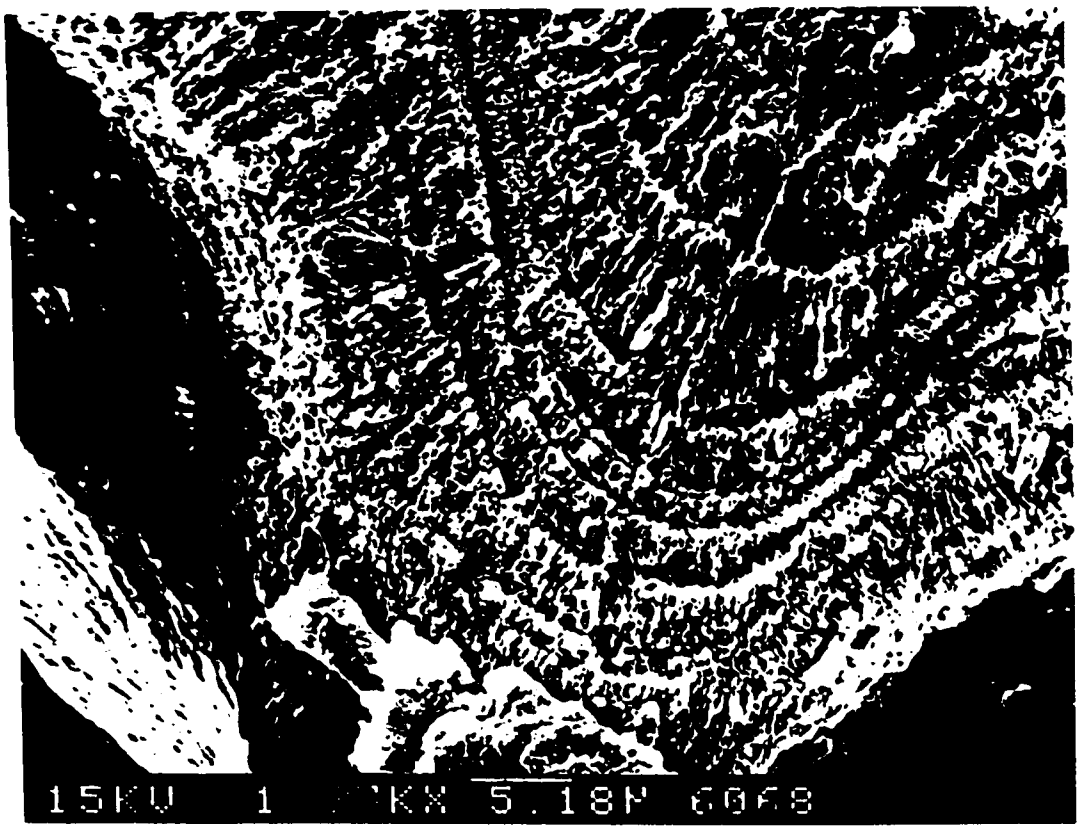

Figure 17: Longitudinal section of epithelium. Interior bands have been truncated, and overlain by new bands.

3.7 Acknowledgements

We thank Klaus Schultes for assistance on the SEM, Cameron Tsujita for drawings and Jack Whorwood for photo plate preparation. The coral was donated by Dr. Barbara Hecker. This work was supported by a Natural Sciences and Engineering Research Council (NSERC) grant to MJR and HPS and NSERC post-graduate support of JES.

3.8 References

Adkins, J.F. and Boyle, E.A. (1995) An investigation of the behavior of stable isotopes and metals in the skeletons of deep-sea corals. *Proceedings of the International Conference of Paleoceanography - V*, Halifax, p. 27 (abstract).

Baker, P.A. & Weber, J.N. 1975: Coral Growth Rates: Variation with Depth. *Earth and Planetary Science Letters* **27**, pp. 57-61.

Barnes, D.J. 1972: The structure and formation of growth-ridges in scleractinian coral skeletons. *Proceedings of the Royal Society of London, B series* **182**, pp. 331-350.

Barnes, D.J. & Lough, J.M. 1993: On the nature and causes of density banding in massive coral skeletons. *Journal of Experimental Marine Biology and Ecology* **167**, pp. 91-108..

Cairns, S.D. (1982) Antarctic and Subantarctic Scleractinina. *Antarctic Research Series* **34** (1), pp. 1-74.

Carriquiry, J.D., Risk, M.J. and Schwarcz, H.P. (1988) Timing and temperature record from stable isotopes of the 1982-1983 El Niño warming event in eastern Pacific corals. *Palaios* **3**: pp. 359-364.

Druffel, E.R.M., King, L.L., Belastock, R.A. and Duesseler, K.O. (1990) Growth rate of a deep-sea coral using Pb-210 and other isotopes. *Geochimica et Cosmochimica Acta* **54**, pp.1492-1500.

Edinger, E.N., Limmon, G.V., Jompa, J., Widjatmoko, W. and Risk, M.J. (1997) The Janus effect: can coral growth rates be taken at face value? Geological Society of America fall meeting, October, Salt Lake City. (abstract)

Emiliani, C., Hudson, J.H., Shinn, E.A. and George, R.Y. (1978) Oxygen and carbon isotopic growth records in a reef coral from Florida Keys and a deep-sea coral from Blake Plateau. *Science* **202**, pp. 627-629.

Grow, J. A. *et al.* 1988: Structure and Evolution of Baltimore Canyon Trough. In *The Geology of North America Volume I-2, The Atlantic Continental Margin: U.S.* The Geological Society of America: Boulder, pp. 269-290.

Highsmith, R.C. 1979: Coral growth rates and environmental control of density banding. *Journal of Experimental Marine Biology and Ecology* **37**, pp. 105-125.

Hudson, J.H., Shinn, E.A., Halley, R.B. and Lidz, B. (1976) Sclerochronology: A tool for interpreting past environments. *Geology* **4** : pp. 361-364.

Hummelinck, P.W. & van der Steen, L.J. 1979: *Desmophyllum cristagalli.* In

Studies on the Fauna of Curacao and the Other Caribbean Islands, Volume LVII. Foundation for Scientific Research in Surinam and the Netherlands Antilles: Utrecht, pp. 117-119.

Keller, N.B. (1989) The comparative characteristics of the coral associations at Atlantic near-continental and mid-oceanic submarine mountains. *Trudy Instituta Okeanologii* **123**, pp. 69-69.

Knutson, D.W. *et al.* 1972. Coral chronometers: Seasonal growth bands in reef corals. *Science* **177**, pp. 270-272.

Mikkelson,N., Erlenkeuser, H., Killingley, J.S. and Berger, W.S. (1982) Norwegian corals: radiocarbon and stable isotopes in *Lophelia pertusa*. *Boreas* **11**, pp. 163-171.

Podoff, N. (1976). *Microstructure of Modern Deep-Water Corals (Flabellidae and Parasmiliinae*). State University of New York at Binghamton, 104 p.

Rye, D.M. and Sommer, M.A. (1980) Reconstructing paleotemperature and paleosalinity regimes with oxygen isotopes. In: Rhodes, D.C. and Lutz, R.H. (eds) *Skeletal Growth of Aquatic Organisms*, Plenum Press, New York, pp. 169-202.

Smith, J.E.; Risk, M.J.; Schwarcz, H.P. and McConnaughey, T.A. (1997) Rapid climate change in the North Atlantic during the Younger Dryas recorded by deep-sea corals. *Nature* **386**, pp. 818-820.

Smith. J.E., Schwarcz, H.P., Risk, M.J., McConnaughey, T.A. and Keller, N.B.

(1996) Isotopic analyses of deep-sea corals yield climatic information after compensating for kinetic isotope effects. Spring Meeting, American Geophysical Union, *EOS* **77**, April 23, 1996 Supplement, S160. (abstract)

Smith, J.E.; Risk, M.J.; Schwarcz, H.P., McConnaughey, T.A. and Keller, N.B. (in revision) Deep-sea corals as paleotemperature indicators: Overcoming 'vital effects'. *Geochimica et Cosmochimica Acta.*

Stanley, G.D. and Cairns, S.D. (1988) Constructional azooxanthellate coral communities: An overview with implications for the fossil record. *Palaios* **3**: pp. 233-242.

Weber, J.N. *et al.* 1975: Correlation of density banding in reef coral skeletons with environmental parameters: the basis for interpretation of chronological records preserved in the coralla of corals. *Paleobiology* **1**, 137-149.

Wellington, G.M. & Glynn, P.W. 1983: Environmental influences on skeletal banding in Eastern Pacific (Panama) corals. *Corals Reefs* **1**, 215-222.

Wells, J.W. (1956) Scleractinia. In: Moore, R.C. (ed) *Treatise on Invertebrate Paleontology.* Part F, Coelenterata. University of Kansas Press, Lawrence, Kansas, pp. F328-F344.

Zibrowius, H. and Gili, J.M. (1990) Deep-water Scleractinia from Namibia, South Africa and Walvis Ridge, southeastern Atlantic. *Scientia Marina* **54**, pp. 19-46.

Chapter 4

Patterns of isotopic disequilibria in azooxanthellate coral skeletons

4.1 Abstract

A specimen of *Desmophyllum cristagalli*, an azooxanthellate (non-photosynthetic) coral was intensively and systematically sampled on all interior and exterior coeval surfaces. Even though the coral grew at an almost-constant temperature estimated to be about 2.5°C, $\delta^{18}O$ varied by almost 3‰ and was up to 3.25‰ depleted with respect to aragonite-seawater oxygen isotope equilibrium. Contour maps of $\delta^{18}O$ show that, although portions of the skeleton approached equilibrium, the location of those areas were unpredictable and were not associated with any readily-identifiable characteristics, such as colour, texture or crystalline structure changes. Although azooxanthellate corals have been shown to have growth banding (Lazier *et al.*, in manuscript), analogous to reef corals, the large and seemingly-random degree of isotopic disequilibrium makes the prospect of documenting temperature changes over the lifetime of an individual coral uncertain.

4.2 Introduction

Oxygen isotopic analyses of foraminiferal and coral carbonates provide much of the available evidence concerning past oceanographic conditions. Temperature affects the partitioning of oxygen isotopes between seawater and precipitating carbonates (McCrea, 1950), while growth and decay of continental ice

sheets affects the oxygen isotopic composition of seawater and hence, of skeletal material (Shackleton, 1967). Recently, carbonates from reef corals have been extensively used as sources of isotopic data, often allowing centuries-long paleoceanographic reconstructions (e.g., Carriquiry *et al.*, 1988). Because of their algal symbionts (zooxanthellae), however, reef corals can only live in shallow tropical waters, thereby biasing the record toward equatorial processes. Azooxanthellate corals have the potential to reflect global conditions, as they have widespread distribution from polar to equatorial waters (Stanley and Cairns, 1988). Although they are often called 'deep-sea' corals, they extend from abyssal waters (>6,000 m) to the surface and sometimes intermingle with true reef corals. Deep-sea corals are also suitable for ^{230}Th-^{234}U disequilibrium dating (Cheng et al., 1995), and may have more-or-less continuous skeletal deposition over periods of decades to centuries (Lazier *et al.*, in manuscript).

Previous attempts to use stable isotopes in deep-sea corals as tools for paleoceanographic reconstructions have been unsuccessful because, like other corals, deep-sea corals do not precipitate in isotopic equilibrium with seawater, and the extent of the disequilibrium varies widely within a particular individual (e.g., Emiliani *et al.*, 1978; Mikkelson *et al.*, 1982; Druffel et al., 1990). McConnaughey (1989) examined both azooxanthellate and reef corals from the Galapagos Islands, and found that a single subsample taken from an azooxanthellate coral could have an isotopic composition several per mil different, both in $\delta^{18}O$ and in $\delta^{13}C$, from a second subsample a few millimetres away. This enormous degree of biological fractionation appeared to overwhelm any environmental signal preserved within the coral.

It has been suggested, however, that some portions of an azooxanthellate coral skeleton may be at or very close to isotopic equilibrium with seawater (Emiliani et al., 1978; Adkins and Boyle, 1995). If areas of equilibrium deposition

were predictable and could be identified beforehand, we could restrict our subsampling to the regions closest to aragonite-seawater equilibrium and perhaps extract an environmental signal that had not been overprinted by kinetic isotope effects. Emiliani *et al.* (1978) performed numerous isotopic analyses on specimens of *Bathypsammia tintinnabulum* from 850 m depth on the Blake Plateau. They reported that individual corals, growing in almost-constant water temperatures, displayed $\delta^{18}O$ and $\delta^{13}C$ values which varied by several per mil. They also noticed, however, that the isotopic values appeared to increase from base to stem, i.e., the skeleton apparently tended toward equilibrium with increasing age. Emiliani *et al.* (1978) speculated that analysing the top (youngest) edges of azooxanthellate corals may give isotopic results that were close to isotopic equilibrium with seawater and were, therefore, suitable for use in paleoceanographic recontructions. Adkins and Boyle (1995) using numerous isotopic values from the septum of an azooxanthellate coral *(Desmophyllum cristagalli)*, demonstrated that the thin, outside edges of the septum showed the smallest degree of kinetic isotope effect and suggested this part of the skeleton may be suitable for paleoenvironmental work.

In order to test whether parts of the coral skeleton were consistently closer to isotopic equilibrium than others, it is best to sample isochronal surfaces, i.e., regions where the skeleton was laid down more-or-less simultaneously. This would allow better mapping of disequilibria patterns, minimizing the confounding effects of ontogeny, growth rate variations, temperature changes, salinity changes, etc.

Lazier *et al.* (in manuscript) described several different sections taken from a specimen of *D. cristagalli*, which were examined with a scanning electron microscope. Photographs of small portions of coral skeleton, taken at 90 - 250x magnification, were pieced together to create large photomosaics. It was hoped that distinct growth lines would be seen that would be analogous to the seasonal

growth bands in reef corals and could be used to develop a sampling strategy for deep-sea corals.

At the centre of each septum and the theca is a trabecular plane (Figure 1). In the septa, the trabecular units form a vertically stacked wall; within the theca, the wall curves around and forms a cylinder. The upward growth of the trabecular plane is not precisely vertical, but rather weaves back and forth in its growth. When the trabecular plane undulates too far in one horizontal direction, a region of stereome is added to the other side of the septum to compensate, serving to keep the septum sub-vertical. Elongate, acicular crystals of aragonite fan out in small bundles perpendicular to the trabecular plane, terminating orthogonally to the septal faces and epitheca. At these outer surfaces banding is apparent; thin lamellae are seen. These bands form a sheath over the septa and epitheca, curling over the trabecular plane at the top of the septa to continue on the other side. As new trabeculae are added vertically, subsequent bands form over the new upper edge of the septum.

The bands are added in successive lamellae to the outer parts of the skeleton. These sheets show continuity from the epitheca to the septa. Each band is added to by the tissue (calicoblastic) layer, as decribed by Barnes (1972), which seals the internal features of the coral, and overlaps and seals the upper portion of the epitheca. Banding can only occur beneath this layer; as the coral grows and the layer ascends, skeletal deposition ceases below the new tissue line. At any given moment, all of the internal surfaces of a coral are covered with tissue depositing new material. The outside of the coral may be entirely covered by tissue (and hence the whole outer layer is coeval) or the tissue line may extend as little as one third the way from the top of the coral (Figure 2). In the latter case, the lower two thirds of coral's outermost layer will be older material. All interior outermost surface layers, and some or all of the exterior outermost surface layers,

are therefore thought to have been deposited simultaneously.

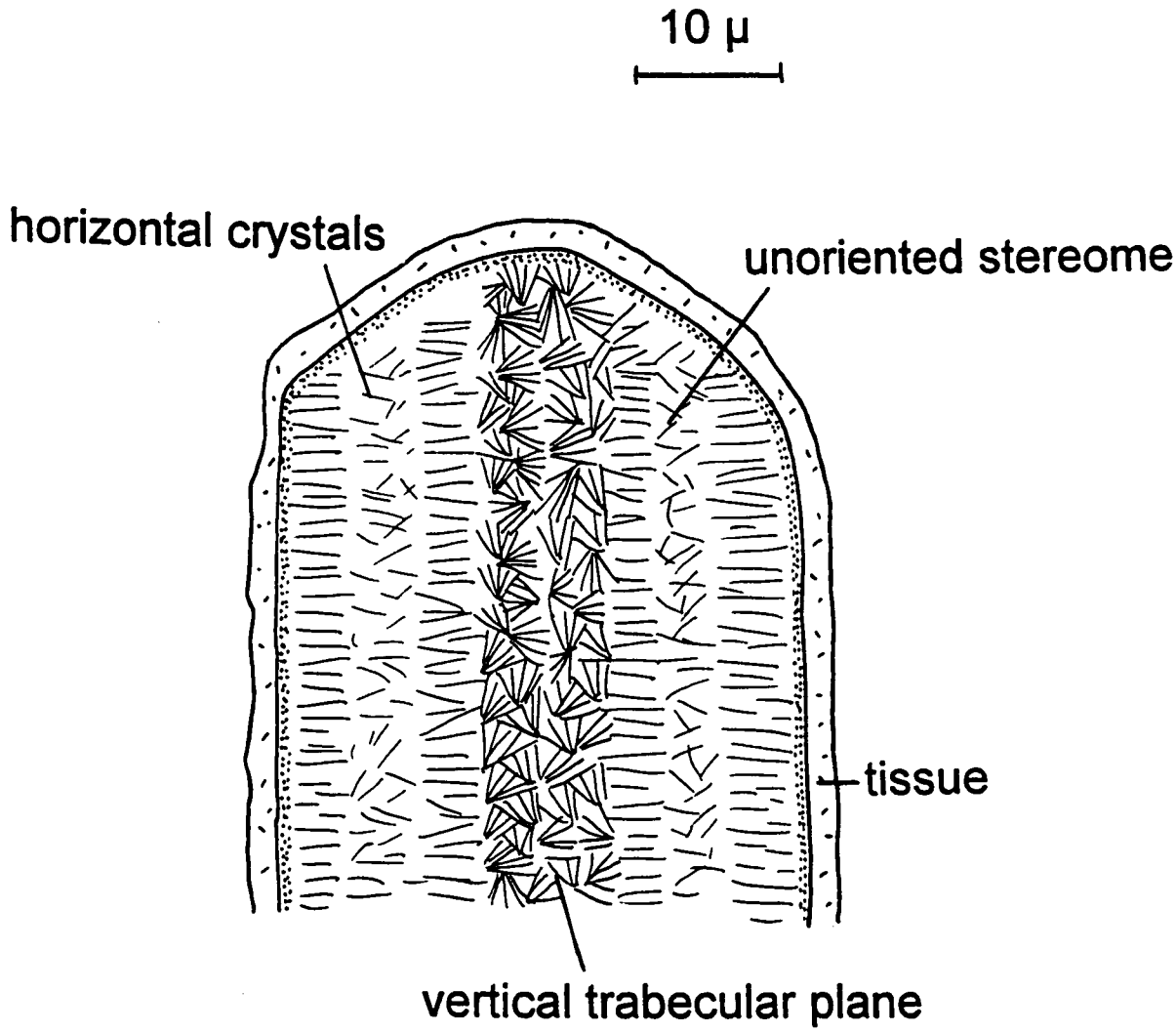

Figure 1: a) Cross-section of thecal wall or septum showing vertically-extending central trabecular plane, horizontally-extending acicular aragonite needles, unoriented stereome for stengthening or straightening and the position of the coral tissue

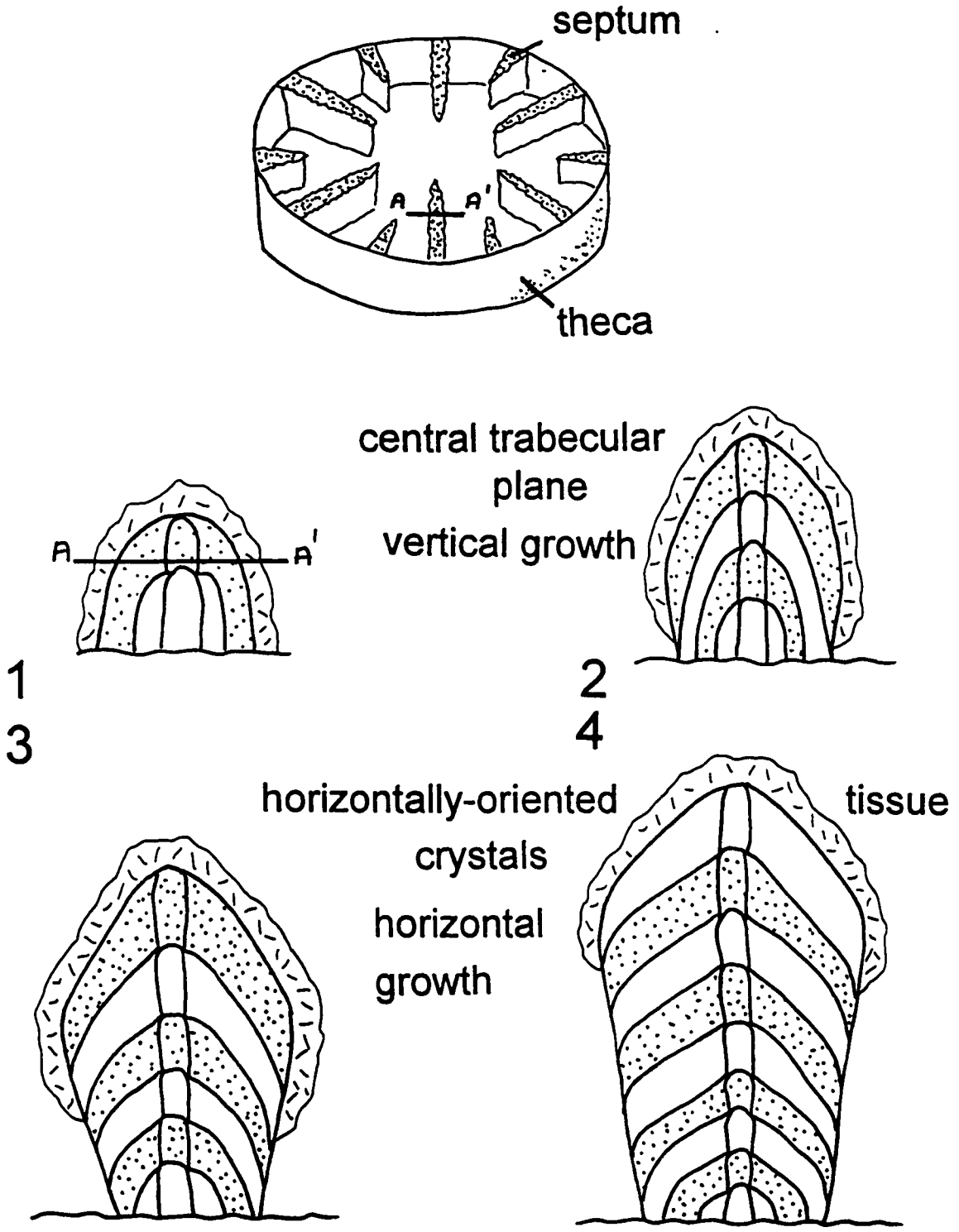

Figure 1b) Layer-by-layer growth of thecal wall or septum, both horizontally and vertically

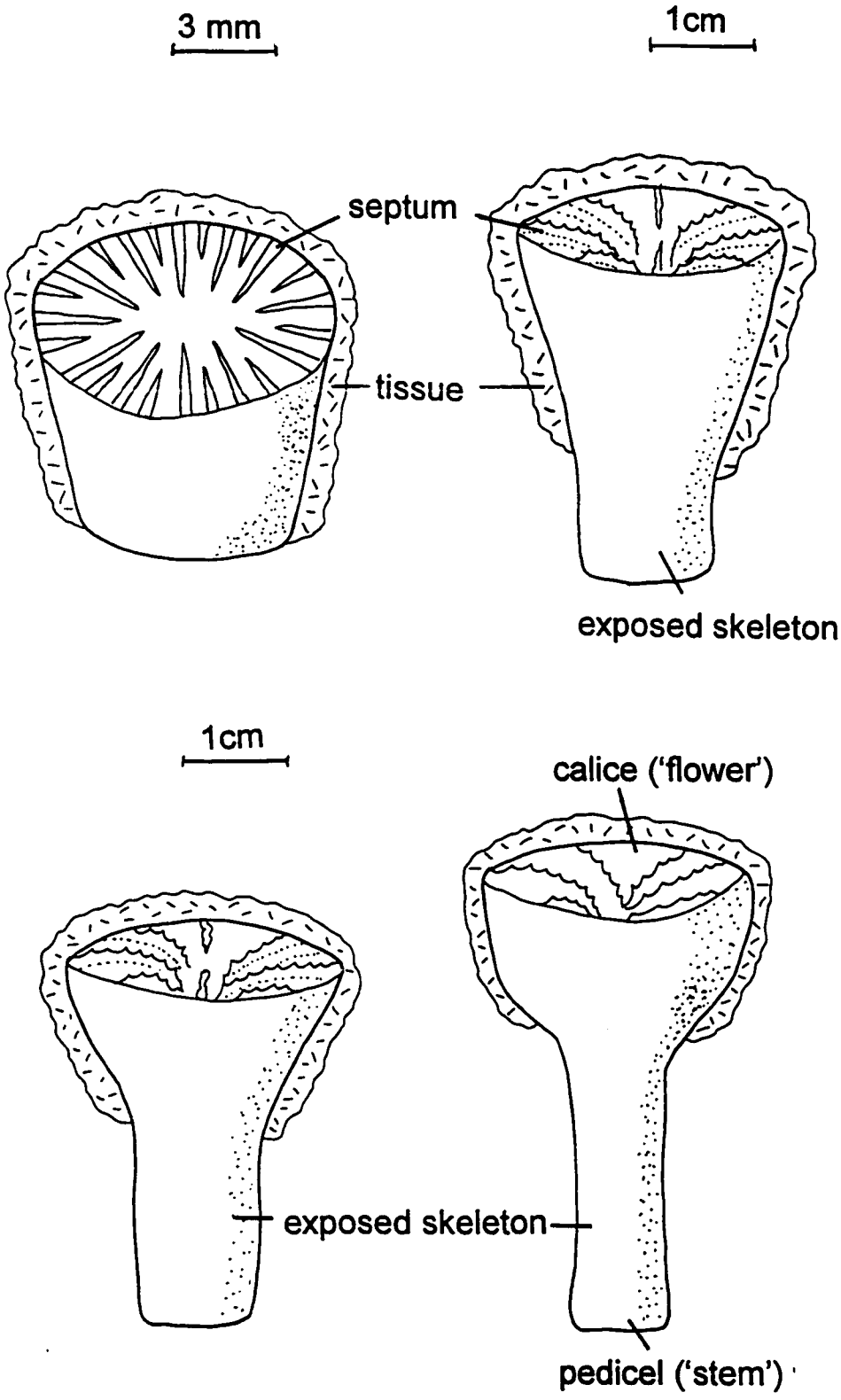

Figure 2: Position of coral tissue at various stages of growth. Skeleton is only precipitated under calicoblastic tissue layer.

4.3 Methods

Patterns of isotopic disequilibria on these surface layers were investigated using a fossil specimen of *Desmophyllum cristagalli* (Figure 3), collected from 1700 m depth in the North Atlantic, 550 km northwest of Newfoundland (50 25.57'N, 46 22.05'W). The coral was halved longitudinally and its various skeletal parts systematically and intensively subsampled. Subsamples of approximately 100 µg were collected from all coral sufaces, interior and exterior, at spacings of a few millimetres (Figure 4). Drilling depths were kept as shallow as possible to avoid penetration into an older layer of the coral. Analyses were performed on a SIRA gas-source mass spectrometer using a common 100% phosphoric-acid bath at 90°C. Precision was 0.07 ‰ for $\delta^{18}O$ and 0.10‰ $\delta^{13}C$; values for $\delta^{18}O$ and $\delta^{13}C$ are reported relative to VPDB.

The oxygen-isotope values obtained from subsamples from various segments were plotted on the "unrolled" surfaces of the coral, and the data were contoured in an attempt to visualize any patterns. The estimate of oxygen aragonite-seawater isotopic equilibrium was 4.2‰ using the following equation:

$(\delta_a - \delta_W) = -0.23\ T\ (°C) + 4.75$ [1]

where δ_a and δ_W are $\delta^{18}O$ value of aragonite and seawater with respect to PDB (Grossman and Ku, 1986). At this site at present, the $\delta^{18}O$ of the water is estimated to have been 0.01‰ and the water temperature is 2.5°C. At the time the coral grew (estimated at 15,000 y BP), the water temperature may have been slightly lower and the $\delta^{18}O$ of the water may have been slightly higher, rendering our estimate of aragonite-seawater isotopic equilibrium a bit too low. Regardless, all surfaces of the coral experienced the same temperature and were precipitated in water of the same isotopic composition.

4.4 Results

Table 1 shows the oxygen isotope results from each subsample: the table is configured to correspond to Figure 4. Figure 5 (left) shows contoured $\delta^{18}O$ values from the exterior surfaces (Figure 4-left) of the specimen, while Figure 5 (right) shows values from the interior surfaces (Figure 4-right). The $\delta^{18}O$ values varied from 0.88 to 3.90‰; the upper limit of these data is close to, but not quite equal to the estimated aragonite-seawater oxygen isotopic equilibrium. Ninety-five percent of the area subsampled differed by >0.2‰ from the equilibrium value. Within an individual 6 x 6 mm region, isotopic values varied by up to 2.75‰. No overall systematic pattern of isotopic variations could be seen on any surface.

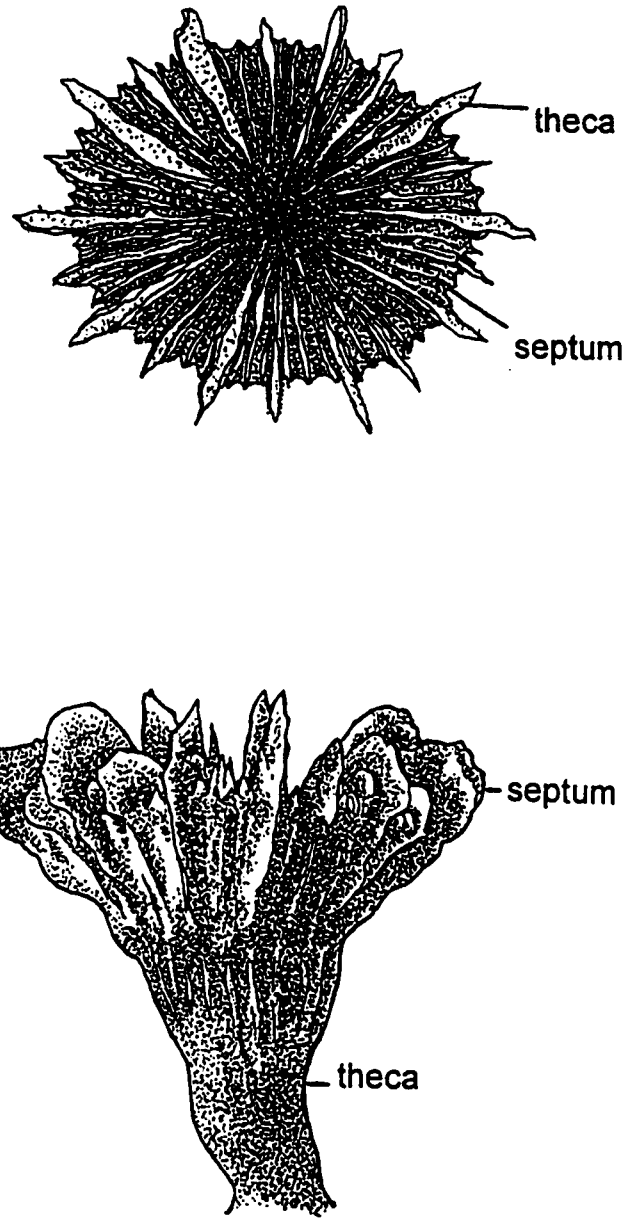

Figure 3: A typical specimen of Desmophyllum cristagalli, with some parts labelled. Drawn by Cameron Tsujita.

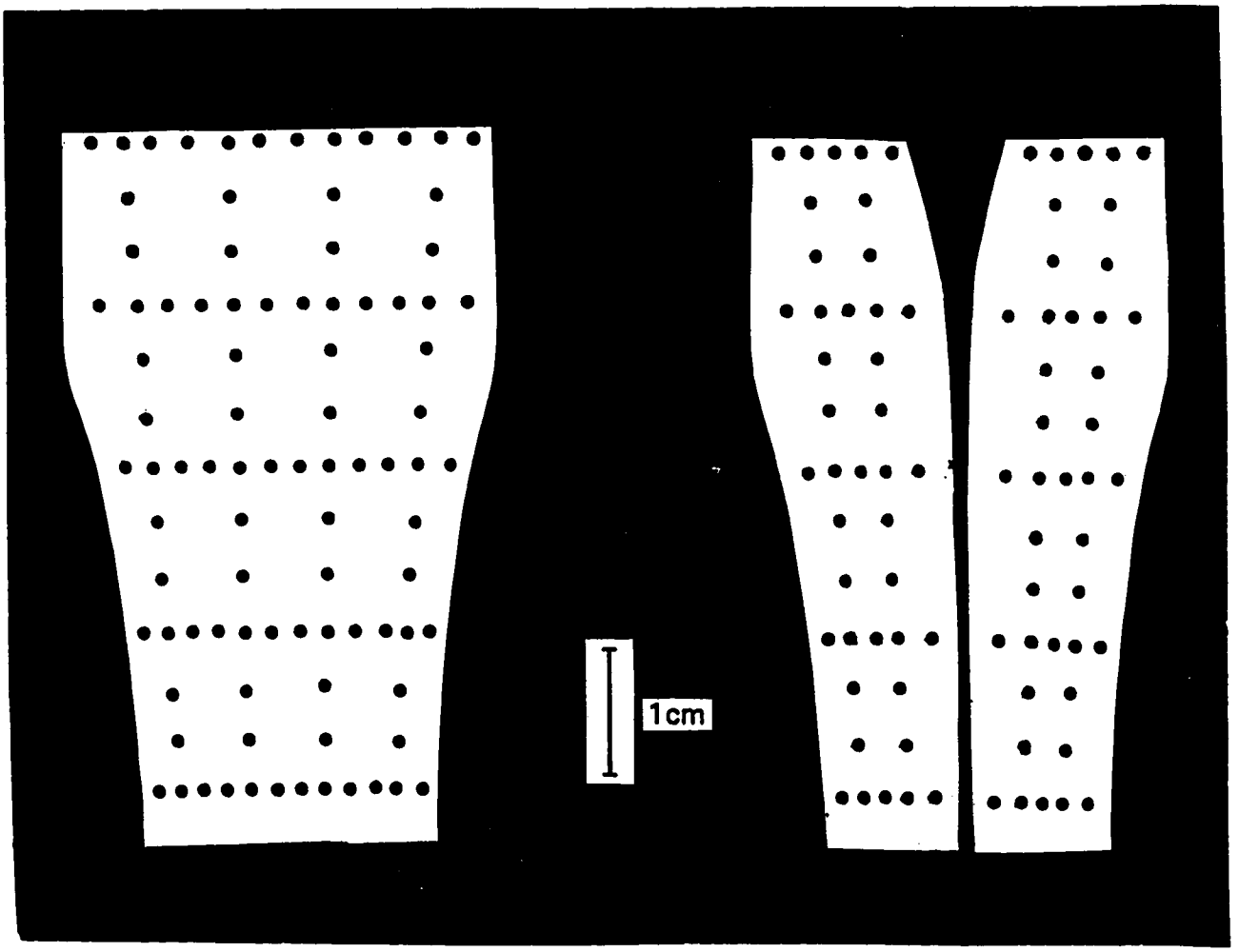

Figure 4: Pattern of subsamples removed from a single specimen, halved longitudinally, for isotopic variability study. Left: exterior surface, samples taken from pedicel, calice and exterior septal edges. Right: interior surface, samples taken from interior septal surfaces within pedicel and calice.

Left											
2.24	2.22	1.73	1.46	1.71	2.14	1.65	1.67	1.74	2.18	0.89	2.33
	2.61			2.23			1.98			1.67	
	2.72			2.12			1.96			1.67	
1.92	1.73	1.15	1.32	1.75	1.96	2.22	2.32	2.84	3.91	2.63	1.67
	1.62			1.96			2.27			2.84	
	2.10			1.84			1.62			2.18	
2.36	2.33	2.41	2.27	2.43	2.12	2.44	2.68	2.89	2.78	2.90	3.14
	2.65			2.92			2.31			3.15	
	2.73			2.33			2.87			3.38	
2.60	2.64	2.75	2.78	2.92	2.96	2.42	2.01	2.41	3.14	3.47	3.34
	2.72			3.22			1.67			2.42	
	2.66			2.78			1.75			2.52	
2.18	2.17	2.16	2.08	2.06	2.05	2.22	2.35	2.54	2.72	2.73	2.75
Right											
1.88	1.92	2.31	2.64	2.34			3.44	3.41	3.45	3.27	3.42
	2.18		2.25					2.85		3.22	
	2.34		2.65					3.18		3.34	
2.31	2.45	2.54	2.59	2.56			2.74	2.96	3.17	3.25	3.32
	2.53		2.78					2.13		2.74	
2.77	2.79	2.68	2.32	3.02			1.52	2.11	2.25	2.34	2.48
	2.87		2.56					1.75		2.03	
	3.08		2.53					1.85		2.23	
3.28	3.08	3.36	3.28	2.94			2.35	23.23	2.21	2.38	2.45
	3.12		3.18					1.74		2.35	
	2.82		2.60					1.23		2.32	
2.56	2.47	2.22	2.13	2.08			3.34	3.34	3.39	3.37	3.30

Table 1: Oxygen isotopic results for each subsample. Table is configured to correspond to sampling pattern in Figure 4

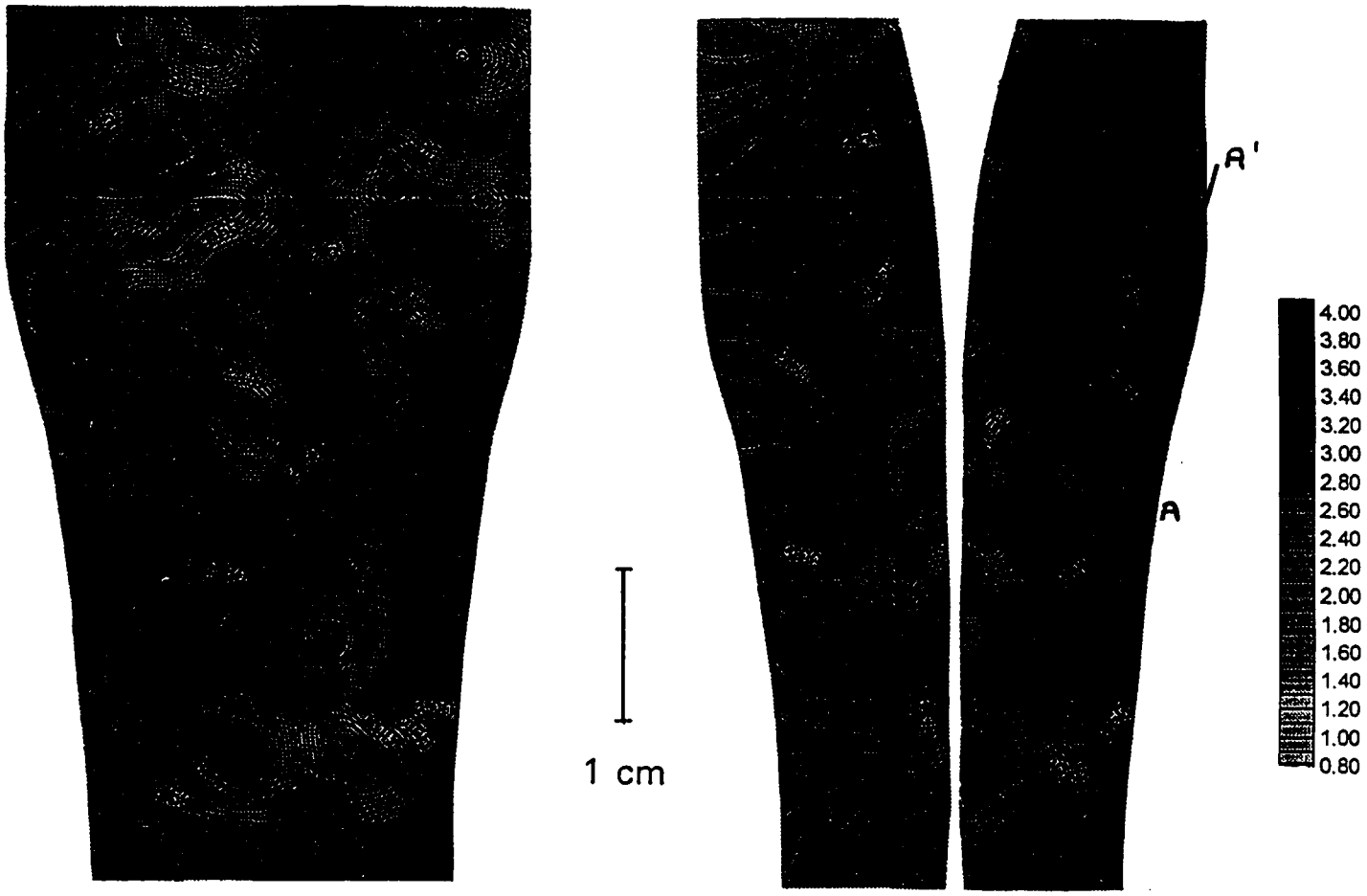

Figure 5: Isotopic contour map of coral surfaces based on analyses of subsamples removed as shown in Figure 2. Left: exterior surface. Right: interior surface. Contour interval is 0.1‰. Although this specimen grew at a constant temperature of approximately 2.5°C, its isotopic values have a range of almost 3‰, varying widely from the equilibrium value of about 4.2‰, with no discernable pattern in their distribution. The equilibrium value is approached at points marked with X's.

4.5 Discussion

This study shows that, even for a deep-sea coral growing at a constant seawater temperature, there is not a unique oxygen isotope value for the skeleton. The $\delta^{18}O$ values varied widely (by about 3‰) and departed by as much as 3.25‰ from aragonite-seawater equilibrium for the conditions of deposition. If the $\delta^{18}O$ values were interpreted as equilibrium data, they would appear to correspond to a temperature range of approximately 12°C. We did not observe that the isotope vaues approached to aragonite-seawater isotopic equilibrium traversing from the base of the coral to the top edge, as reported by Emiliani et al. (1978). We also did not duplicate the results of Adkins and Boyle (1995) who found the thin septal edges to be closest to equilibrium. This may be just an artifact of scale: Adkins and Boyle (1995) sampled a small area of the coral, but did so very intensively. They may have uncovered a significant systematic change in isotopic values missed by our more widely-spaced subsampling.

On the contour maps, regions approaching aragonite-seawater equilibrium are the mostly darkly shaded: they generally appear as isotopic 'hills', with values falling on all sides around them. Visual, petrographic and scanning electron investigation of the area showed no changes in texture, structure or colour (Figure 6). While some portions of the various coral surfaces do approach isotopic equilibrium, there seems no way to identify these *a priori* .

Note, however, that some areas on the coral skeleton that could produce a series of $\delta^{18}O$ values which appear to vary unidirectionally along a transect (e.g., A to A' on Figure 5), however, a second transect, taken a few millimetres away, would give a different trend. This is probably why Emiliani et al. (1978) found a systematic change in the oxygen isotope values along their transect when there was unlikely to have been a significant variation present.

It would be useful if azooxanthellate corals could be employed as tools for the reconstruction of ambient temperature fluctuations during their lifetime. These corals do have growth banding: although the lamellae are confusing and poorly developed, it is possible to identify regions of sequential growth (Lazier *et al.*, in manuscript). The finding that $\delta^{18}O$ values vary so widely on coeval surfaces and that there are no readily-identifiable areas of equilibrum deposition, however, renders the prospect of time series analyses doubtful on any surface.

Although the oxygen isotope values for the surfaces of this coral vary by as much as 3‰ plots of $\delta^{13}C$ vs. $\delta^{18}O$ reveal a strong linear correlation (Figure 7). This phenomenon has been noted several times previously for azooxanthellate corals. Figure 7 shows very little scatter of points and a regression line with an r^2 value of 0.94. This further suggests that all samples analyzed were deposited at the same temperature, as linear arrays of isotopic analyses from corals growing at different temperatures are positioned differently in($\delta^{13}C$, $\delta^{18}O$) space (Smith *et al.*, in revision).

Figure 6: SEM photograph of a portion of coral surface containing an 'isotopic hill', i.e., a region closely approaching equilibrium. There are no visual changes in texture, colour or morphology to readily indicate this phenemenon.

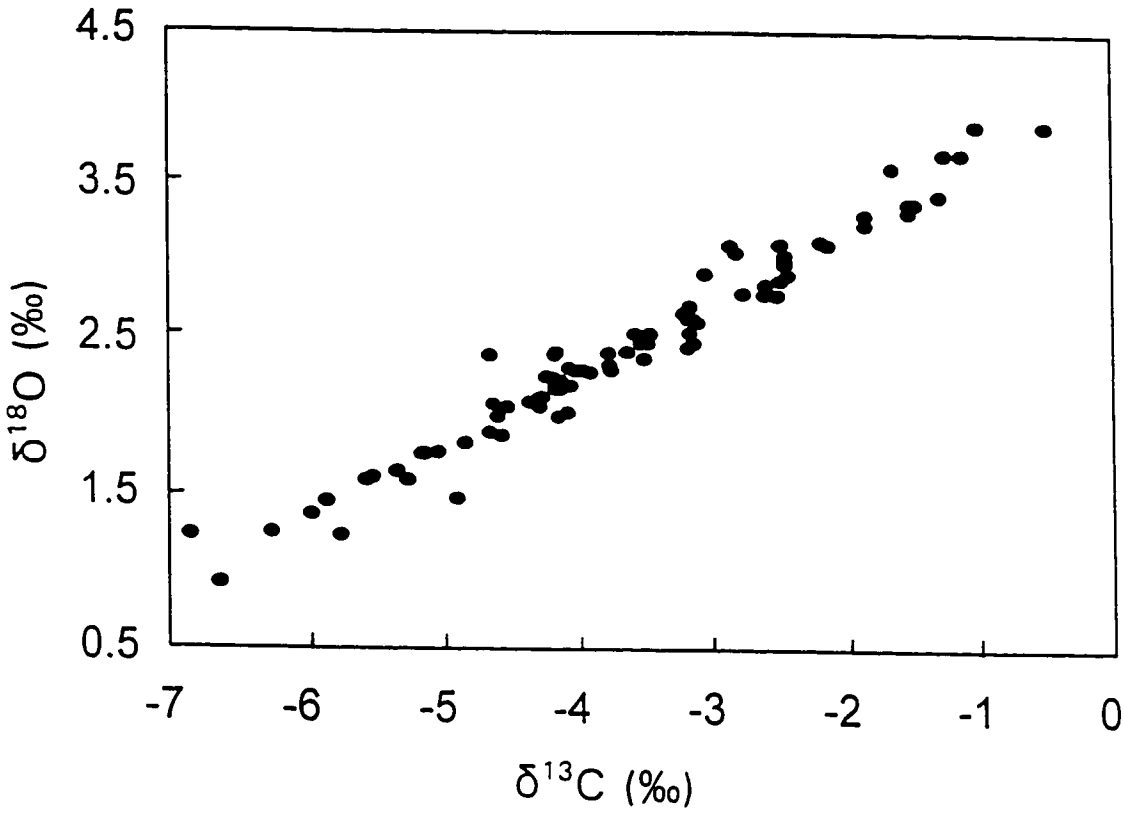

Figure 7: $\delta^{13}C$ vs $\delta^{18}O$ for contoured coral. Although the isotopic values each span several per mil, the data nonetheless display a strong linear correlation.

4.6 Conclusions

Oxygen isotope ratios of multiple samples from all interior and exterior coeval surfaces of an azooxanthellate coral show that the $\delta^{18}O$ values vary by almost 3‰ and differ by up to 3.5‰ from the calculated oxygen isotope aragonite-seawater equilbrium point. Contour maps show that the extent of disequilibrium does not vary in any systematic, significant manner on the coral skeleton. Portions of the skeleton which do approach oxygen isotope equilibrium cannot readily be identified beforehand. If oxygen isotope data from a coeval surface cannot give an estimate of the temperature of depositon, it will be difficult to develop a sampling strategy whereby environmental reconstruction over the course of the coral's life can be made.

4.7 Acknowledgements

We thank the Atlantic Geoscience Centre (Geological Survey of Canada) for donating the coral, and Martin Knyf and Ines Guerraro for helping with laboratory analyses. Stephen Cairns and Helmut Zibrowius provided useful information. This study was funded by a Natural Sciences and Engineering Research Council (NSERC) collaborative grant to HPS, MJR and NBK and NSERC graduate student support to JES.

4.8 References

Adkins, J.F. and Boyle, E.A. (1995) An investigation of the behavior of stable isotopes and metals in the skeletons of deep-sea corals. *Proceedings of the*

International Conference of Paleoceanography - V, Halifax, p. 27 (abstract).

Barnes, D.J. 1972: The structure and formation of growth-ridges in scleractinian coral skeletons. *Proceedings of the Royal Society of London, B series* 182, 331-350.

Carriquiry, J.D., Risk, M.J. and Schwarcz, H.P. (1988) Timing and temperature record from stable isotopes of the 1982-1983 El Niño warming event in eastern Pacific corals. Palaios 3: pp. 359-364.

Cheng, W., Adkins, J.F. and Boyle, E.A. (1995) ^{230}Th dating of deep-sea solitary corals. AGU Abstracts with Programs. Fall meeting, San Francisco, p. F292.

Druffel, E.R.M., King, L.L., Belastock, R.A. and Duesseler, K.O. (1990) Growth rate of a deep-sea coral using Pb-210 and other isotopes. *Geochimica et Cosmochimica Acta* **54**, pp.1492-1500.

Emiliani, C., Hudson, J.H., Shinn, E.A. and George, R.Y. (1978) Oxygen and carbon isotopic growth records in a reef coral from Florida Keys and a deep-sea coral from Blake Plateau. *Science* **202**, pp. 627-629.

Grossman, E.L. and Ku, T-L. (1986) Oxygen and carbon isotope fractionation in biogenic aragonite: temperature effects. *Chemical Geology (Isotope Geoscience Section)* **59**, pp. 59-74.

Lazier, A.V., Smith, J.E. , Risk, M.J. and Schwarcz, H.P. (in manuscript) The skeletal structure of Desmophyllum cristagalli: the use of deep-water corals in

sclerochronology. for submission to Lethaia

McConnaughey, T.A. (1989) ^{13}C and ^{18}O isotopic disequilibrium in biological carbonates: 1. Patterns. *Geochimica et Cosmochimica Acta* **53**, pp. 151-162.

McCrea, J.M. (1950) On the isotope chemistry of carbonates and a paleotemperature scale. *Journal of Chemical Physics* **18**: 849-857.

Mikkelson,N., Erlenkeuser, H., Killingley, J.S. and Berger, W.S. (1982) Norwegian corals: radiocarbon and stable isotopes in *Lophelia pertusa*. *Boreas* **11**, pp. 163-171.

Shackleton, N.J. (1967) Oxygen isotope analyses and Pleistocene temperatures reassessed. *Nature* **215**, pp. 15-17.

Smith, J.E.; Risk, M.J.; Schwarcz, H.P., McConnaughey, T.A. and Keller, N.B. (in revision) Deep-sea corals as paleotemperature indicators: Overcoming 'vital effects'. *Geochimica et Cosmochimica Acta.*

Stanley, G.D. and Cairns, S.D. (1988) Constructional azooxanthellate coral communities: An overview with implications for the fossil record. *Palaios* **3**: pp. 233-242.

CHAPTER 5

Paleotemperatures from deep-sea corals: overcoming 'vital effects'

5.1 Abstract

Thirty-five azooxanthellate (non-photosynthetic) corals belonging to 18 species were collected at sites ranging from the Norwegian Sea to the Antarctic and of depths ranging from 10 to 5220 m. All specimens showed distinct, well-defined linear correlations between carbonate oxygen and carbon isotopic composition, with slopes ranging from 0.23 to 0.67 (mean 0.45 ± 0.9) and linear correlation r^2 values which averaged 0.89. These pronounced isotopic disequilibria have, to date, rendered azooxanthellate corals unsuitable for use in paleothermometry. Most, but not all, of the heaviest skeletal $\delta^{18}O$ values reached or approached equilibrium. If the isotopically-heavy ends of the $\delta^{18}O$ vs $\delta^{13}C$ regression lines reliably approximated isotopic equilibrium with seawater, these values could be used to estimate the temperature of the water in which the coral grew. The $\delta^{13}C$ values of the heavy ends of each line, however, were always depleted compared to carbon isotopic equilibrium with ambient bicarbonate by varying amounts.

Despite the disequilibria, a reliable method for obtaining paleotemperature data was obtained. It was found that, if a $\delta^{18}O$ vs $\delta^{13}C$ regression line from an individual coral could be generated, the $\delta^{18}O_{arag}$ value corresponding to $\delta^{13}C_{arag} = \delta^{13}C_{water}$ and corrected for $\delta^{18}O_{water}$ was a linear function of temperature: $\delta^{18}O = -0.25\ T(°C) + 4.97$.

5.2 Introduction

Oxygen isotopic analyses of foraminiferal and coral carbonates provide much of the available evidence concerning past oceanographic conditions. Temperature affects the partitioning of oxygen isotopes between seawater and precipitating carbonates (McCrea, 1950), while growth and decay of continental ice sheets affects the oxygen isotopic composition of seawater and hence, of skeletal material (Shackleton, 1967). Carbonate from foraminifera has been a useful source of isotopic data. Forams are, however, difficult to date accurately beyond the range of ^{14}C and bioturbation of the bottom sediments often limits age resolution (CLIMAP, 1984). Carbonates from reef corals have also been extensively used for paleoceanographic reconstructions which may be several centuries long (e.g., Carriquiry *et al.*, 1988; Hudson *et al.*, 1976). Because of their algal symbionts (zooxanthellae), however, reef corals can only live in shallow tropical waters, thereby biasing the record toward equatorial processes. Azooxanthellate corals (Figure 1) have the potential to reflect global conditions, as they have widespread distribution from polar to equatorial waters. Although they are often called 'deep-sea' corals, they extend from abyssal waters (>6,000 m) to the surface and sometimes intermingle with true reef corals (Stanley and Cairns, 1988). Deep-sea corals are also suitable for ^{230}Th / ^{234}U dating (e.g., Edwards *et al.*, 1987), and may have more-or-less continuous skeletal deposition over periods of decades to centuries (Lazier *et al.*, in manuscript).

Previous attempts to use stable isotopes in deep-sea corals as tools for paleoceanographic reconstructions have been unsuccessful because, like other corals, deep-sea corals do not precipitate in isotopic equilibrium with seawater, and the extent of the disequilibrium varies widely within a particular individual.

Emiliani *et al.* (1978) performed isotopic analyses on *Bathypsammia tintinnabulum* from 850 m depth on the Blake Plateau, and found that individual corals, growing in almost-constant water temperatures, displayed $\delta^{18}O$ and $\delta^{13}C$ values which varied by several per mil. Emiliani *et al.* (1978) reported a strong linear correlation between $\delta^{18}O$ and $\delta^{13}C$.

Mikkelson *et al.* (1982) analysed samples along the presumed growth axis of a portion of a *Lophelia pertusa* colony from a Norwegian fjord and compared the $\delta^{18}O$ values with mean monthly seawater temperatures. They concluded that the temperature and salinity range in the area could not explain the excessive variation in the oxygen and carbon isotope values, which they attributed to "vital effects", i.e., biogenic fractionation. They also reported a significant linear correlation between $\delta^{18}O$ and $\delta^{13}C$ in all of their specimens

McConnaughey (1989) examined both azooxanthellate and reef corals from the Galapagos Islands, and found that a single subsample taken from an azooxanthellate coral could have an isotopic composition several per mil different, both in $\delta^{18}O$ and in $\delta^{13}C$, from a second subsample a few millimetres away. This enormous degree of biological fractionation appeared to overwhelm any environmental signal preserved within the coral. He found that skeletal isotope ratios showed a strong positive correlation and tended to fall along lines in ($\delta^{13}C$, $\delta^{18}O$) space extending roughly between equilibrium and a point 10-15‰ depleted in ^{13}C, 4‰ depleted in ^{18}O.

These observations by McConnaughey (1989) raise the possibility that multiple data points from single corals, plotted as $\delta^{13}C$ vs $\delta^{18}O$, could be used to estimate the seawater-aragonite isotopic equilibria. This would, in turn, provide an estimate of the temperature at the site where the coral had grown. Using a unique collection of azooxanthellate corals, we demonstrate how, despite considerable isotopic disequilibria, deep-sea corals can be used as monitors of

past oceanographic conditions.

5.3 Methods and Materials

We gathered isotopic data from 35 individual azooxanthellate corals, representing 18 different species (Table 1). Specimens 1 to 20 were collected by Russian oceanographic research vessels between 1955 and 1982 in a variety of locations, including the Aleutian trench, The Sierra Leone Rise and Antarctic shores, from depths of 80-5220 m and temperatures from 1 to 15°C. Corals were retrieved using Sigsbee trawls, beam trawls or geological dredges and archived by one of us (NBK). Specimens 21 to 23 were collected in 1984 by the deep-sea submersible Alvin, of the Woods Hole Oceanographic Institute, investigating deep-water canyons off the American northeast coast. Depths varied from 905 to 1984 m, and temperatures from 3.5 to 6°C. Specimen 24 was collected from the Celebes Sea in 1996 by JES and MJR, using SCUBA. The coral was retrieved from 10 m depth in 28°C water. Specimen 25, obtained from the Canadian Museum of Nature, had been collected by dredge during a scientific cruise to Iceland in 1971. The coral came from 8°C water at 128 m depth. Specimens 26-29, also from the Canadian Museum of Nature, were dredged during an investigation of the Mid-Atlantic Ridge and Nova Scotian shelf, from depths of 549 to 1200 m and 5.5 to 8.5°C temperatures. Specimens 30 and 31 were retrieved in 1995 by the deep-sea submersible Johnson Sea Link (Harbor Branch Oceanographic Institute) near Bahamas (253 and 295 m; 18-20°C). Specimen 32 grew in the Norwegian Sea at 270 m depth and 7.2°C. It was recently collected by R/V Victor Hensen (Alfred Wegner Institute of Bremerhaven) with the aid of an echosounder. All specimens in Table 1 were alive when collected and subsequently air dried.

Equilibrium $CaCO_3$-H_2O fractionation factors for oxygen isotopes were estimated as:

$$(\delta_a - \delta_w) = -0.23\ T\ (°C) + 4.75 \quad [1]$$

where δ_a and δ_w are $\delta^{18}O$ value of aragonite and seawater with respect to PDB. (Grossman and Ku, 1986). Average annual ambient temperatures were either measured *in situ*, or were retrieved from the literature (Levitus and Boyer, 1994). The $\delta^{18}O$ values for the seawater were estimated from salinity data which were retrieved from the literature (Levitus *et al.*, 1994), using generalized δ-S relations reported by Craig and Gordon (1965) for the appropriate water mass. Where necessary, data given with respect to SMOW were converted to the PDB scale (Craig, 1965). Equilibrium carbon isotope fractionations for each coral were estimated using the equation of Romanek *et al.* (1992) for ^{13}C:

$$\varepsilon^{13}C(\text{aragonite-}HCO_3^-) = +2.7 \quad [2]$$

This equation was derived using data for synthetic aragonite, but is believed to be generally applicable to biogenic aragonite. The $\delta^{13}C$ of local seawater HCO_3^- was estimated from depth profiles of $\delta^{13}C$ reported by Kroopnick (1985).

In an attempt to capture the entire range of $\delta^{18}O$ and $\delta^{13}C$ from each specimen, 17 to 27 subsamples were removed from random locations on each coral skeleton (depending on the individual's size). Analyses were performed on a SIRA gas-source mass spectrometer using a common 100% phosphoric-acid bath at 90°C. Precision was 0.07 ‰ for $\delta^{18}O$ and 0.10‰ $\delta^{13}C$; values for $\delta^{18}O$ and $\delta^{13}C$ are reported relative to VPDB.

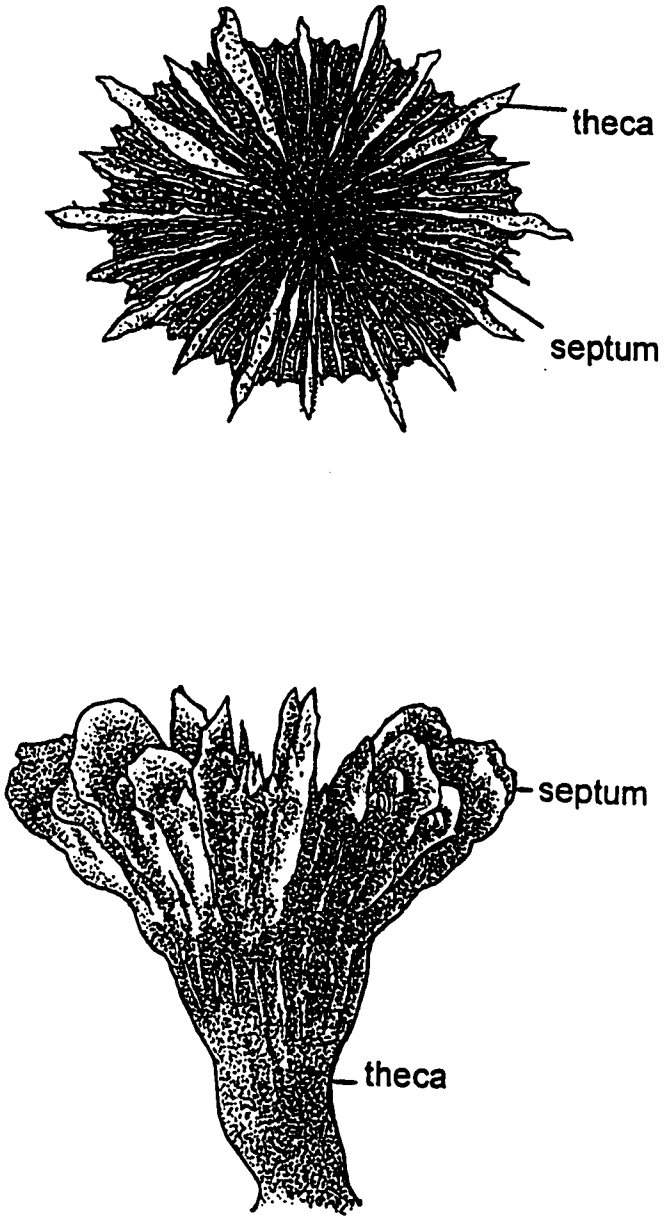

Figure 1: A typical deep-sea coral. Top: view of calice ('flower') showing septal insertion pattern from above. Bottom: side view showing pedicel ('stem') and exterior septal edges. This particular specimen is *Desmophyllum cristagalli* from Lydonia Canyon on the northeastern US coastline and is about 40 cm in length (#21 in Table 1).

Specimen			Location		Depth	Temp.	$\delta^{13}C$	$\delta^{18}O$
Number	Species	Place	Latitude	Longitude	(m)	(°C)	PDB	PDB
1	*Caryophyllia aleutica*	Aleutian trench	45°26'N	154°12'E	1680	2	-0.60	-0.27
2	*Fungiacyathus aleuticus*	Aleutian trench	45°26'N	154°12'E	5220	1.25	0.20	-0.27
3a	*Lophelia pertusa*	Great Meteor Bank	30°N	28.5°W	960	8	0.80	0.01
3b	*Desmophyllum cristagalli*	Great Meteor Bank	30°N	28.5°W	960	8	0.80	0.01
4a	*Deltocyathus moseleyi*	Great Meteor Bank	30°N	28.5°W	510	12.5	0.90	0.28
4b	*Flabellum chunii*	Great Meteor Bank	30°N	28.5°W	510	12.5	0.90	0.28
5	*Caryophyllia calvery*	Great Meteor Bank	30°N	28.5°W	310	15	1.00	0.66
6	*Desmophyllum cristagalli*	Tirrenian Sea	40°53'N	10°26'E	815	11	0.50	0.66
7	*Desmophyllum cristagalli*	Tirrenian Sea	40°52'N	10°25'E	700	11	0.50	0.66
8	*Desmophyllum cristagalli*	Tirrenian Sea	40°51'N	10°24'E	635	11	0.50	0.66
9	*Flabellum alabastrum*	Sierra Leone Rise	6°55'N	21°52'W	1170	4.5	0.60	0.01
10	*Gardineria antarctica*	Antarctic shores	66°26'S	59°16E	410	1	0.50	-0.59
11	*Flabellum impensum*	Antarctic shores	65°59'S	57°08'E	265	1	0.60	-0.59
12	*Flabellum apertum*	Southwest Atlantic	35°44'S	22°33'E	1400	3	0.40	0.01
13	*Gardineria antarctica*	Antarctic shores	64°03'S	98°33'E	525	1	0.50	-0.59
14	*Gardineria antarctica*	Antarctic shores	67°21'S	179°53'E	500-900	1.75	0.6-0.9	-0.59
15	*Flabellum thouarsii*	Argentinian shores	42°33'S	60°58'W	80	8	1.50	0.37
16	*Flabellum thouarsii*	Falkland Islands	52°40'S	56°08'W	1660	2.5	0.40	0.01
17a	*Balanophyllia malouinensis*	Falkland Islands	52°08'S	57°16'W	720	3	0.50	0.28
17b	*Flabellum thouarsii*	Falkland Islands	52°08'S	57°16'W	720	3	0.50	0.28
18	*Caryophyllia ambrosia*	Reykjanes Ridge	58°45'N	27°13'W	2190	3.5	1.10	0.01
19	*Caryophyllia calvery*	Reykjanes Ridge	58°23'N	31°47'W	1700	3.5	1.10	0.01
20	*Desmophyllum cristagalli*	Reykjanes Ridge	35°07'N	12°51'W?	1000	8	1.10	0.01
21	*Desmophyllum cristagalli*	Lydonia Canyon	40°21'N	67°39'W	905	6	0.80	0.01
22	*Desmophyllum cristagalli*	Lydonia Canyon	40°11'N	67°38'W	1984	3.5	1.00	0.01
23	*Desmophyllum cristagalli*	Baltimore Canyon	38°05'N	73°47'W	1024	5.5	0.80	0.01
24	*Dendrophyllia sp.*	Manado, Indonesia	2°32'N	124°58'E	10	28	1.50	0.09
25	*Solenosmilia variabilis*	Iceland shelf	60°58'N	29°15'W	128	8	1.50	0.47
26	*Desmophyllum cristagalli*	Mid-Atlantic Ridge	45°N	29°W	800	8.5	0.90	0.28
27	*Desmophyllum cristagalli*	Mid-Atlantic Ridge	45°N	29°W	900	7.5	0.90	0.28
28	*Desmophyllum cristagalli*	Mid-Atlantic Ridge	45°N	29°W	1200	5.5	0.90	0.01
29	*Desmophyllum cristagalli*	Nova Scotia shelf	43°58'N	58°59'W	549	7	1.10	0.28
30	*Desmophyllum cristagalli*	Bahamas	26°28'N	78°42'W	253	18	1.00	0.66
31	*Desmophyllum cristagalli*	Bahamas	25°07'N	77°16'W	295	20	1.00	0.66
32	*Lophelia pertusa*	Sula Ridge	64°05'N	8°03'E	270	7.2	1.10	0.47

Table 1: List of coral specimen used for isotopic analyses with environmental information

5.4 Results

Results from all corals are presented in Table 2. Typical plots of $\delta^{13}C$ vs $\delta^{18}O$ are shown in Figure 2 from six of the corals, representing three different species, which grew at different temperatures and in different parts of the world. The $\delta^{18}O$ and $\delta^{13}C$ values for each coral show a strong positive correlation, which passes close to the equilibrium point for that individual. Since the equilibrium $\delta^{18}O$ value decreases with increasing temperature, each regression line is offset vertically from the others. Most subsamples from the six corals, and all of the other specimens in the collection, show $\delta^{18}O$ and $\delta^{13}C$ values which are depleted in the heavy isotope with respect to the equilibrium between aragonite and seawater. McConnaughey (1989) attributed this systematic depletion in azooxanthellate corals as the superposition of kinetic and metabolic isotope effects. Slower CO_2 hydration and hydroxylation reactions by molecules bearing the heavy isotopes ^{18}O and ^{13}C are believed to cause kinetic effects. Skeletal incorporation of ^{13}C-depieted respired CO_2 causes the metabolic effects. On most specimens, the heaviest oxygen isotopic ratios reach or nearly reach oxygen equilibrium; some are significantly depleted, however, by up to 3‰. The heaviest carbon-isotope values were always depleted with respect to equilibrium; some approached equilibrium (as close as 0.5‰), but others were depleted by as much as 11.4‰.

Table 2: $\delta^{18}O$ and $\delta^{13}C$ values for each of the deep-sea corals

Specimen 1		Specimen 2		Specimen 3a		Specimen 3b		Specimen 4a		Specimen 4b		Specimen 5		Specimen 6		Specimen 7	
$\delta^{13}C$	$\delta^{18}O$	$\delta^{13}C$	$\delta^{18}O$	$\delta^{13}C$	$\delta^{18}O$	$\delta^{13}C$	$\delta^{18}O$	$\delta^{13}C$	$\delta^{18}O$	$\delta^{13}C$	$\delta^{18}O$	$\delta^{13}C$	$\delta^{18}O$	$\delta^{13}C$	$\delta^{18}O$	$\delta^{13}C$	$\delta^{18}O$
-11.02	-0.44	-3.60	2.94	0.27	2.51	0.71	2.31	2.12	2.70	-0.48	1.66	-0.94	0.86	-5.23	-0.12	-3.90	0.12
-10.93	-0.15	-2.33	3.41	2.24	3.36	0.19	2.38	1.88	2.68	-0.72	1.12	-2.10	0.19	-2.96	1.09	-2.18	0.97
-9.69	0.40	-3.04	3.02	2.26	3.37	1.39	2.65	1.63	2.61	-2.18	0.59	-2.15	0.51	-3.50	0.81	0.25	1.93
-8.04	1.05	-3.55	2.96	2.52	3.47	1.39	3.05	1.12	2.16	-1.54	0.84	-3.47	-0.55	-1.76	1.64	-1.61	1.06
-8.00	1.12	-3.09	3.06	2.26	3.27	-1.79	1.56	1.12	2.21	-2.65	-0.13	-3.35	-0.28	-3.24	1.06	-5.87	-1.56
-8.30	0.98	-3.23	3.07	2.36	3.52	-2.35	1.79	1.30	2.33	-2.06	0.37	-1.65	0.30	-5.92	-0.88	-5.27	0.77
-8.88	0.91	-3.38	3.00	1.16	2.87	-0.69	2.34	1.59	2.45	-2.33	0.41	-0.90	0.71	-3.93	0.10	-1.45	1.49
-4.57	2.50	-2.60	3.35	1.67	3.03	0.82	3.17	1.60	2.48	0.44	2.19	-0.07	1.30	-2.67	1.06	-1.08	1.78
-9.30	0.55	-2.88	3.16	1.53	2.88	-2.36	1.62	1.88	2.58	0.36	2.21	1.68	1.97	-2.30	1.12	-4.25	0.14
-9.19	0.61	-3.20	3.02	2.06	3.08	-0.85	2.31	1.78	2.65	-2.53	-0.05	0.89	2.06	-4.58	-0.09	-4.88	1.03
-7.81	1.17	-2.69	3.22	1.29	2.66	1.65	2.95	1.78	2.57	-1.25	0.82	-1.91	0.39	-6.31	-0.90	-3.47	0.75
-7.75	1.13	-2.40	3.31	2.52	3.44	0.95	2.63	2.01	2.70	0.21	1.75	-2.01	-0.18	-4.34	0.19	-1.64	1.45
-7.51	1.24	-2.43	3.39	1.51	2.98	-1.50	1.82	1.95	2.66	-0.66	1.52	-3.70	-1.05	-3.72	0.46	0.45	2.66
-9.06	0.73	-3.44	2.91	2.00	3.33	-0.18	2.54	1.23	2.24	-0.80	1.20	-3.30	-0.61	-4.25	0.23	-1.15	2.34
-10.24	0.29	-2.90	3.09	2.20	3.22	0.39	2.72	1.18	2.34	-2.22	0.35	-4.24	-0.85	-3.14	0.77	-2.35	1.16
-7.25	1.50	-2.49	3.35	0.75	2.81	-1.00	1.82	1.90	2.73	-1.42	1.03	0.55	1.67	-4.57	0.28	-3.65	0.59
-6.51	1.50	-2.53	3.25	1.75	3.00	1.00	2.88	1.99	2.72	-0.15	1.59	1.12	1.97	-2.84	0.89	-1.96	1.33
		-3.37	2.95			1.38	2.83	1.35	2.39							-3.65	0.59
								1.40	2.30							-0.35	2.04
								2.05	2.69							-5.23	-0.11

Specimen 8		Specimen 9		Specimen 10		Specimen 11		Specimen 12		Specimen 13		Specimen 14		Specimen 15		Specimen 16	
$\delta^{13}C$	$\delta^{18}O$	$\delta^{13}C$	$\delta^{18}O$	$\delta^{13}C$	$\delta^{18}O$	$\delta^{13}C$	$\delta^{18}O$	$\delta^{13}C$	$\delta^{18}O$	$\delta^{13}C$	$\delta^{18}O$	$\delta^{13}C$	$\delta^{18}O$	$\delta^{13}C$	$\delta^{18}O$	$\delta^{13}C$	$\delta^{18}O$
-2.49	1.12	-1.84	2.72	-3.12	3.39	-3.38	2.63	-6.50	1.40	-4.81	1.66	-1.63	3.24	-4.97	-0.44	-4.26	1.70
-1.39	1.64	-1.80	2.87	-2.54	3.64	-4.67	1.97	-7.56	0.92	-4.63	2.08	-3.69	2.52	-4.98	-0.67	-4.28	1.69
-0.15	2.61	-1.59	2.80	-1.66	3.98	-2.45	2.94	-8.02	0.63	-2.40	3.23	-2.10	2.93	-4.65	0.27	-5.02	1.32
-0.39	2.05	-1.00	3.13	-1.68	3.96	-5.07	1.85	-6.29	1.64	-3.33	2.83	-4.76	2.07	-4.74	-0.27	-4.31	1.78
-1.14	1.63	-1.21	3.07	-2.40	3.51	-4.27	2.29	-6.96	1.44	-1.02	3.57	-4.93	1.86	-4.76	-0.45	-5.74	1.14
-0.89	1.31	-1.42	2.95	-3.10	3.31	-3.73	2.65	-6.63	1.71	-5.03	1.61	-4.93	2.07	-4.96	-0.53	-5.41	1.07
-0.63	2.07	-1.79	2.94	-4.05	3.03	-4.93	2.16	-7.60	1.26	-3.52	2.36	-6.92	1.14	-4.89	-0.44	-3.78	1.67
-1.53	1.94	-2.10	2.67	-7.91	1.28	-3.36	2.81	-5.22	1.86	-2.59	2.92	-7.17	0.95	-3.29	0.71	-2.84	2.48
-1.84	1.87	-2.22	2.62	-9.15	0.87	-1.09	3.45	-6.46	1.43	-5.91	1.20	-4.42	2.31	-2.13	1.35	-3.78	1.82
-2.32	1.31	-2.39	2.59	-6.66	1.82	-2.50	3.42	-8.75	0.22	-5.63	1.51	-6.15	1.82	-1.31	1.68	-3.80	1.99
-1.62	1.61	-3.25	2.19	-2.39	3.69	-1.90	3.68	-9.44	0.21	-5.16	1.67	-6.01	1.94	-1.35	1.78	-3.27	2.20
-2.21	1.36	-3.17	2.00	-1.47	3.87	-2.93	3.33	-8.20	0.83	-6.79	0.57	-6.79	1.42	-3.28	0.57	-4.63	1.53
-1.65	1.62	-2.89	2.28	-2.06	3.68	-2.37	3.20	-5.33	2.03	-7.87	0.41	-5.87	1.31	-4.02	0.29	-5.26	1.33
-0.64	2.02	-3.02	2.22	-0.87	4.14	-3.53	2.72	-5.96	1.69	-7.47	0.78	-5.24	1.43	-3.86	0.28	-4.65	1.61
-0.56	2.06	-2.96	2.27	-0.70	4.04	-2.01	3.38	-7.24	1.16	-5.53	1.76	-3.45	2.33	-3.66	0.28	-3.52	2.04
-0.85	1.92	-1.68	2.86	-3.06	3.21	-4.32	2.32	-8.21	0.72	-4.36	2.30	-5.10	1.95	-1.84	1.55	-4.03	1.80
-0.12	2.26	-1.24	3.06	-6.20	1.80	-3.25	2.79	-8.60	0.54	-2.65	2.92	-4.27	2.17	-1.68	1.50	-3.62	1.99
-0.90	1.91	-2.27	2.62	-7.50	1.23	-2.32	3.26	-6.03	1.71	-5.74	1.42	-5.13	1.67	-3.34	0.54	-4.87	1.44
-1.36	1.63			-4.28	2.63	-1.96	3.42			-4.87	1.80	-4.58	2.17	-5.58	-0.63		
				-5.54	2.45	-1.47	3.61			-6.02	1.32	-6.80	1.03	-3.81	-0.11		
				-4.76	2.48							-4.83	2.29	-4.91	-0.83		
				-2.43	3.32							-6.95	0.99	-4.25	-0.60		
				-4.82	2.69							-5.75	1.93	-4.47	-0.60		
				-1.74	3.73							-5.84	1.88	-4.83	-0.83		
				-2.71	3.34									-4.18	-0.15		
				-2.30	3.35									-4.35	-0.61		
				-2.32	3.48									-4.17	-0.06		
														-4.47	-0.29		

Specimen 17a		Specimen 17b		Specimen 18		Specimen 19		Specimen 20		Specimen 21		Specimen 22		Specimen 23		Specimen 24	
$\delta^{13}C$	$\delta^{18}O$	$\delta^{13}C$	$\delta^{18}O$	$\delta^{13}C$	$\delta^{18}O$	$\delta^{13}C$	$\delta^{18}O$	$\delta^{13}C$	$\delta^{18}O$	$\delta^{13}C$	$\delta^{18}O$	$\delta^{13}C$	$\delta^{18}O$	$\delta^{13}C$	$\delta^{18}O$	$\delta^{13}C$	$\delta^{18}O$
-4.09	1.65	-1.75	2.64	-0.86	3.17	-4.72	1.65	-1.34	2.24	0.32	3.77	-0.32	3.75	0.24	3.48	-10.44	-5.90
-5.32	1.34	-2.56	2.40	-1.13	3.03	-6.08	1.09	-1.66	2.00	-1.26	3.18	-2.32	2.72	1.02	3.80	-11.05	-5.81
-5.34	0.87	-1.51	2.90	-0.87	3.16	-6.26	0.81	-5.57	0.09	-2.36	2.70	-2.40	2.08	-2.04	2.19	-9.47	-5.27
-4.72	1.33	-1.96	2.68	-1.16	3.06	-4.50	1.57	-4.67	0.50	-0.13	3.48	-3.70	2.11	-1.02	2.73	-8.36	-4.87
-6.31	0.61	-1.42	2.95	-1.73	3.00	-6.86	0.52	-3.55	1.15	-3.85	1.91	-3.63	2.15	-4.24	1.21	-7.67	-4.63
-7.00	0.19	-1.25	2.91	0.02	3.59	-6.71	0.46	-2.75	1.55	0.70	3.95	-3.74	1.89	-2.37	2.01	-8.07	-4.80
-4.82	1.44	-2.69	2.39	0.40	3.72	-5.93	0.83	-2.85	1.40	0.49	3.95	-3.95	1.88	-3.75	1.26	-8.60	-4.80
-5.24	1.06	-2.07	2.66	-0.17	3.48	-5.08	1.31	-4.29	0.97	-0.57	3.28	-2.66	2.65	-3.62	1.43	-8.56	-4.99
-5.07	1.01	-3.00	2.00	-0.70	3.30	-5.40	1.11	-3.48	1.09	-1.24	3.09	-4.24	1.64	-0.33	3.29	-11.06	-5.95
-5.28	1.07	-3.03	2.06	-0.53	3.40	-4.87	1.51	-1.24	2.29	-2.03	2.74	-4.21	1.75	-0.99	2.64	-11.73	-6.33
-5.28	1.10	-2.07	2.47	0.33	3.79	-5.20	1.36	-2.43	1.39	-1.02	3.19	-3.63	2.15	0.16	3.29	-12.38	-6.40
-4.50	1.51	-3.26	2.05	0.22	3.67	-6.13	0.90	-3.54	1.08	1.37	3.56	-1.57	3.01	0.96	3.79	-11.60	-6.00
-3.68	1.70	-2.35	2.65	0.80	3.78	-6.51	0.70	-1.13	2.26	-3.65	2.03	-1.85	2.96	-0.25	3.13	-10.92	-5.68
-4.75	1.36	-3.00	2.33	-0.07	3.49	-5.95	1.09	-4.23	0.73	-2.31	2.52	-0.37	3.72	-2.37	2.00	-10.11	-5.34
-5.92	0.79	-2.75	2.18	0.28	3.82	-6.73	0.52	-3.22	1.47	-1.12	3.15	-0.98	3.51	-4.16	1.24	-9.54	-5.33
-4.78	1.56	-2.36	2.36	0.22	3.43	-7.11	0.38	-4.12	0.77	1.00	3.53	-1.35	3.12	-2.65	1.86	-8.98	-5.08
-6.57	0.59	-1.75	2.90	-1.04	3.06	-7.14	0.38	-3.26	1.18	-0.02	3.81	-2.70	2.53	-4.12	1.23	-8.81	-4.94
-4.59	1.65			-1.06	3.09	-7.15	0.46	-1.12	2.37	-0.37	3.40	-4.49	1.71	-3.26	1.53	-9.45	-5.28
-7.05	0.48			-3.26	2.17	-5.11	0.86	-2.30	1.73	-2.37	2.59	-2.66	2.45	-3.22	1.23	-9.84	-5.29
-4.92	1.59			-1.47	2.95	-4.54	1.78			-3.64	2.13	-1.96	2.81	-1.96	1.67	-10.49	-5.65
-5.02	1.54			-0.42	3.46	-5.74	1.35					-3.95	1.78	-1.86	2.37	-10.76	-5.80
-3.97	1.96			-0.51	3.44	-5.31	1.51					-0.98	3.31			-10.34	-6.02
-2.62	2.61			-1.79	3.00	-3.77	2.07									-10.06	-5.88
				-2.30	2.47	-4.79	1.30									-10.21	-6.40
				-1.39	3.03	-5.61	1.29									-10.32	-6.34
				-1.49	2.90	-3.37	2.17									-10.45	-5.94

Specimen 25		Specimen 26		Specimen 27		Specimen 28		Specimen 29		Specimen 30		Specimen 31		Specimen 32	
$\delta^{13}C$	$\delta^{18}O$	$\delta^{13}C$	$\delta^{18}O$	$\delta^{13}C$	$\delta^{18}O$	$\delta^{13}C$	$\delta^{18}O$	$\delta^{13}C$	$\delta^{18}O$	$\delta^{13}C$	$\delta^{18}O$	$\delta^{13}C$	$\delta^{18}O$	$\delta^{13}C$	$\delta^{18}O$
-0.80	2.89	-4.49	2.32	-3.66	1.12	-2.83	2.38	-6.31	0.59	-2.59	-0.56	-3.22	-1.77	-1.35	2.39
1.00	3.15	-4.83	2.13	-4.05	0.91	-5.77	1.51	-5.74	-0.16	-2.59	0.32	-6.01	-3.42	-1.97	2.26
-0.99	2.63	-1.12	2.15	-4.50	0.83	-4.68	1.91	-6.30	0.00	-1.71	0.10	-4.12	-2.00	-0.75	2.70
0.82	3.51	-3.43	2.68	-3.80	0.91	-3.17	2.65	-5.52	0.60	-1.12	0.22	-6.45	-3.59	-0.45	2.31
-0.51	3.09	-3.46	2.69	-3.62	1.13	-4.11	2.80	-6.32	-0.03	-2.44	-0.16	-2.24	-1.01	0.02	3.01
1.22	3.59	-3.68	2.59	-2.70	1.25	-3.19	2.14	-6.13	-0.06	-0.11	0.48	-3.18	-1.29	-0.62	2.36
-1.59	1.98	-1.28	2.62	-3.00	1.47	-3.83	1.78	-5.68	0.62	-1.80	-0.11	-5.17	-2.86	-2.95	1.38
0.46	2.87	-0.83	2.32	-1.96	2.08	-4.33	2.12	-5.91	0.60	-1.33	0.21	-4.90	-2.54	-4.65	0.72
-0.09	3.21	-2.27	2.14	-1.26	2.49	-4.15	1.82	-6.28	0.22	-1.51	-0.13	-2.37	-1.99	-5.42	0.77
-0.41	2.64	-2.16	2.12	0.11	3.16	-3.67	2.43	-6.89	-0.11	-0.72	0.31	-4.57	-2.18	-3.40	1.37
-1.75	2.07	-5.35	1.44	0.99	3.40	-3.81	2.19	-4.84	0.85	0.07	0.79	-2.37	-1.56	-3.54	1.60
-1.38	2.44	-3.75	1.74	0.56	3.52	-2.42	2.54	-4.76	1.19	0.26	0.53	-5.12	-2.98	-1.65	2.51
-0.72	2.38	-4.68	2.05	-1.09	2.44	-6.21	1.44	-4.92	1.05	1.03	1.02	-6.84	-3.76	0.25	2.57
-0.79	2.17	-4.69	2.20	1.00	3.66	-4.50	2.25	-6.65	0.31	1.64	0.97	-1.13	-0.10	0.90	2.60
0.07	2.66	-4.93	1.76	-3.17	1.57	-5.18	1.90	-0.71	2.79	0.67	0.82	-2.46	-1.08	-0.68	2.20
-0.22	2.42	-6.12	1.61	-2.94	1.66	-7.10	1.02	-1.54	2.22	-0.49	0.40	-6.15	-3.70	-1.64	1.83
-1.25	2.09	-7.36	0.67	-3.08	1.48	-6.69	1.04	-2.26	2.03	0.77	0.84	-3.03	-2.12	-2.41	1.65
0.09	2.80	-3.02	1.50	-3.81	1.26	-5.02	1.87	-0.51	2.74	0.98	0.79	-6.15	-2.79	-1.30	2.12
1.01	3.52	-7.44	1.27	-3.84	1.33	-7.20	0.99	-2.02	1.95	1.27	0.80	-6.12	-3.09	-2.81	1.72
0.52	2.94	-6.38	0.64	-3.94	1.07	-6.53	1.06	-1.24	2.19	1.21	0.84	-2.79	-1.35	-2.16	1.73
0.33	2.63	-6.56	1.37	-1.11	2.71	-3.39	1.52	-1.29	2.16	2.00	1.06	-1.79	-0.44	-1.38	2.04
0.03	2.93	-7.98	0.90	-0.53	3.30	-7.09	1.08	-3.40	1.26	1.54	1.02	-4.57	-2.32	-1.51	1.69
-0.74	2.77	-6.71	0.99	-0.77	2.60	-4.54	2.35	-2.66	1.55	1.06	0.94	-5.24	-2.94	-0.85	2.38
-1.44	2.53	-5.90	1.38			-4.82	2.48	-4.63	0.52	0.57	0.63	-0.75	-0.37	-0.73	1.99
-0.25	2.69	-6.87	1.22			-4.46	2.37	-5.75	0.18			-4.80	-2.49		
-0.70	2.65	-7.27	1.50					-4.33	0.81			-3.49	-1.67		
0.28	2.71	-7.71	1.03					-6.32	0.08						

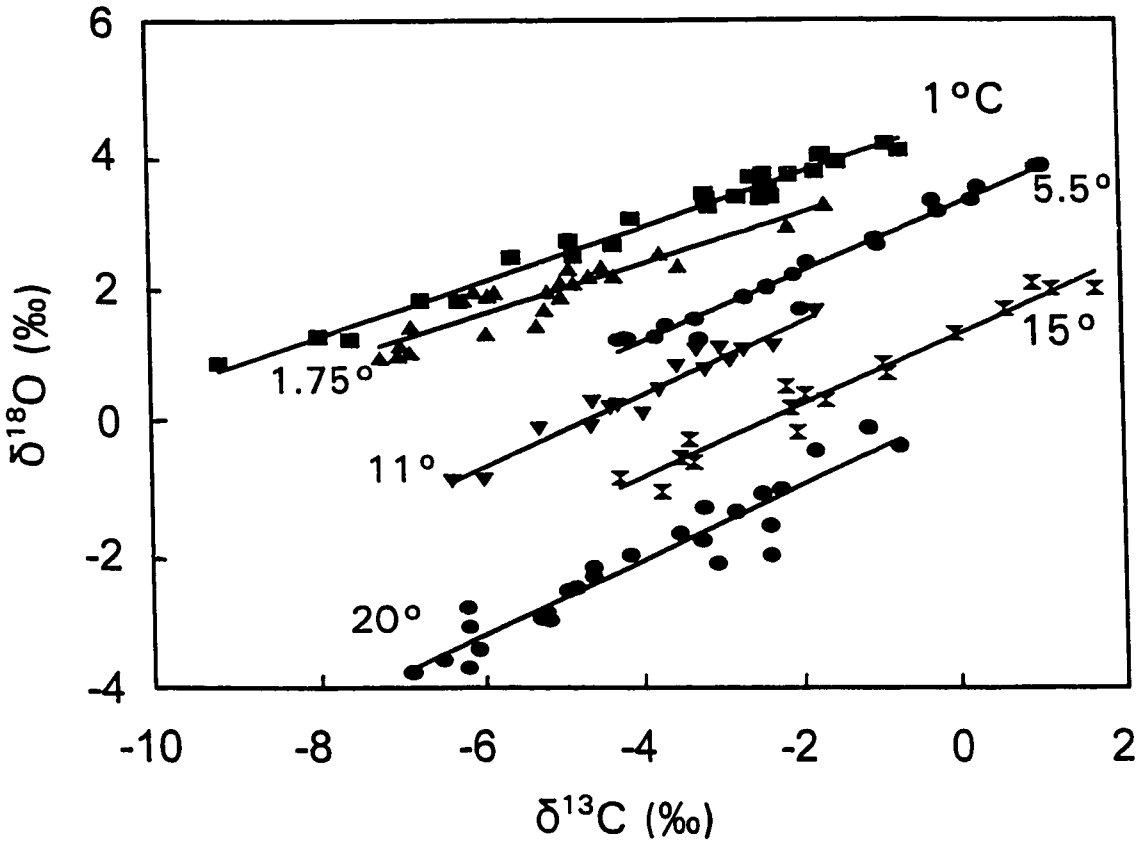

Figure 2: The $\delta^{18}O$ and $\delta^{13}C$ values for six of the coral specimens, along with the least-squares regression line for each coral's data set. Squares (■) are Specimen 10, *Gardineria antarctica*, T = 1°C; triangles (▲) are Specimen 14, *Gardineria antarctica* T = 1.75°C; upper set of circles (●) are Specimen 23, *Desmophyllum cristagalli*, T = 5.5°C; upside-down triangles (▼) are Specimen 6, *Desmophyllum cristagalli*, T = 11°C water; hourglass symbols (⧗) are Specimen 5, *Caryophyllia calvery*, T = 15°C and the lower set of circles is Specimen 31, *Desmophyllum cristagalli*, T = 20°C.

5.5 Discussion

5.5.1 Temperature / oxygen isotope relationships

Theoretically, isotopic equilibrium for the environment should lie near the isotopically heavy end of the ($\delta^{13}C$, $\delta^{18}O$) regression line (McConnaughey, 1989), so it should be possible to estimate the growth temperature. This technique was used successfully in a study of pre-Holocene azooxanthellate corals from the North Atlantic: regression lines for individual corals clearly differentiated between glacial and interglacial organisms (Smith *et al.*, 1997).

When we analyse randomly selected subsamples from an individual coral, however, it would not be clear whether the regression line would reach aragonite-seawater isotopic equilibrium. Even though 26 analyses were undertaken on Specimen 24, for example, the heaviest end of the regression line was almost 3 ‰ depleted with respect to aragonite-seawater oxygen equilibrium.

An alternative approach would be to analyse only those parts of the coral skeleton previously shown to be at or near aragonite-seawater isotopic equilibrium, such as the top portion of the calice (Emiliani *et al.*, 1978) or the septal edges (Adkins and Boyle, 1995). A recent study performed numerous systematic isotopic analyses on all exterior and interior surfaces of a specimen of *Desmophyllum cristagalli* (Smith *et al.*, in manuscript). Even though the coral grew at an almost-constant 2.5°C temperature, oxygen isotope analyses of these subsamples varied by almost 3‰ and were up to 3.25‰ depleted with respect to aragonite-seawater oxygen isotope equilibrium. Contour maps of the $\delta^{18}O$ values showed that, although portions of the skeleton approached equilibrium, the location of those areas were unpredictable and were not associated with any readily-identifiable characteristics, such as colour, texture or crystalline structure changes.

Another approach is to make use of the $\delta^{13}C$ vs $\delta^{18}O$ regression line equation for each coral. A regression analysis produces a linear equation of the form $\delta^{18}O = m\,\delta^{13}C + b$, where m is the slope and b is the $\delta^{18}O$ intercept when $\delta^{13}C = 0$. Coral skeletons are precipitated from a mixture of seawater ($\delta^{13}C \sim 0‰$) and metabolic HCO_3^- (McConnaughey et al., 1997). We measured the $\delta^{13}C$ of azooxanthellate coral tissue as -23.8‰ and assumed this was the isotopic value for respired CO_2. The mixture of these two elements gives a net $\delta^{13}C \sim 0‰$ (see Discussion, below). Thus, if $\delta^{13}C$ of aragonite is relatively independent of temperature, as suggested by Romanek *et al.*(1992), then the $\delta^{18}O_{arag} - \delta^{18}O_{water}$ value corresponding to the $\delta^{13}C$ of local seawater HCO_3^- should give a good estimate of aragonite-seawater oxygen isotopic equilibrium and hence, the temperature at which the coral grew.

Table 3 lists the regression data for each coral specimen; Figure 3 shows $\delta^{18}O_{arag} - \delta^{18}O_{water}$ values when $\delta^{13}C_{arag} = \delta^{13}C_{water}$ from the linear regressions for each of the 32 data sets, plotted against temperature. The data define a line with the equation:

$$\delta^{18}O_{arag} - \delta^{18}O_{water} = (-0.25 \pm 0.01)\,T\,(°C) + (4.97 \pm 0.24)\,‰ \quad (r^2 = 0.95,\ p < 0.01) \quad [3]$$

Thus, by obtaining sufficient subsamples from an individual coral, the ambient temperature can be calculated with a precision of a few percent. Isotopic analyses are performed on the subsamples and regression analysis done on the $\delta^{13}C$ vs $\delta^{18}O$ data. The value of $\delta^{18}O_{arag} - \delta^{18}O_{water}$ when $\delta^{13}C_{arag} = \delta^{13}C_{water}$ can be inserted into equation [3] to obtain an estimate of the temperature at which the coral grew.

The precision of the slope and intercept of equation [3] (± 0.01 and ±

0.24, respectively) were obtained by using standard statistical analyses for the precision of regression coefficients for $\alpha = 0.05$ and $n = 35$ (see, for example, Freund, 1973, p 415). Thus, for the slope, the probability is 0.95 that the interval -0.24 to -0.26 contains the true value. Likewise, there is a 95% probability that the interval 4.73 to 5.21 contains the true intercept value. Calculations of the true $\delta^{18}O$ value for a given temperature (i.e., the true mean of y for a given x) were performed using standard statistical equations for $\alpha = 0.05$ and $n = 35$ (see Freund, 1973, p 417). Temperature estimates are more precise for corals growing in cold waters: at 1.0°C, the calculated $\delta^{18}O$ value is 4.72 ± 0.09, translating into a temperature uncertainty of 0.36 at 95% confidence limits. At 28.0°C, the calculated $\delta^{18}O$ value is -2.53 ± 0.25, giving a temperature estimate of ± 1.0°C (95% confidence limits).

Note that equation [3] is almost coincident with equation [1], obtained experimentally by Grossman and Ku (1986) from analyses of foraminifera and molluscs. If we had used $\delta^{18}O$ intercepts at aragonite $\delta^{13}C$ equilibrium values, i.e., $\delta^{13}C_{water}$ + 2.7‰, the result would be a line parallel to that of Grossman and Ku (1986), but with $\delta^{18}O$ values displaced by approximately 0.9‰. The agreement of our regression line suggests our assumption that net skeletal $\delta^{13}C$ ~ 0‰ is correct, and that incorporation of isotopically-light respiratory HCO_3^- is of sufficient magnitude (approximately 3‰) to offset Romanek et al.'s (1992) isotopic enrichment. Furthermore, our data suggest that, once the confounding influence of 'vital effects' is removed from azooxanthellate corals, they can be used successfully as paleotemperature indicators or, for periods when $\delta^{18}O_{water}$ varied, as indicators of equilibrium $\delta^{18}O_{arag}$.

Often, however, the isotopic composition of the seawater is not known. Using the same 35 data sets and regression lines, the $\delta^{18}O_{arag}$ value corresponding to $\delta^{13}C_{arag} = 0$ (i.e., assuming $\delta^{13}C_{water} = 0$) and by assuming that

$\delta^{18}O_{water} = 0$, an equation similar to equation [3] was generated (Figure 4):

$$\delta^{18}O = (-0.22 \pm 0.01)\ T\ (°C) + (4.51 \pm 0.35) \quad r^2 = 0.97,\ p < 0.01 \qquad [4]$$

Using the same statistical techniques as described above, the slope of equation [4] was found to be precise to within ± 0.01 and the intercept is precise to within ± 0.35 (both at the 95% confidence level). Temperature estimates using equation [4] are somewhat less precise than with equation [3]: at 1.0°C, the calculated $\delta^{18}O$ value is 4.30 ± 0.13, translating into a temperature uncertainty of 0.52°C at 95% confidence limits. At 28.0°C, the calculated $\delta^{18}O$ value is -2.09 ± 0.28 giving a temperature estimate of ± 1.12°C (95% confidence limits). These error margins may be too large to be useful for some applications, but should be suitable for many others.

Temp (°C)	Specimen Number	No. of Observ.	Slope	Intercept	R-sqrd
1	10	27	0.41	4.50	0.98
1	11	20	0.46	4.31	0.91
1	13	20	0.49	4.22	0.97
1.25	2	18	0.38	4.27	0.93
1.75	14	24	0.38	3.84	0.87
2	1	17	0.41	4.40	0.97
2.5	16	18	0.45	3.63	0.93
3	12	18	0.45	4.41	0.94
3	17a	23	0.50	3.79	0.91
3	17b	17	0.48	3.60	0.88
3.5	18	26	0.41	3.56	0.95
3.5	19	26	0.47	3.78	0.90
3.5	22	21	0.50	3.84	0.95
4.5	9	18	0.47	3.64	0.96
5.5	23	21	0.52	3.24	0.96
5.5	28	25	0.33	3.46	0.67
6	21	20	0.44	3.64	0.94
7	29	27	0.43	2.85	0.93
7.2	32	24	0.34	2.58	0.82
7.5	27	23	0.52	3.10	0.97
8	3a	17	0.44	2.33	0.87
8	3b	18	0.34	2.43	0.83
8	15	27	0.66	2.65	0.94
8	20	19	0.49	2.85	0.97
8	25-	27	0.42	2.86	0.66
8.5	26	27	0.23	2.84	0.62
11	6	17	0.55	2.54	0.93
11	7	20	0.44	2.20	0.76
11	8	19	0.43	2.29	0.68
12.5	4a	20	0.54	1.61	0.92
12.5	4b	17	0.67	1.82	0.95
15	5	17	0.54	1.31	0.95
18	30	24	0.29	0.55	0.86
20	31	26	0.57	0.16	0.91
28	24	26	0.41	-1.49	0.78

Table 3: Regression data for each of the 35 deep-sea coral data sets

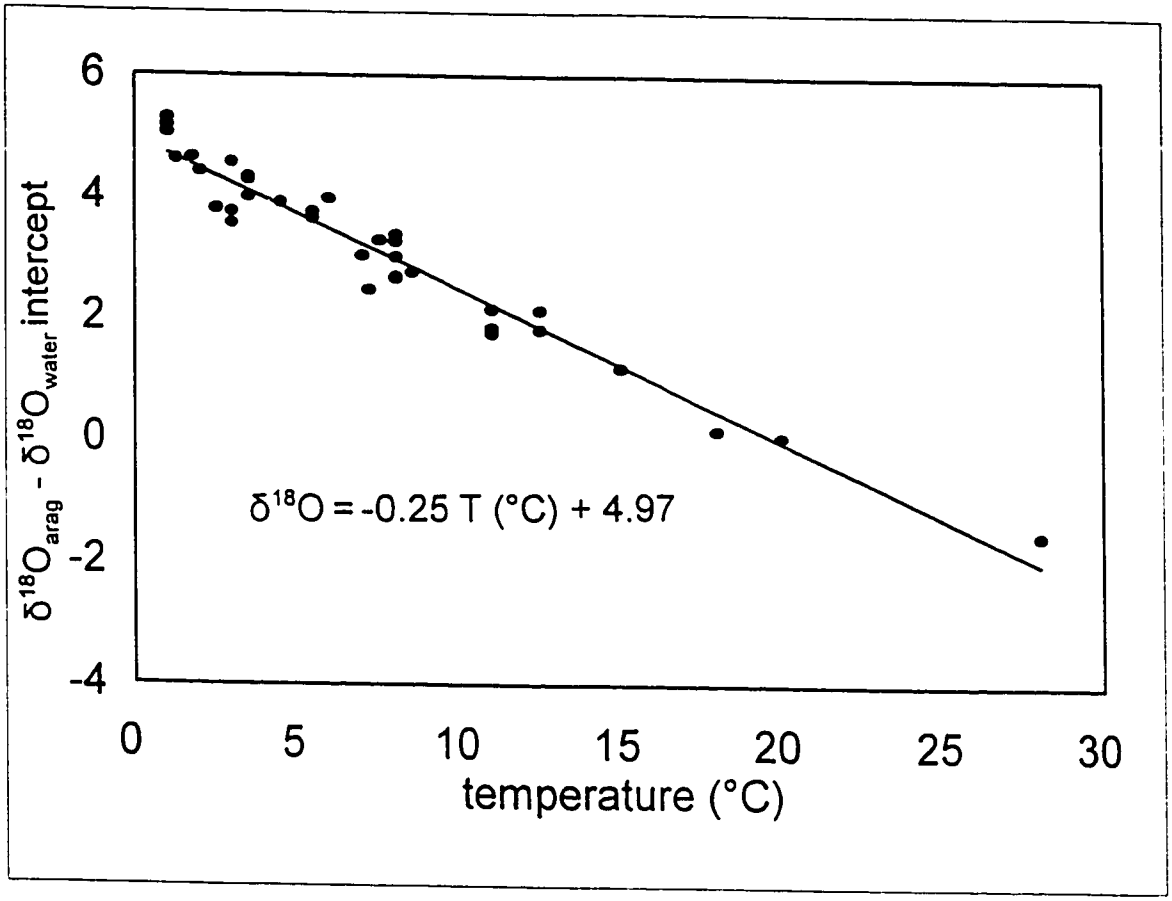

Figure 3: $\delta^{18}O_{arag} - \delta^{18}O_{water}$ when $\delta^{13}C_{arag} = \delta^{13}C_{water}$ for each regression line for each of the 35 corals. The least-squared regression line for the intercept data is included.

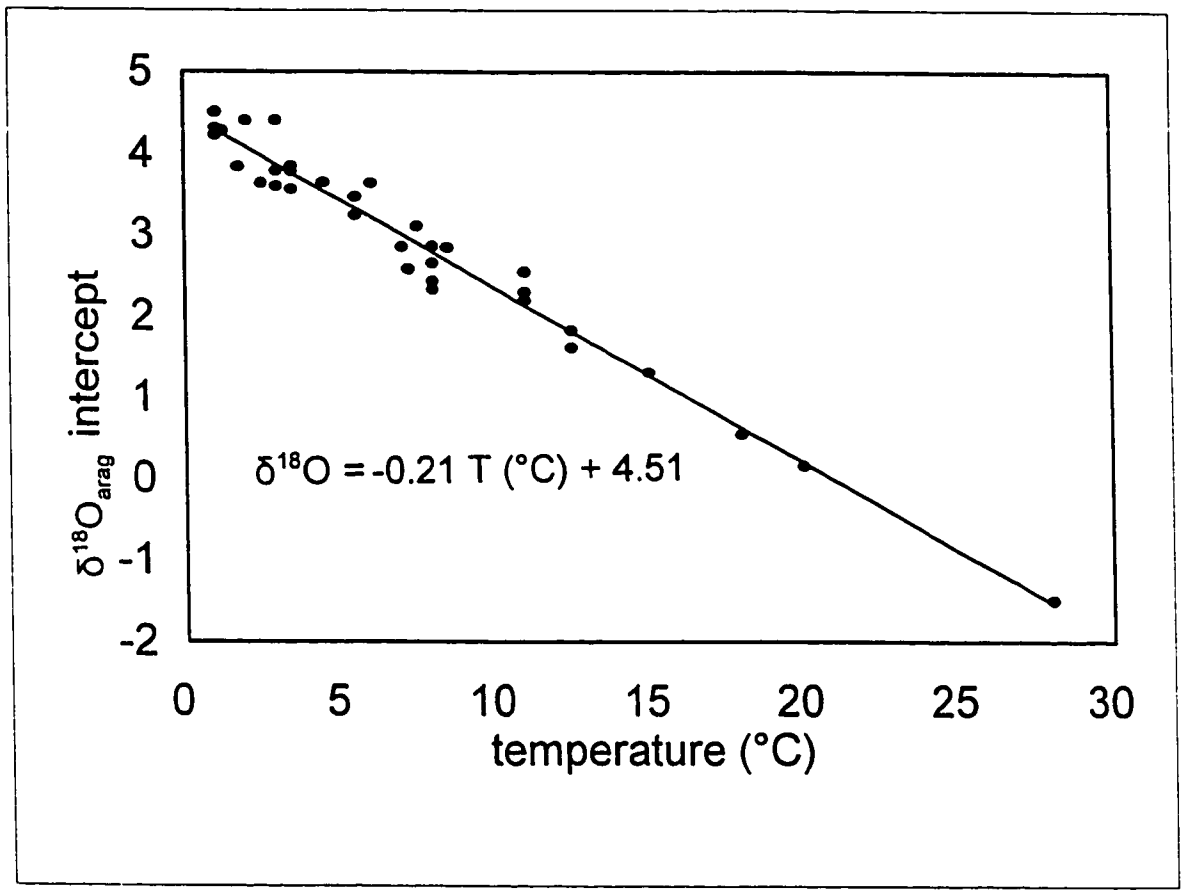

Figure 4: $\delta^{18}O_{arag}$ when $\delta^{13}C_{arag} = 0$, i.e., assuming $\delta^{18}O_{water} = \delta^{13}C_{water} = 0$ for each regression line for each of the 35 corals. The least-squared regression line for the intercept data is included.

5.5.2 Minimum number of points required

For the data used to construct equation [3], numerous subsamples and isotopic analyses were performed on each coral (up to 27 per specimen). We, of course, would prefer to do this using as few points as necessary to give an accurate estimate of the equilibrium point for a given skeletal deposit. Let us assume, arbitrarily, that an acceptable margin of error in the intercept should be ± 0.25‰, corresponding to an uncertainty in temperature of ±1.15°C. Isotopic ratios were randomly removed from each data set, one pair at a time, until the $\Delta_{a\text{-}w}$ for $\delta^{13}C_{arag} = \delta^{13}C_{water}$ deviated by more than 0.25‰ from the original value. It was found that nine pairs of $\delta^{18}O$ and $\delta^{13}C$ ratios gave an 'acceptable' intercept value, with a still-significant correlation coefficient. Thus, as few as 9 randomly-selected samples define the $\delta^{18}O$ - $\delta^{13}C$ correlation for a given coral with adequate precision to determine the average annual temperature of the water in which the coral grew. An uncertainty of ±1.15°C may be too large to be useful in some studies, like those investigating changes in abyssal-depth waters, but may be tolerable in many others.

It may also be possible to reconstruct changes in the equilibrium point during an individual coral's lifespan. If successive growth segments of a deep-sea coral can be identified, constructing 9-point lines from each section could yield a chronological record of the C-O lines at various points in time. These long-lived organisms, then, may provide unique decadal- to century-long records of equilibrium compositions at various deep ocean locations, perhaps with annual resolution.

5.5.3 Using $\delta^{18}O$ value as a paleotemperature indicator

We seem to be able to estimate the equilibrium value of $\delta^{18}O_{arag}$ for a single modern coral or a part thereof, as long as we can know the isotopic composition of the seawater in which the coral grew. To be really useful, though, it is necessary to determine how this relationship would translate into oceans of the past in which both the $\delta^{18}O$ of seawater and the $\delta^{13}C$ of HCO_3^- have varied. Information regarding the isotopic composition of the water in which a fossil coral grew may be able to be obtained from benthic aragonitic forams at the same site, if they were of comparable age, and of a species whose skeleton chemistry is suitable for estimation of oxygen and carbon isotopic aragonite / seawater equilibria. If so, this information can be used with equation [3] in the same manner as for modern corals. If forams are required to calibrate the deep-sea coral isotopic data, it may appear that the latter offer no advantage as a paleotemperature indicator. Although azooxanthellate corals require multiple $\delta^{18}O$ / $\delta^{13}C$ pairs for a reliable temperature and provide discontinuous records, their advantages lie with their suitability for accurate and precise dating, and in their immunity to bioturbation. Recent forams can be radiocarbon dated, but those older than 50,000 y BP or so require age interpolation between datable strata in a core, for example, ash layers or magnetic reversals. The precision of such interpolations may be very low, especially if bioturbation has occurred, or if sedimentation rates have fluctuated over time. Corals can be dated directly using either ^{14}C or the uranium-series method, with 2σ uncertainties of about 1% (Edwards, et al., 1987). A single specimen of azooxanthellate coral could possess a 100-year-long record of high-resolution paleoceanographic information; it may be possible, therefore, to determine paleotemperature variations on a decadal scale. This degree of resolution in an

isotopic record would only be obtainable on sediment cores with extremely high sedimentation rates, as bioturbation normally limits resolution to a few hundred years.

If it is not possible to use foraminifera to determine the paleo-isotopic composition of seawater, an estimate of temperature of Holocene fossils can still be made by assuming that the $\delta^{13}C$ and $\delta^{18}O$ of the ambient seawater were both equal to zero. Equation [4] demonstrates that, even without known $\delta^{18}O_{water}$ and $\delta^{13}C_{HCO3-}$, the $\delta^{18}O$ / temperature correlation is still high and in agreement with Grossman and Ku's (1986) curve (equation [1]).

5.5.4 Slopes

The slopes of the 35 regression lines vary from 0.23 to 0.67, with a mean of 0.45 and a standard deviation of 0.09; the slopes are normally distributed. There does not appear to be a unique relationship between slope and any of: temperature, depth, isotopic composition of the seawater, nutrient supply or taxon. The slope would appear to be a locally determined variable, perhaps due to a combination of any or all of the above. There are variations in the slope (by as much as 0.1) among various segments of an individual coral, however, so ontogeny may play a role in the determination of the slope of the $\delta^{13}C$ vs $\delta^{18}O$ regression line.

5.5.5 Species dependence

Figure 2 also shows that the relationship between temperature and $\delta^{18}O$ is independent of the species analysed. Eighteen different species of deep-sea

corals were included, yet the intercepts for each regression line all fall virtually on the same line. This is quite different from the behaviour of reef corals: zooxanthellate corals also do not precipitate their skeletons in isotopic equilibrium with seawater, but the relationship between temperature and $\delta^{18}O_{arag}$ - $\delta^{18}O_{water}$ is unique to each species of scleractinian coral (Weber and Woodhead, 1970).

5.5.6 Carbon isotope data and the respired CO_2 effect

So far we have been unable to extract environmental information from the carbon isotope data of deep-sea corals. As with the $\delta^{18}O$ data, $\delta^{13}C$ values display large variations which are not correlated with temperature or the isotopic composition of the appropriate reservoir ($\delta^{18}O$ of seawater for oxygen, $\delta^{13}C$ of the bicarbonate ion for carbon).

The carbon isotope data can, however, give some information regarding the provenance of the carbon in coral aragonite. Two carbon sources are potentially available to corals for skeletogenesis: dissolved inorganic carbon ($\delta^{13}C$ ~ 0‰) from seawater and respired CO_2 ($\delta^{13}C$ ~ 23.8‰). Carbonates which precipitate in isotopic equilibrium with cell fluids might therefore be somewhat depleted in ^{13}C compared to isotopic equilibrium with ambient. Assuming that the coral $\delta^{18}O$ - $\delta^{13}C$ regression lines represent a mixture of kinetic isotope effects and equilibrium with oxygen and HCO_3^- (McConnaughey, 1989), the depression of skeletal $\delta^{13}C$ which results from respired CO_2 incorporation can be estimated by extending the coral $\delta^{18}O$ - $\delta^{13}C$ regression line to oxygen isotopic equilibrium. The projected skeletal $\delta^{13}C$ at that point can then be compared with the aragonite ^{13}C equilibrium with seawater DIC (see Figure 6,

McConnaughey *et al.*, 1997). As before, we can use Grossman and Ku's (1986) equation for oxygen isotopic equilibrium in aragonite and the Romanek et al. (1992) relation for carbon isotopic equilibrium.

For three specimens from the South Atlantic (*Flabellum thouarsii*, #16 and #17b, and *Balanophyllia malouinensis*, #17a), the corals' regression lines intersect oxygen isotopic equilibrium (approximately+4.1‰) at $\delta^{13}C$ = +0.5 to 1.2‰ (Figure 5). Regressions calculated separately for all 3 corals were rather similar, even though they occupied different ranges of $\delta^{18}O$ and $\delta^{13}C$. Environmental DIC is approximately 0.4 - 0.6‰ for this region (Kroopnick, 1985). Aragonite $\delta^{13}C$ equilibrium with environmental DIC should have a $\delta^{13}C$ of ca. +3.1 to +3.3‰. The respired CO_2 effect is the difference between these numbers, ranging from about -1.9‰ (#16) to -2.8‰ (#17a). Similarly calculated respired CO_2 effects for the other range vary from -1.9 to -4.4‰.

Cell membranes are quite permeable to CO_2 (Gutknecht *et al.*, 1977), so respired CO_2 easily escapes, while environmental CO_2 diffuses in. The rate of inward CO_2 diffusion can be estimated as the product of the membrane CO_2 permeability (about $10^{-2.5}$ m s^{-1} in human erythrocytes; Gutknecht *et al.*, 1977) and the concentration of molecular CO_2, approximately $10^{-4.5}$ molar (or $10^{-1.5}$ moles m^{-3}) in abyssal waters. The inward CO_2 flux is therefore on the order of 10^{-4} moles m^{-2} s^{-1} if membrane permeabilities limit CO_2 diffusion. Aqueous boundary layers probably also limit carbon diffusion at least as much (McConnaughey *et al.*, 1997). For comparison, the rate of respiration in reef corals is on the order of 10^{-6} moles m^{-2} s^{-1} (Muscatine, 1980; Davies, 1984). Environmental CO_2 is therefore likely to dominate as a source for skeletal carbon. Griffin *et al.* (1989), reported that the ^{14}C content skeletons of azooxanthellate coral skeleton resembled ambient DIC, rather than living tissues or potential food sources.

The estimates of respired CO_2 effects reported for these azooxanthellate corals (-1.9 to -4.4‰) are for the most part larger than expected from the analyses of McConnaughey *et al.* (1997). Their work showed that skeletal incorporation of respired CO_2 in marine invertebrates typically varies from near zero to about 10%. Analysis of a Galapagos azooxanthellate coral demonstrated that respired CO_2 affected the $\delta^{13}C$ of the skeleton by about -1.5‰.

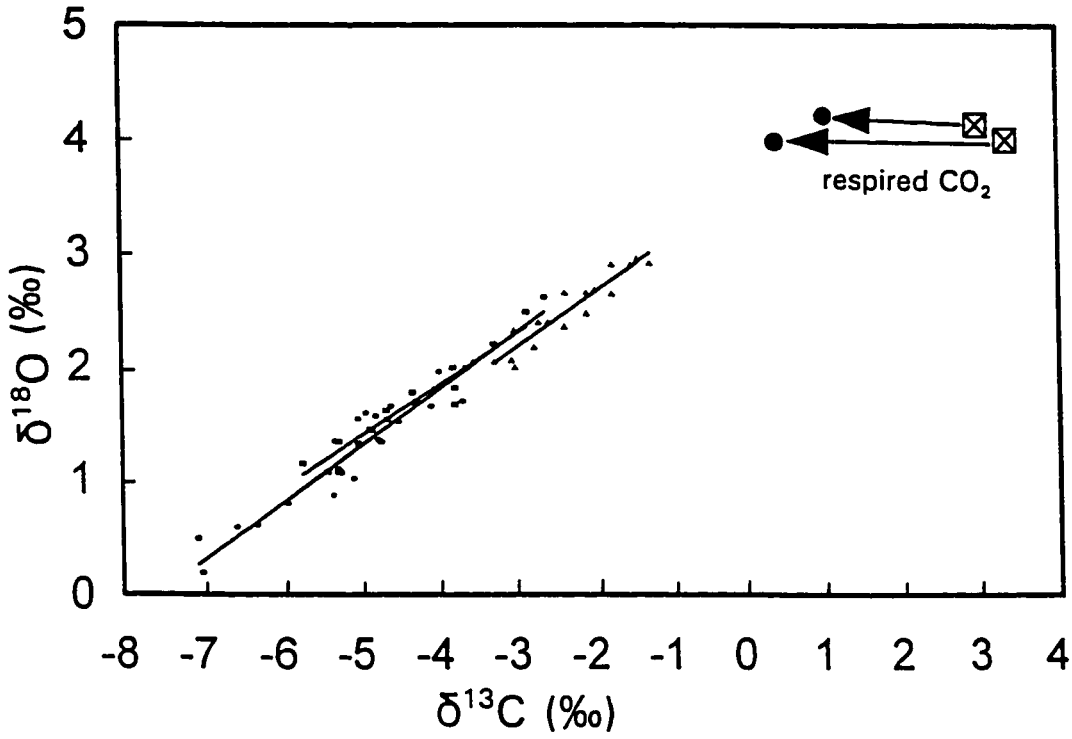

Figure 5: Plot of $\delta^{13}C$ vs $\delta^{18}O$ for Specimens 16 (■), 17a (●) and 17b (▲) with their regression lines. Boxed crosses (⊠) signify theoretical aragonite-seawater equilibrium for sites 16 (left) and 17 (right). Arrows show where the points would lie if there was no respired CO_2 included in the coral skeletons, i.e., on the extension of the $\delta^{13}C$ vs $\delta^{18}O$ regression lines. In this case, respired CO_2 lightens the skeleton by 2-3‰.

5.6 Conclusions

The principal aim of the study was to provide an additional tool for paleoceanographic reconstructions. Modelling past climatic changes is complicated by a lack of knowledge regarding deep-water circulation, especially its connections with surface waters and the atmosphere. Our results demonstrate that, although the oxygen isotope signal from each individual deep-sea coral is a mixture of equilibrium and biologically-fractionated components, the environmentally-controlled portion (reflecting the ambient temperature and isotopic composition of the water) is extractable and may be used for climatic reconstructions.

We showed that isotopic analyses of subsamples removed randomly from modern azooxanthellate corals (the exact number depending upon the degree of precision required), can be used to give the temperature at which the coral grew. From the $\delta^{13}C$ vs $\delta^{18}O$ regression line for an individual coral, the $\delta^{18}O_{arag}$ value corresponding with $\delta^{13}C_{arag}$ equal to $\delta^{13}C_{water}$, corrected by $\delta^{18}O_{water}$ is a function of temperature (equation [3]). Figure 8 demonstrates that this technique is successful as a tool for paleotemperature determination with a precision varying from ± 0.36 to 1.0 C.

If the isotopic composition of the seawater is not known, such as in the study of fossil corals, coeval benthic aragonitic forams may be used for calibration. For Holocene fossils, if foraminifera are not available, it is possible to assume that the $\delta^{13}C$ and $\delta^{18}O$ of the ancient seawater are equal to zero. The $\delta^{18}O_{arag}$ value corresponding to $\delta^{13}C_{arag} = 0$, without correction for seawater $\delta^{18}O$, used in equation [4] gives less precise estimate of the temperature in which the coral grew, but one likely to be useful in many circumstances.

Fossil azooxanthellate corals, while offering advantages in temporal

resolution of isotopic records, require independent estimates of the $\delta^{13}C$ and $\delta^{18}O$ of the seawater for the most precise temperature estimate, which foraminifera of comparable age may offer. Foraminfera are ubiquitous, usually provide continuous records and only require one isotopic analysis per depth in the sediment core. On the other hand, the ability of corals to be accurately and precisely dated directly by uranium-series methods, and their utility in producing high-resolution isotopic records free of the impacts of bioturbation and fluctuating sedimentation rates, render them as valuable complementary tools of paleotemperature indicators.

5.7 Acknowledgments

We thank Barbara Hecker, Judith Fournier, Paul Tyler, Craig Young and Andre Freivald for donating coral specimens and environmental information. Martin Knyf and Ines Guerrero helped with laboratory analyses. Stephen Cairns and Helmut Zibrovius provided useful information. This study was funded by a Natural Sciences and Engineering Research Council (NSERC) collaborative grant to HPS, MJR and NBK and NSERC graduate student support to JES. We thank Michael Tevesz and Jess Adkins for constructive comments.

5.8 References

Adkins, J.F. and Boyle, E.A. (1995) An investigation of the behavior of stable isotopes and metals in the skeletons of deep-sea corals. *Proceedings of the International Conference of Paleoceanography - V*, Halifax, p. 27 (abstract).

Carriquiry, J.D., Risk, M.J. and Schwarcz, H.P. (1988) Timing and temperature

record from stable isotopes of the 1982-1983 El Niño warming event in eastern Pacific corals. *Palaios* **3**: pp. 359-364.

CLIMAP (1984) The last interglacial ocean. *Quaternary Research* **21**: pp. 123-224.

Craig, H. and Gordon, L.I. (1965) Deuterium and oxygen-18 variations in the ocean and the marine atmosphere. *Proc. Congr. on Stable Isotopes in Oceanographic Studies and Paleotemperatures.* Spoleto, 26-30 July 1965, pp 9-130.

Davies, P.S. (1984) The role of zooanthellae in the nutritional energy requirements of *Pocillopora eydouxi. Coral Reefs* **2,** pp.181-186.

Druffel, E.R.M., King, L.L., Belastock, R.A. and Duesseler, K.O. (1990) Growth rate of a deep-sea coral using Pb-210 and other isotopes. *Geochimica et Cosmochimica Acta* **54**, pp.1492-1500.

Edwards, L.R., Chen, J.H., Ku, T.-L. And Wasserburg, G.J. (1987) Precise time of the last interglacial period from mass spectrometric determination of thorium-230 in corals. *Science* **236**, pp. 1547-1553.

Emiliani, C., Hudson, J.H., Shinn, E.A. and George, R.Y. (1978) Oxygen and carbon isotopic growth records in a reef coral from Florida Keys and a deep-sea coral from Blake Plateau. *Science* **202**, pp. 627-629.

Freund, J.W. (1973) Elementary Statistical Analysis. Plenum Press, New York, 389 pp.

Griffin, S.; Griffin, E. And Druffel, E.R.M. (1989) Sources of carbon to deep-sea corals. *Radiocarbon* **31**, pp. 53-543.

Grossman, E.L. and Ku, T-L. (1986) Oxygen and carbon isotope fractionation in biogenic aragonite: temperature effects. *Chemical Geology (Isotope Geoscience Section)* **59**, pp. 59-74.

Gutknecht, J.; Bisson, M.A. and Tosteson, F.C. (1977) Diffusion of carbon dioxide through lipid bilayer membranes: effects of carbonic anhydrase, bicarbonate and unstirred layers. *Journal of General Physiology* **69**, pp. 779-794.

Hudson, J.H., Shinn, E.A., Halley, R.B. and Lidz, B. (1976) Scleroschronology: A tool for interpreting past environments. *Geology* **4** : pp. 361-364.

Kroopnick, P (1985) The distribution of ^{13}C of ΣCO_2 in the world oceans. *Deep-Sea Research* **32**, pp. 57-84.

Lazier, A.V., Smith, J.E. , Risk, M.J. and Schwarcz, H.P. (in manuscript) The skeletal structure of Desmophyllum cristagalli: the use of deep-water corals in sclerochronology. for submission to Lethaia.

Levitus, S. and Boyer, T.P. (1994) *World Ocean Atlas. Volume 4: Temperature.* National Oceanic and Atmospheric Administration, Washington, D.C.

Levitus, S.; Burgett, R. And Boyer, T.P. (1994) *World Ocean Atlas. Volume 3: Salinity*. National Oceanic and Atmospheric Administration, Washington, D.C.

McConnaughey, T.A. (1989) ^{13}C and ^{18}O isotopic disequilibrium in biological carbonates: 1. Patterns. *Geochimica et Cosmochimica Acta* **53**, pp. 151-162.

McConnaughey, T.A.; Burdett, J.; Whelan, J.F. and Paull, C.K. (1997) Respiration and photosynthesis: effects on the carbon-13 content of biological carbonates. *Geochimica et Cosmochimica Acta* **61**, pp. 611-622.

McCrea, J.M. (1950) On the isotope chemistry of carbonates and a paleotemperature scale. *Journal of Chemical Physics* **18**: 849-857.

Mikkelson,N., Erlenkeuser, H., Killingley, J.S. and Berger, W.S. (1982) Norwegian corals: radiocarbon and stable isotopes in *Lophelia pertusa*. *Boreas* **11**, pp. 163-171.

Muscatine, L. (1980) Productivity of zooxanthellae. In: Falkowski, P.G. (ed.) *Primary Productivity in the Sea*. Plenum, New York, pp. 381-402.

Orbach, E. and Finkelstein, A. (1980) The non-electrolyte permeability of planar lipid bilayer membranes. *Journal of General Physiology* **75**, pp. 427-436.

Romanek, C.S., Grossman, E.L. and Morse, J.W. (1992) Carbon isotopic fractionation in synthetic aragonite and calcite: effects of temperature and precipitation rate. *Geochimica et Cosmochimica Acta* **56**, pp. 419-430.

Shackleton, N.J. (1967) Oxygen isotope analyses and Pleistocene temperatures reassessed. *Nature* **215**, pp. 15-17.

Smith, J.E.; Risk, M.J.; Schwarcz, H.P. and McConnaughey, T.A. (1997) Rapid climate change in the North Atlantic during the Younger Dryas recorded by deep-sea corals. *Nature* **386**, pp. 818-820.

Smith, J.E.; Risk, M.J.; Schwarcz, H.P. and McConnaughey, T.A. (in manuscript) Patterns of isotopic disequilibria in azooxanthellate coral skeletons. To be submitted to Palaeogeograpy, Palaeoclimatology, Palaeoecology

Weber, J.N. and Woodhead, P.M. (1970) Carbon and oxygen isotope fractionation in skeletal carbonate of reef-building corals. *Chemical Geology* **6**, pp. 93-102.

Chapter 6

Mid-Atlantic ridge hydrothermal events recorded by deep-sea corals

6.1 Abstract

Trace-element and stable-isotope analyses were perfomed on two sets of azooxanthellate corals from the North Atlantic, from different tectonic settings. One set was from Orphan Knoll, near Newfoundland; the other from the mid-Atlantic ridge. The mid-Atlantic-ridge corals had significantly greater quantities of Fe, Mn, Cu, Ni and Zn contained within their skeletons than did the Orphan Knoll corals. The metal concentrations were not homogeneous within the mid-Atlantic-ridge coral skeletons, however, but occurred as episodic pulses during a decade or two of each coral's lifetime. We believe these metals originated in a hydrothermal discharge zone associated with the mid-Atlantic spreading centre. If so, it is evidence that the duration of an individual hydrothermal event is from a decade up to 30 years or so. With sufficient specimens of known ages, it may be possible to reconstruct the history of a particular segment of a spreading centre.

6.2 Introduction

Studies of key oceanic and atmospheric phenomena have focused increasingly on the use of corals as paleoenvironmental monitors. Corals, as recorders of ocean/atmosphere variability, have no rivals for fidelity

and resolution. They provide excellent chronologic control, with age errors generally <1% using $^{230}Th/^{234}U$ dating, and incorporate several independent tracers which can record changes in various environmental parameters. Certain trace elements substitute readily for calcium in carbonate skeletons; trace element histories in corals, then, offer a record of an element's concentration in seawater and thus of specific environmental processes (e.g., Shen *et al.*, 1987). Recent stable-isotope analyses on several species of deep-sea corals have shown that, despite considerable kinetic effects, an environmental signal is retained and can be extracted (Smith *et al.*, 1995, 1997, in press). To date, most coralline studies of oceanic distributions of trace elements have been performed on reef species which are confined to shallow, tropical water by their algal symbionts (zooxanthellae), providing records of low-latitude environmental phenomena only. Azooxanthellates experience no such geographic or bathymetric restrictions, so can attain much wider distributions (Stanley and Cairns, 1988). The purpose of this study was to determine the ability of these little-known taxa to reflect the trace-element and/or stable-isotope composition of the seawater in which their skeletons were precipitated and consequently, to assess further their usefulness as paleoenvironmental monitors. Two distinct populations of the deep-water coral *Desmophyllum cristagalli* (Milne-Edwards and Haime, 1848), from different regions of the North Atlantic, were selected for study (Figure 1). One suite of specimens was dredged from 1700 m from the top of Orphan Knoll, a bathymetric high which lies at the edge of the continental rise 550 km northeast of Newfoundland (50° 25.57' N, 46° 22.05' W). Orphan Knoll is a piece of Laurasia which was separated from its parent block during the initial opening of the North Atlantic. It is

composed of shallow-marine Devonian limestone and has not been subjected to any tectonic activity since at least the Jurassic. The second group was retrieved from the mid-Atlantic ridge (45° 14.12' N, 28° 34.12' W) from a depth of 1200 m (Figure 2). This is a locality characterized by active seafloor spreading and concurrent hydrothermal activity. The corals had been fixed to relatively-fresh basalt with negligible sediment cover. We hypothesized that the geochemistry of these skeletons may have been affected by the proximity of the population to the spreading centre and attachment to fresh basalt.

6.3 Methods

Trace-element and stable-isotope analyses were performed on three coral specimens from each tectonic setting, i.e., from Orphan Knoll (OK1, OK2, OK3) and from the mid-Atlantic ridge (MAR1, MAR2, MAR3). In each case subsampling proceeded along the coral's growth axis (Lazier *et al.*, in manuscript); the geochemical record of an individual coral, then, reflects changes in the ambient seawater during its lifetime. Previous XRD work has ascertained that the corals are at least 98% aragonite (Smith, 1993).

Subsamples for stable isotope analyses (about 100µg each) were removed with a high-speed hand-held drill. Fifteen subsamples were taken from each coral. Analyses were performed on a SIRA gas-source mass spectrometer using a common 100% phosphoric-acid bath at 90°C. Precision was 0.07 ‰ for $\delta^{18}O$ and 0.10‰ $\delta^{13}C$; values for $\delta^{18}O$ and $\delta^{13}C$ are reported relative to VPDB.

Nine to thirteen subsamples, depending on the size of the

individual, were taken from each coral specimen for trace-element analyses (Figure 3). In these abyssal environments *D. cristagalli* grows about 1 mm per year (Smith, 1993); each analysis required a piece of thecal wall 5 mm in height, an amount of skeletal material representing approximately five-years' growth. To remove possible metal contaminants adsorbed onto the epitheca from the surrounding seawater, the outer 0.5 mm of theca from each specimen was mechanically removed. The remaining material was cleaned by etching in 10% HCl for a few seconds, quenched in a sodium bicarbonate bath and then rinsed in distilled water with ultrasonic agitation. As these specimens were long dead, it was deemed unnecessary to invoke procedures for the removal of organic residues. The samples were dissolved in 10 ml 3% HNO_3. Trace-element analyses were performed on a Varian SprectrAA 400 Atomic Absorption Spectrophotometer using an air-acetylene flame. Average accuracy and reproducibility of AAS analyses were determined using NBS (NIST) standard reference materials #634 and #636. Relative precision and accuracy was ± 5% for Fe, Mn, Cu, Zn, and Ni. Every third subsample from each coral was split and analyzed separately, as an extra precision check: for these, the reported result is the mean of the two analyses. Blanks of reagent-grade HNO_3 were inserted every 10 analyses. Results are reported in parts per million (ppm).

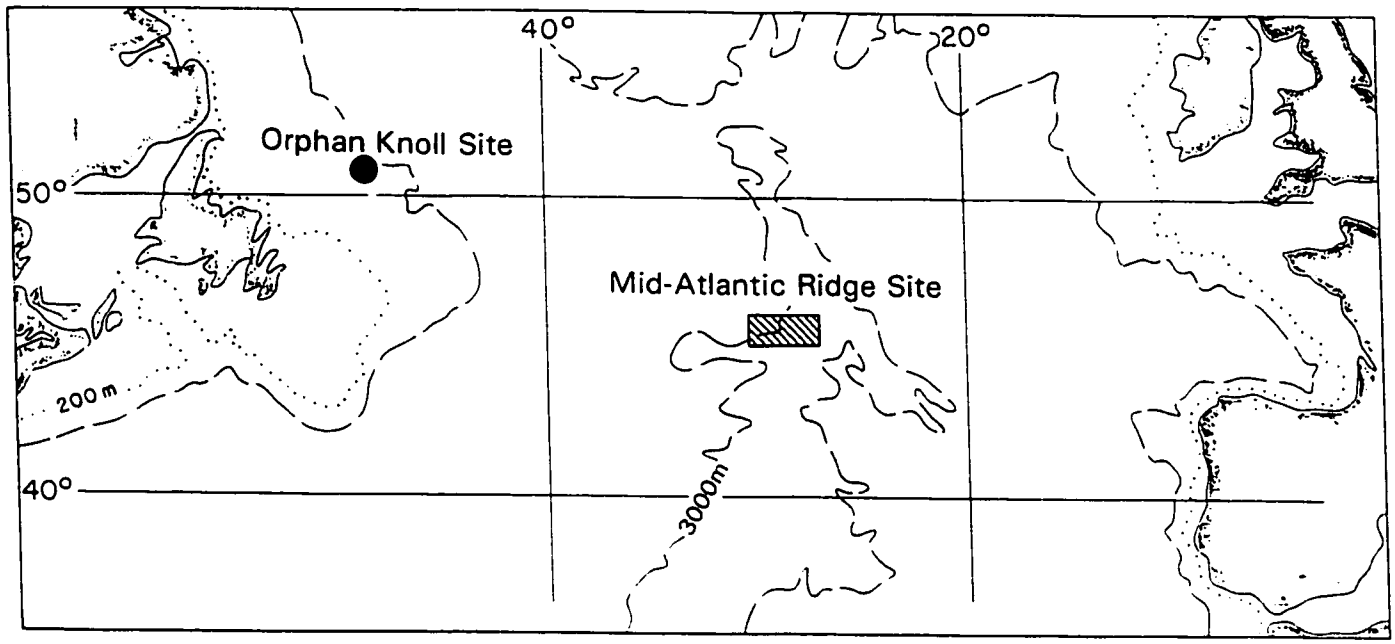

Figure 1: Location of Orphan Knoll and Mid-Atlantic-Ridge sampling sites

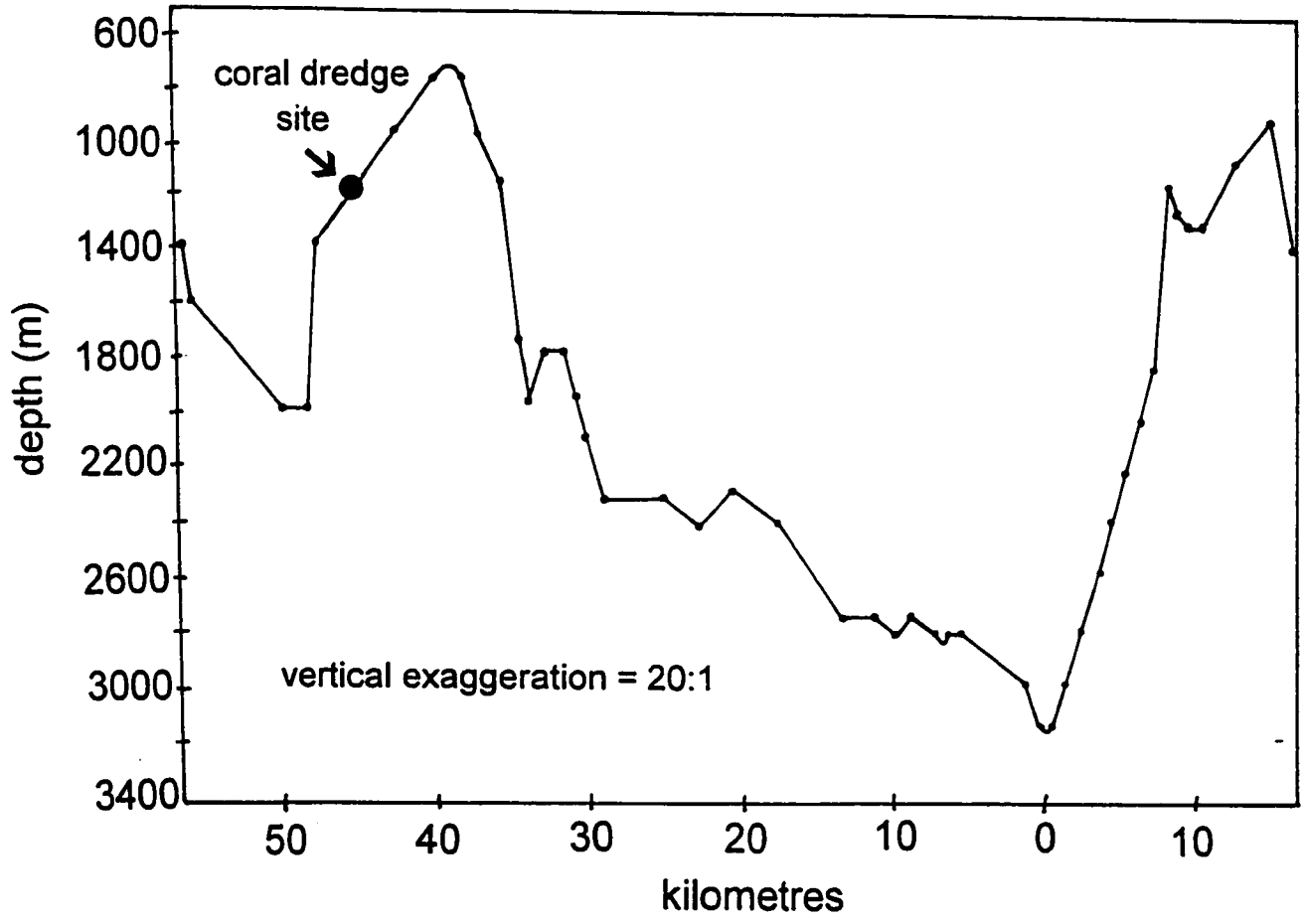

Figure 2: Bathymetry of Mid-Atlantic-Ridge site and coral dredging location

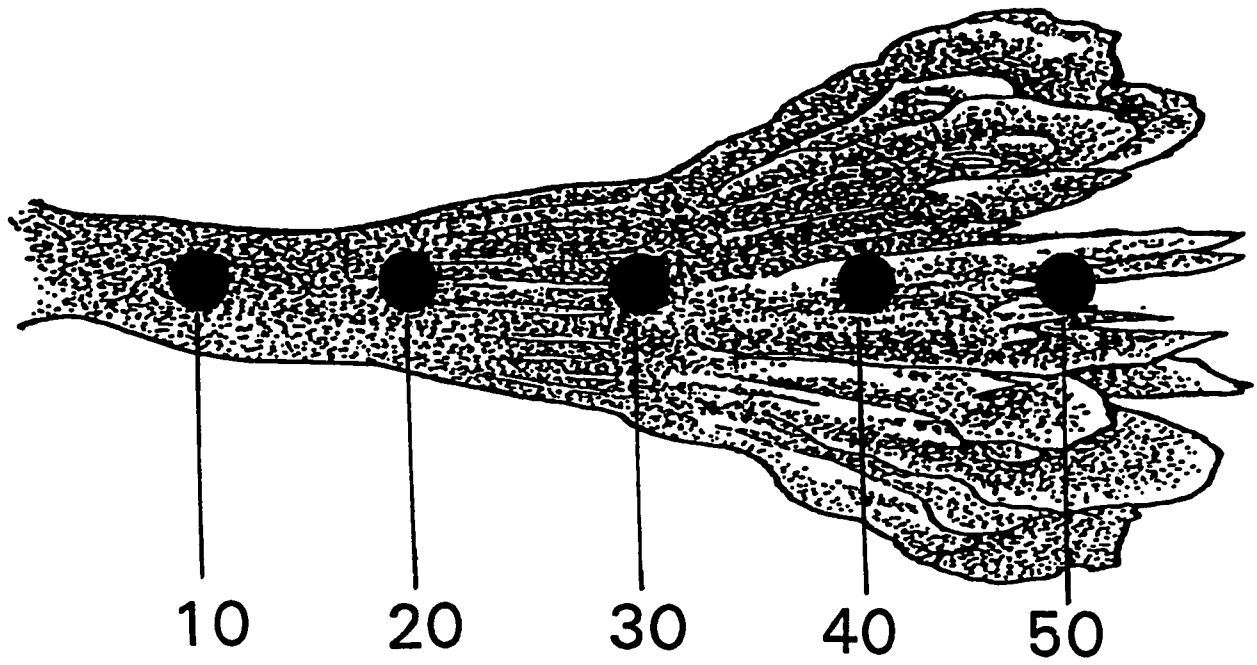

Figure 3: Sampling scheme on *D. cristagalli* (not all sampling sites marked)

6.4 Results

Stable isotope data for each specimen are shown in Table 1. As expected, the $\delta^{13}C$ and $\delta^{18}O$ values show a strong positive correlation (Smith *et al.*, in revision; Figure 4), with r^2 values ranging from 0.78 to 0.93. Trace element data for each specimen are shown in Tables 2 to 6. Figures 5-16 are plots of the concentration of each metal present for each coral versus height on the coral (mm from the base) from which the sample was removed. The height in millimetres from the base is approximately equal to the coral's age in years.

The mid-Atlantic coral population had significantly higher concentrations of copper, zinc, nickel, iron and manganese within their structure than did the Orphan Knoll specimens (difference of means tests, $\alpha = 0.05$, $p < 0.01$) (Table 7). Below is a correlation matrix for the five trace elements discussed above. Iron / manganese displays a very high positive correlation (0.97), and copper / zinc / nickel show high positive correlations with each other (ranging from 0.74 to 0.79). Cadmium and lead were also analysed for, and all values from both sites were below detection limits.

	Cu	Zn	Mn	Ni	Fe
Cu	1.000				
Zn	0.736	1.000			
Mn	-0.122	-0.070	1.000		
Ni	0.790	0.778	-0.137	1.000	
Fe	-0.035	0.003	0.959	-0.049	1.000

The mid-Atlantic ridge corals also displayed episodic 'peaks' in their trace element constituents over time. One mid-Atlantic-ridge

specimen (MAR 2, Figure 6) shows an iron and manganese enrichment in a segment of its skeleton precipitated early in its life. Since each data point comprises about 5 years skeletal growth, the increased metal assimilation occurred over approximately ten years. The remainder of the skeleton has Fe and Mn concentrations not significantly different than those from Orphan Knoll (Figures 8-10). Cu, Zn and Ni maxima also occur within a fifteen-year period in about the middle of the coral's life, between about years 20 - 35. Again, during times of non-enrichment, metal concentrations are similar to those recorded in the Orphan Knoll corals. MAR 1 (Figure 5) records Cu, Zn and Ni spikes during the first 15 - 20 years of its life. In contrast, MAR 3 (Figure 7) records only Fe and Mn anomalies between its ages of 20 and 30.

1		2		3		
$\delta^{13}C$	$\delta^{18}O$	$\delta^{13}C$	$\delta^{18}O$	$\delta^{13}C$	$\delta^{18}O$	MAR
-4.46	2.02	-3.67	2.43	-5.72	1.46	
-4.82	1.90	-4.15	1.82	-3.12	2.60	
-4.54	1.81	-4.33	2.12	-4.06	2.75	
-7.09	1.08	-3.83	1.78	-3.14	2.09	
-3.39	2.38	-3.19	2.14	-3.78	1.73	
-6.53	1.16	-4.11	2.80	-4.28	2.07	
-7.20	0.99	-3.17	2.65	-4.10	1.77	
-5.02	1.87	-4.68	1.91	-3.62	2.38	
-6.69	1.04	-5.77	1.51	-3.76	2.14	
-7.10	1.02	-2.83	2.38	-2.37	2.49	
-6.21	1.45	-5.04	1.85	-6.16	1.39	
-4.50	1.95	-6.19	1.87	-4.45	2.20	
-6.21	1.44	-4.52	2.37	-5.13	1.850	
-2.42	2.54	-6.68	0.99	-7.05	0.97	
-3.81	2.19	-4.46	2.30	-6.64	0.99	
$\delta^{13}C$	$\delta^{18}O$	$\delta^{13}C$	$\delta^{18}O$	$\delta^{13}C$	$\delta^{18}O$	OK
-6.03	1.71	-2.62	2.61	-1.73	2.78	
-8.60	0.54	-3.97	1.96	-2.38	2.39	
-8.21	0.72	-5.02	1.54	-2.75	2.16	
-7.24	1.16	-4.92	1.59	-3.00	2.33	
-5.96	1.69	-7.05	0.48	-2.35	2.65	
-5.33	2.03	-4.59	1.65	-3.26	2.05	
-8.20	0.83	-6.57	0.59	-2.07	2.47	
-9.44	0.21	-4.78	1.56	-3.03	2.06	
-8.75	0.42	-5.92	0.79	-3.02	1.99	
-6.46	1.43	-4.75	1.36	-2.07	2.66	
-5.22	1.86	-3.68	1.70	-2.69	2.39	
-7.60	1.06	-4.50	1.51	-1.25	2.91	
-6.63	1.51	-5.28	1.10	-1.42	2.95	
-6.96	1.44	-5.07	1.01	-1.96	2.68	
-6.29	1.64	-5.24	1.06	-1.51	2.90	

Table 1: Stable isotope data for all six corals

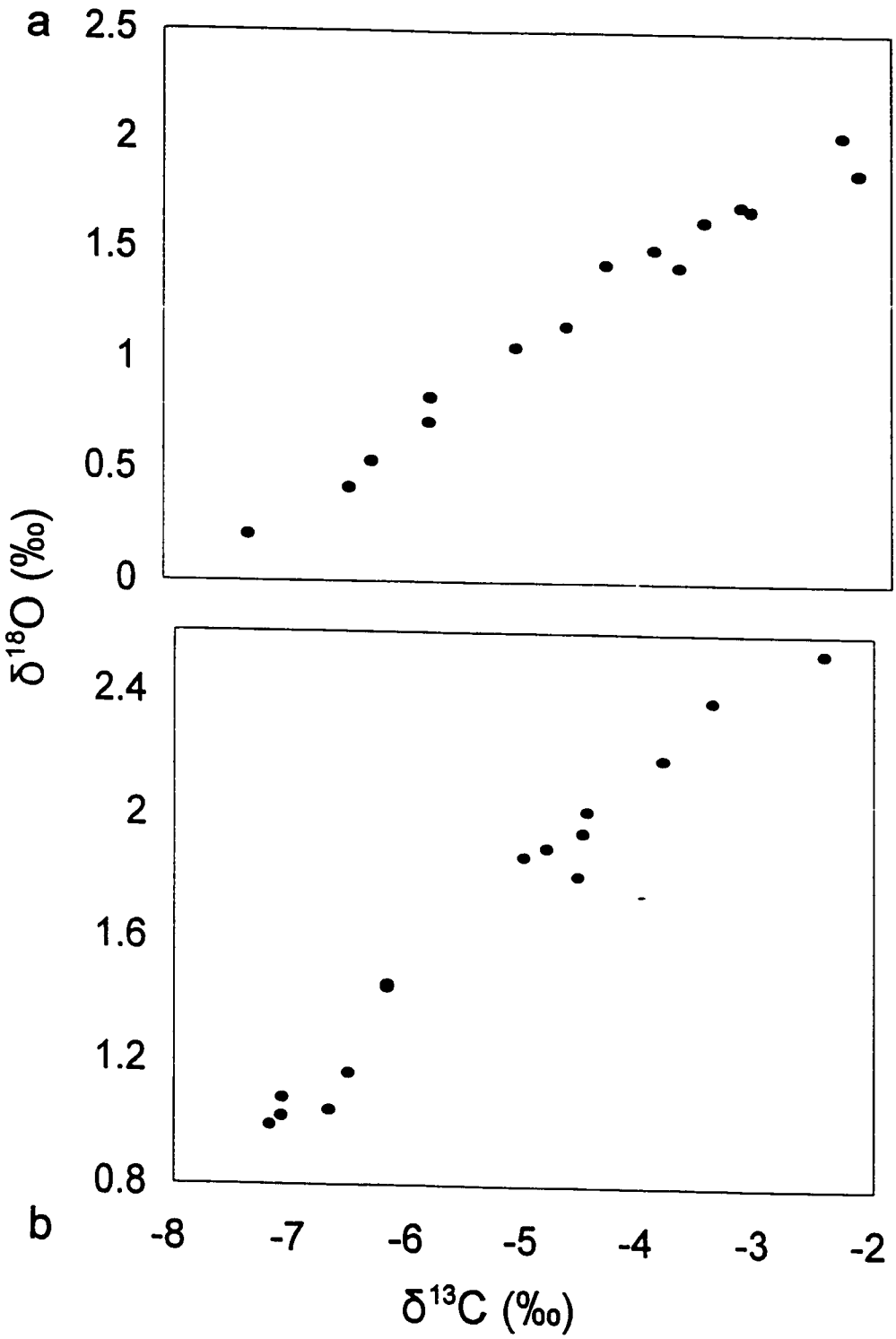

Figure 4: $\delta^{13}C$ vs $\delta^{18}O$ for OK1 (top) and MAR 1 (bottom)

Copper

Sample		AAS ppm	Weight	Coral ppm
MAR1	1	0.212	0.100	21.27
	2	0.190	0.076	25.23
	3A	0.109	0.046	23.41
	3B	0.142	0.060	23.73
	4	0.099	0.081	12.29
	5	0.096	0.076	12.72
	6A	0.097	0.075	12.91
	6B	0.081	0.061	13.25
	7	0.112	0.084	13.27
	8	0.120	0.074	16.24
	9A	0.000	0.094	13.13
	9B	0.089	0.070	12.75
	10	0.100	0.087	11.44
MAR2	1	0.109	0.077	14.17
	2A	0.100	0.070	14.34
	2B	0.076	0.053	14.98
	3	0.100	0.061	16.50
	4	0.118	0.076	15.53
	5A	0.000	0.053	19.02
	5B	0.135	0.074	18.20
	6	0.119	0.053	22.37
	7	0.108	0.071	15.23
	8A	0.119	0.083	14.44
	8B	0.114	0.082	13.86
	9	0.119	0.078	15.22
	10	0.112	0.081	13.84
MAR3	1A	0.085	0.089	9.62
	1B	0.067	0.074	9.08
	2	0.070	0.077	9.06
	3	0.061	0.056	10.97
	4A	0.100	0.075	13.27
	4B	0.082	0.065	12.59
	5	0.061	0.059	10.27
	6	0.062	0.054	11.46
	7A	0.058	0.053	10.99
	7B	0.076	0.074	10.23
	8	0.039	0.036	10.99
	9	0.067	0.065	10.31
	10A	0.049	0.037	13.12
	10B	0.055	0.043	12.68
	11	0.076	0.082	9.28
	12	0.061	0.067	9.16
	13	0.055	0.060	9.24

Sample		AAS ppm	Weight	Coral pp
OK1	1	0.120	0.089	13.56
	2	0.107	0.064	16.72
	3A	0.086	0.067	12.87
	3B	0.071	0.058	12.21
	4	0.086	0.058	14.83
	5	0.123	0.076	16.12
	6A	0.120	0.088	13.62
	6B	0.097	0.075	12.98
	7	0.114	0.069	16.43
	8	0.111	0.081	13.75
	9A	0.100	0.082	12.25
	9B	0.067	0.056	11.95
OK2	1	0.051	0.059	8.72
	2	0.043	0.042	10.36
	3A	0.057	0.050	11.55
	3B	0.054	0.049	11.03
	4	0.059	0.056	10.48
	5	0.035	0.030	11.71
	6A	0.057	0.052	10.97
	6B	0.072	0.063	11.47
	7	0.060	0.060	10.05
	8	0.057	0.050	11.42
	9A	0.060	0.057	10.58
	9B	0.082	0.075	10.94
	10	0.048	0.049	9.84
	11	0.048	0.045	10.64
	12A	0.052	0.040	12.87
	12B	0.091	0.073	12.51
	13	0.059	0.051	11.57
OK3	1	0.044	0.038	11.46
	2A	0.050	0.045	11.19
	2B	0.074	0.063	11.73
	3	0.048	0.043	11.16
	4	0.053	0.054	9.83
	5A	0.051	0.050	10.27
	5B	0.052	0.053	9.89
	6	0.058	0.074	7.89
	7	0.054	0.058	9.31
	8A	0.034	0.038	9.12
	8B	0.055	0.058	9.54
	9	0.044	0.047	9.43

Table 2: Copper data for all six corals

Zinc

Sample		AAS ppm	Weight	Coral ppm
MAR1	1	0.124	0.100	12.44
	2	0.275	0.076	36.41
	3A	0.047	0.046	10.10
	3B	0.044	0.045	9.72
	4	0.034	0.081	4.22
	5	0.033	0.076	4.37
	6A	0.046	0.075	6.10
	6B	0.048	0.081	5.92
	7	0.024	0.084	2.84
	8	0.024	0.074	3.25
	9A	0.031	0.094	3.30
	9B	0.019	0.054	3.48
	10	0.022	0.087	2.52
MAR2	1	0.051	0.077	6.63
	2A	0.052	0.070	7.44
	2B	0.035	0.048	7.22
	3	0.058	0.061	9.57
	4	0.037	0.076	4.87
	5A	0.081	0.053	15.21
	5B	0.123	0.078	15.75
	6	0.096	0.053	18.12
	7	0.026	0.071	3.67
	8A	0.030	0.083	3.62
	8B	0.018	0.046	3.88
	9	0.051	0.078	6.52
	10	0.030	0.081	3.71
MAR3	1A	0.062	0.089	7.02
	1B	0.037	0.056	6.68
	2	0.043	0.077	5.55
	3	0.030	0.056	5.43
	4A	0.028	0.075	3.73
	4B	0.022	0.054	4.01
	5	0.027	0.059	4.63
	6	0.018	0.054	3.37
	7A	0.025	0.053	4.77
	7B	0.033	0.079	4.21
	8	0.018	0.036	5.01
	9	0.023	0.065	3.54
	10A	0.020	0.037	5.38
	10B	0.032	0.062	5.12
	11	0.055	0.082	6.77
	12	0.036	0.067	5.37
	13	0.024	0.060	4.03

Sample		AAS ppm	Weight	Coral pp
OK1	1	0.043	0.089	4.86
	2	0.030	0.064	4.69
	3A	0.010	0.037	2.81
	3B	0.015	0.048	3.21
	4	0.031	0.058	5.34
	5	0.025	0.076	3.28
	6A	0.022	0.088	2.54
	6B	0.016	0.072	2.24
	7	0.018	0.069	2.59
	8	0.023	0.081	2.86
	9A	0.026	0.082	3.13
	9B	0.018	0.065	2.79
OK2	1	0.017	0.059	2.89
	2	0.012	0.042	3.01
	3A	0.022	0.050	4.44
	3B	0.022	0.046	4.68
	4	0.014	0.056	2.49
	5	0.011	0.030	3.79
	6A	0.023	0.052	4.51
	6B	0.026	0.054	4.89
	7	0.024	0.060	4.06
	8	0.031	0.050	6.12
	9A	0.017	0.057	2.93
	9B	0.023	0.073	3.11
	10	0.012	0.049	2.56
	11	0.012	0.045	2.60
	12A	0.018	0.040	4.38
	12B	0.022	0.051	4.22
	13	0.011	0.051	2.08
OK3	1	0.012	0.038	3.21
	2A	0.011	0.045	2.48
	2B	0.010	0.047	2.16
	3	0.015	0.043	3.56
	4	0.021	0.054	3.87
	5A	0.010	0.050	2.04
	5B	0.019	0.084	2.28
	6	0.042	0.074	5.78
	7	0.024	0.058	4.17
	8A	0.012	0.038	3.17
	8B	0.015	0.044	3.37
	9	0.144	0.420	3.43

Table 3: Zinc data for all six corals

Manganese

Sample		AAS ppm	Weight	Coral ppm
MAR1	1	0.126	0.100	12.64
	2	0.110	0.076	14.57
	3A	0.064	0.046	13.88
	3B	0.068	0.047	14.56
	4	0.077	0.081	9.57
	5	0.056	0.076	7.42
	6A	0.064	0.075	8.54
	6B	0.040	0.045	8.82
	7	0.038	0.084	4.50
	8	0.033	0.074	4.47
	9A	0.045	0.094	4.72
	9B	0.035	0.069	5.04
	10	0.045	0.087	5.15
MAR2	1	0.429	0.077	55.79
	2A	0.688	0.070	98.81
	2B	0.495	0.048	103.21
	3	0.064	0.061	10.56
	4	0.129	0.076	16.97
	5A	0.070	0.053	13.09
	5B	0.093	0.068	13.61
	6	0.105	0.053	19.74
	7	0.094	0.071	13.26
	8A	0.132	0.083	15.94
	8B	0.104	0.064	16.22
	9	0.104	0.078	13.30
	10	0.228	0.081	28.18
MAR3	1A	0.165	0.089	18.59
	1B	0.163	0.091	17.89
	2	0.181	0.077	23.42
	3	0.093	0.056	16.73
	4A	0.547	0.075	72.96
	4B	0.413	0.058	71.22
	5	0.439	0.059	73.91
	6	0.161	0.054	29.76
	7A	0.193	0.053	36.55
	7B	0.140	0.039	35.79
	8	0.110	0.036	30.99
	9	0.195	0.065	30.00
	10A	0.060	0.037	16.14
	10B	0.087	0.052	16.66
	11	0.076	0.082	9.28
	12	0.074	0.067	11.11
	13	0.061	0.060	10.25

Sample		AAS ppm	Weight	Coral pp
OK1	1	0.118	0.089	13.33
	2	0.058	0.064	9.06
	3A	0.055	0.037	15.18
	3B	0.066	0.045	14.68
	4	0.095	0.068	13.97
	5	0.103	0.076	13.50
	6A	0.104	0.088	11.84
	6B	0.052	0.045	11.58
	7	0.045	0.069	6.48
	8	0.044	0.081	5.45
	9A	0.061	0.082	7.45
	9B	0.047	0.061	7.71
OK2	1	0.089	0.059	15.21
	2	0.036	0.042	8.67
	3A	0.039	0.050	7.90
	3B	0.045	0.055	8.22
	4	0.040	0.056	7.10
	5	0.031	0.030	10.37
	6A	0.038	0.052	7.39
	6B	0.044	0.057	7.69
	7	0.049	0.060	8.21
	8	0.048	0.050	9.62
	9A	0.046	0.057	8.04
	9B	0.052	0.069	7.48
	10	0.045	0.049	9.22
	11	0.045	0.045	9.98
	12A	0.047	0.040	11.64
	12B	0.066	0.054	12.24
	13	0.043	0.051	8.43
OK3	1	0.046	0.038	11.98
	2A	0.040	0.045	8.91
	2B	0.048	0.056	8.61
	3	0.054	0.043	12.56
	4	0.058	0.054	10.76
	5A	0.048	0.050	9.65
	5B	0.063	0.068	9.31
	6	0.066	0.074	8.98
	7	0.066	0.058	11.38
	8A	0.050	0.038	13.26
	8B	0.053	0.041	12.88
	9	0.078	0.065	12.00

Table 4: Manganese data for all six corals

Nickel

Sample		AAS ppm	Weight	Coral ppm
MAR1	1	0.135	0.100	22.27
	2	0.118	0.076	26.23
	3A	0.083	0.046	25.26
	3B	0.084	0.035	23.88
	4	0.107	0.081	13.29
	5	0.099	0.076	13.11
	6A	0.104	0.075	13.88
	6B	0.063	0.048	13.08
	7	0.096	0.084	11.37
	8	0.115	0.074	15.56
	9A	0.133	0.094	14.12
	9B	0.117	0.086	13.66
	10	0.130	0.087	14.87
MAR2	1	0.132	0.077	17.17
	2A	0.108	0.070	15.57
	2B	0.137	0.084	16.33
	3	0.103	0.061	17.00
	4	0.108	0.076	14.21
	5A	0.096	0.053	18.01
	5B	1.230	0.710	17.33
	6	0.109	0.053	20.49
	7	0.102	0.071	14.39
	8A	0.127	0.083	15.33
	8B	0.090	0.056	16.11
	9	0.113	0.078	14.45
	10	0.116	0.081	14.34
MAR3	1A	0.125	0.089	14.05
	1B	0.071	0.049	14.55
	2	0.084	0.077	10.87
	3	0.084	0.056	15.11
	4A	0.085	0.075	11.27
	4B	0.059	0.054	10.87
	5	0.086	0.059	14.48
	6	0.079	0.054	14.60
	7A	0.073	0.053	13.75
	7B	0.093	0.065	14.29
	8	0.046	0.036	12.96
	9	0.089	0.065	13.69
	10A	0.055	0.037	14.86
	10B	0.133	0.084	15.78
	11	0.136	0.082	16.61
	12	0.115	0.067	17.27
	13	0.095	0.060	15.97

Sample		AAS ppm	Weight	Coral pp
OK1	1	0.135	0.100	13.54
	2	0.118	0.076	15.63
	3A	0.081	0.046	17.36
	3B	0.155	0.084	18.42
	4	0.107	0.081	13.29
	5	0.096	0.076	12.72
	6A	0.100	0.075	13.32
	6B	0.117	0.091	12.84
	7	0.112	0.084	13.27
	8	0.120	0.074	16.24
	9A	0.119	0.094	12.64
	9B	0.085	0.064	13.24
OK2	1	0.100	0.087	11.44
	2	0.047	0.042	11.26
	3A	0.058	0.050	11.74
	3B	0.103	0.082	12.56
	4	0.080	0.056	14.16
	5	0.036	0.030	12.16
	6A	0.073	0.052	14.08
	6B	0.089	0.069	12.94
	7	0.092	0.060	15.45
	8	0.062	0.050	12.46
	9A	0.081	0.057	14.37
	9B	0.042	0.032	13.21
	10	0.055	0.049	11.23
	11	0.057	0.045	12.62
	12A	0.060	0.040	14.93
	12B	0.051	0.036	14.11
	13	0.082	0.051	16.02
OK3	1	0.048	0.038	12.52
	2A	0.061	0.045	13.62
	2B	0.055	0.043	12.88
	3	0.052	0.043	12.15
	4	0.073	0.054	13.54
	5A	0.056	0.050	11.26
	5B	0.113	0.096	11.82
	6	0.112	0.074	15.23
	7	0.080	0.058	13.87
	8A	0.049	0.038	13.02
	8B	0.099	0.084	11.82
	9	0.094	0.075	12.57

Table 5: Nickel data for all six corals

Iron

Sample		AAS ppm	Weight	Coral ppm
MAR1	1	0.492	0.100	49.35
	2	0.498	0.076	65.96
	3A	0.295	0.046	63.55
	3B	0.339	0.056	60.59
	4	0.340	0.081	42.24
	5	0.236	0.076	31.26
	6A	0.276	0.075	36.85
	6B	0.266	0.076	34.97
	7	0.164	0.084	19.43
	8	0.168	0.074	22.73
	9A	0.214	0.094	22.65
	9B	0.126	0.058	21.67
	10	0.175	0.087	20.02
MAR2	1	1.628	0.077	211.70
	2A	1.886	0.070	270.93
	2B	2.422	0.091	266.13
	3	0.357	0.061	58.91
	4	0.500	0.076	65.79
	5A	0.264	0.053	49.65
	5B	0.396	0.083	47.71
	6	0.427	0.053	80.26
	7	0.404	0.071	56.98
	8A	0.533	0.083	64.45
	8B	0.385	0.062	62.03
	9	0.470	0.078	60.10
	10	0.943	0.081	116.56
MAR3	1A	0.654	0.089	73.69
	1B	0.407	0.058	70.23
	2	0.751	0.077	97.15
	3	0.289	0.056	51.98
	4A	1.168	0.075	155.70
	4B	0.792	0.052	152.32
	5	1.232	0.059	207.41
	6	0.438	0.054	80.96
	7A	0.582	0.053	110.24
	7B	0.688	0.061	112.86
	8	0.290	0.036	81.69
	9	0.458	0.065	70.46
	10A	0.206	0.037	55.45
	10B	0.156	0.029	53.69
	11	0.258	0.082	31.50
	12	0.211	0.067	31.68
	13	0.190	0.060	31.93

Sample		AAS ppm	Weight	Coral pp
OK1	1	0.434	0.089	49.10
	2	0.379	0.064	59.22
	3A	0.081	0.037	22.15
	3B	0.129	0.054	23.87
	4	0.385	0.095	40.53
	5	0.247	0.076	32.32
	6A	0.331	0.088	37.62
	6B	0.386	0.094	41.02
	7	0.280	0.069	40.35
	8	0.249	0.081	30.86
	9A	0.270	0.082	32.95
	9B	2.369	0.750	31.59
OK2	1	0.289	0.059	49.40
	2	0.129	0.042	31.08
	3A	0.171	0.050	34.42
	3B	0.307	0.084	36.54
	4	0.159	0.056	28.24
	5	0.127	0.030	42.47
	6A	0.174	0.052	33.62
	6B	0.218	0.062	35.24
	7	0.171	0.060	28.64
	8	0.160	0.050	32.06
	9A	0.178	0.057	31.40
	9B	0.176	0.063	27.86
	10	0.144	0.049	29.51
	11	0.147	0.045	32.59
	12A	0.154	0.040	38.37
	12B	0.268	0.065	41.23
	13	0.128	0.051	25.10
OK3	1	0.201	0.038	52.34
	2A	0.155	0.045	34.81
	2B	0.211	0.063	33.51
	3	0.253	0.043	58.84
	4	0.224	0.054	41.56
	5A	0.188	0.050	37.94
	5B	0.367	0.092	39.88
	6	0.344	0.074	46.80
	7	0.278	0.058	47.93
	8A	0.207	0.038	55.19
	8B	0.278	0.048	57.87
	9	1.908	0.532	35.86

Table 6: Iron data for all six corals

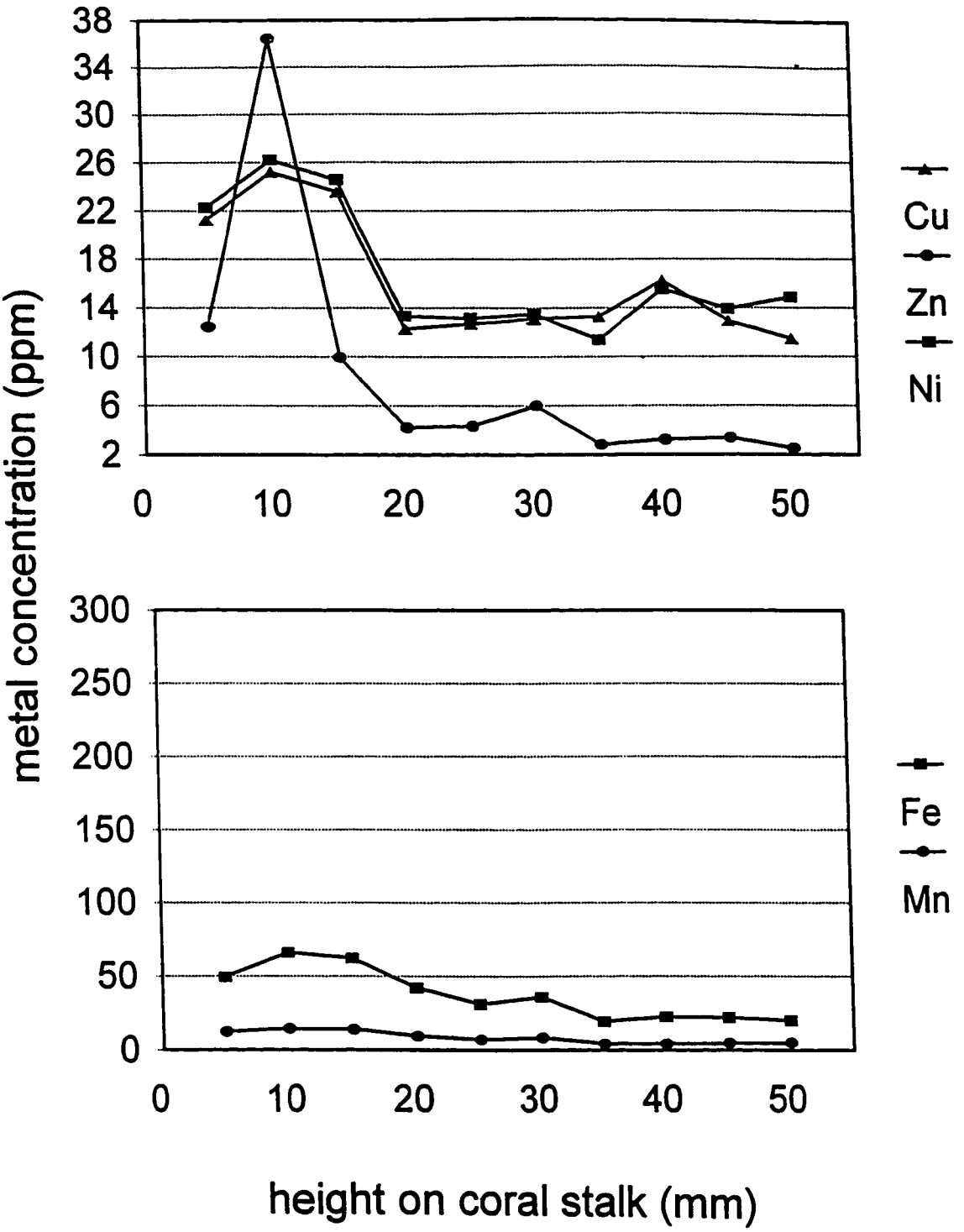

Figure 5: Cu, Zn, Ni (top) and Fe, Mn (bottom) concentrations for MAR1 plotted against height on coral stalk

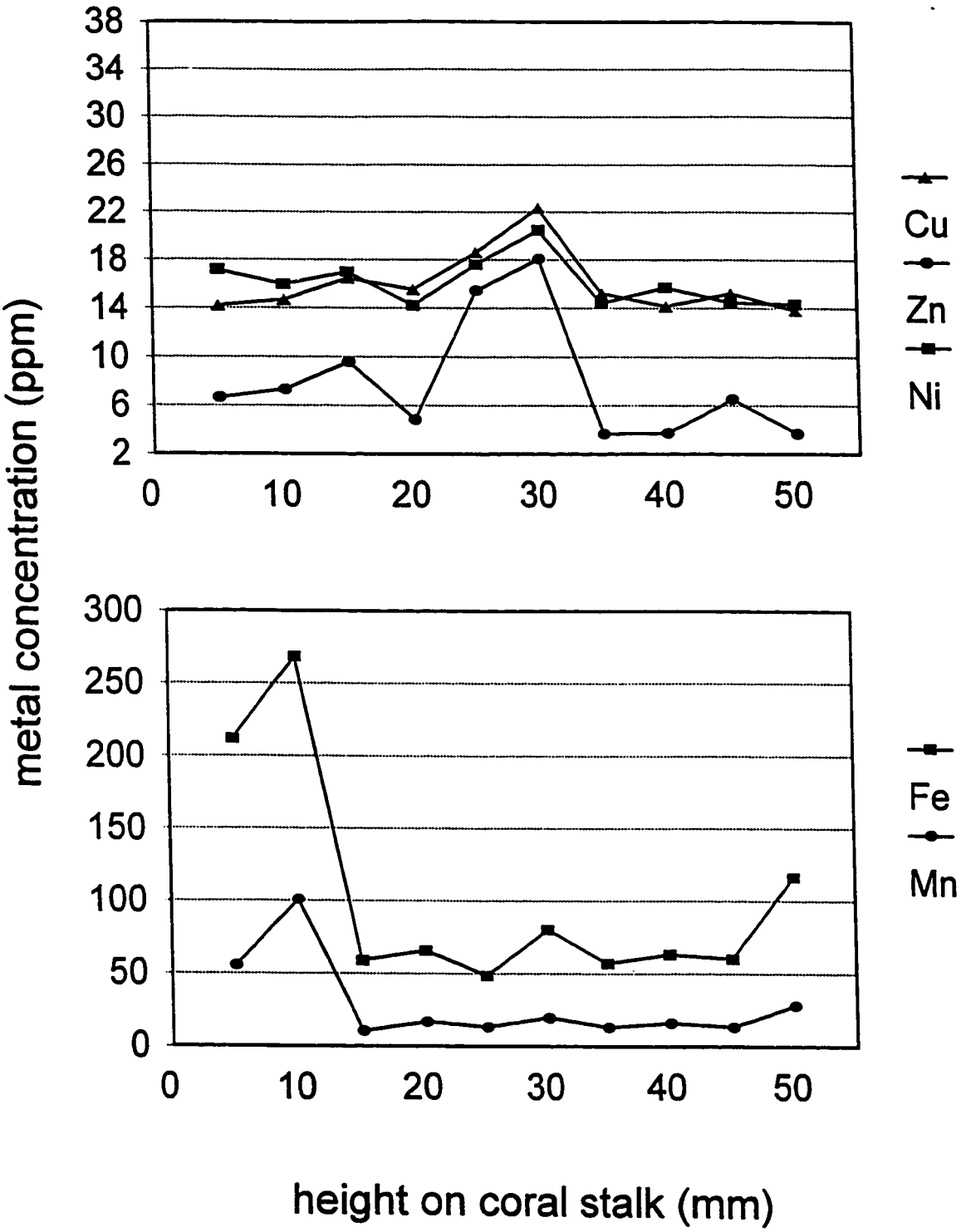

Figure 6: Cu, Zn, Ni (top) and Fe, Mn (bottom) concentrations for MAR 2 plotted against height on coral stalk

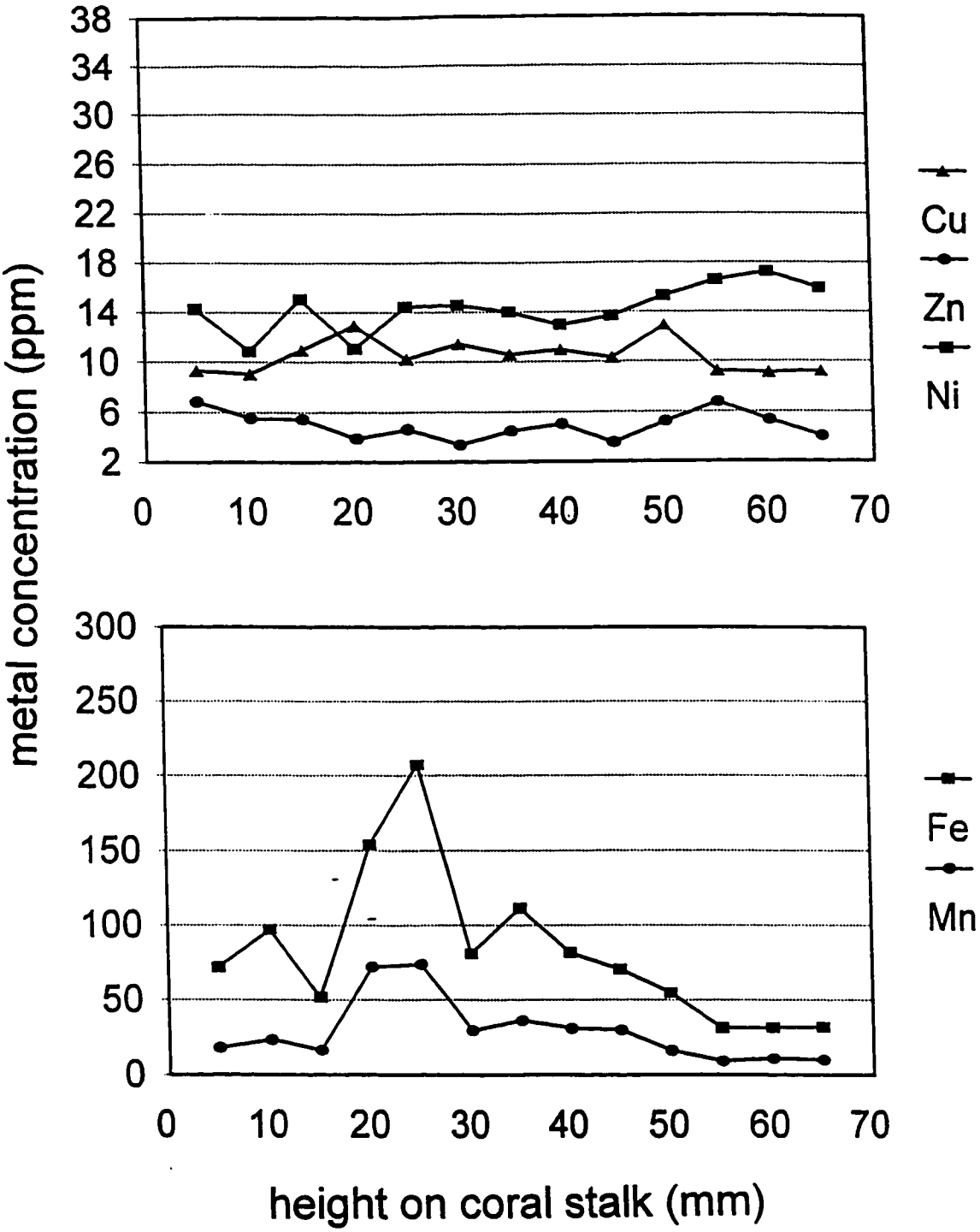

Figure 7: Cu, Zn, Ni (top) and Fe, Mn (bottom) concentrations for MAR 3 plotted against height on coral stalk

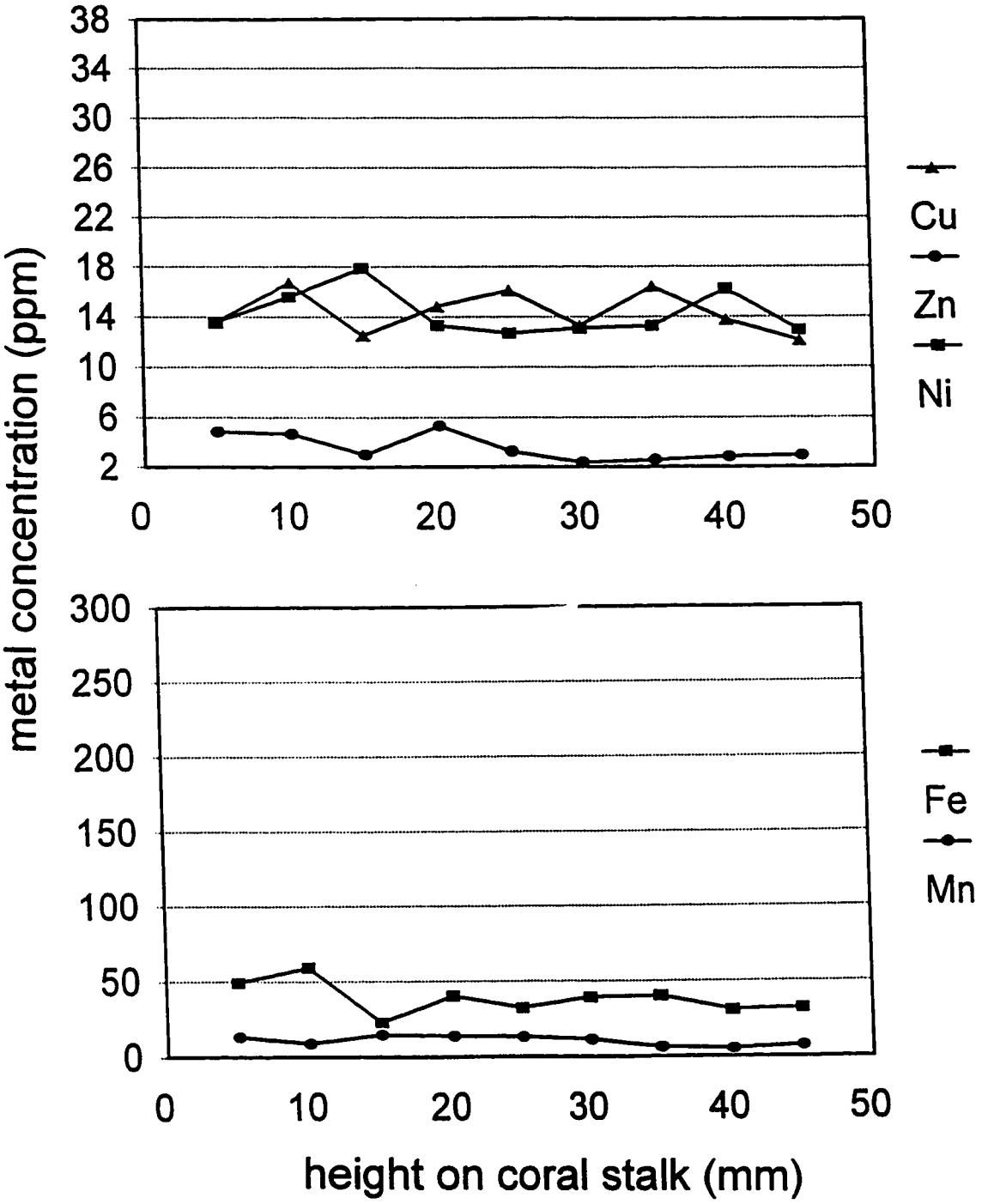

Figure 8: Cu, Zn, Ni (top) and Fe, Mn (bottom) concentrations in OK1 plotted against height on coral stalk

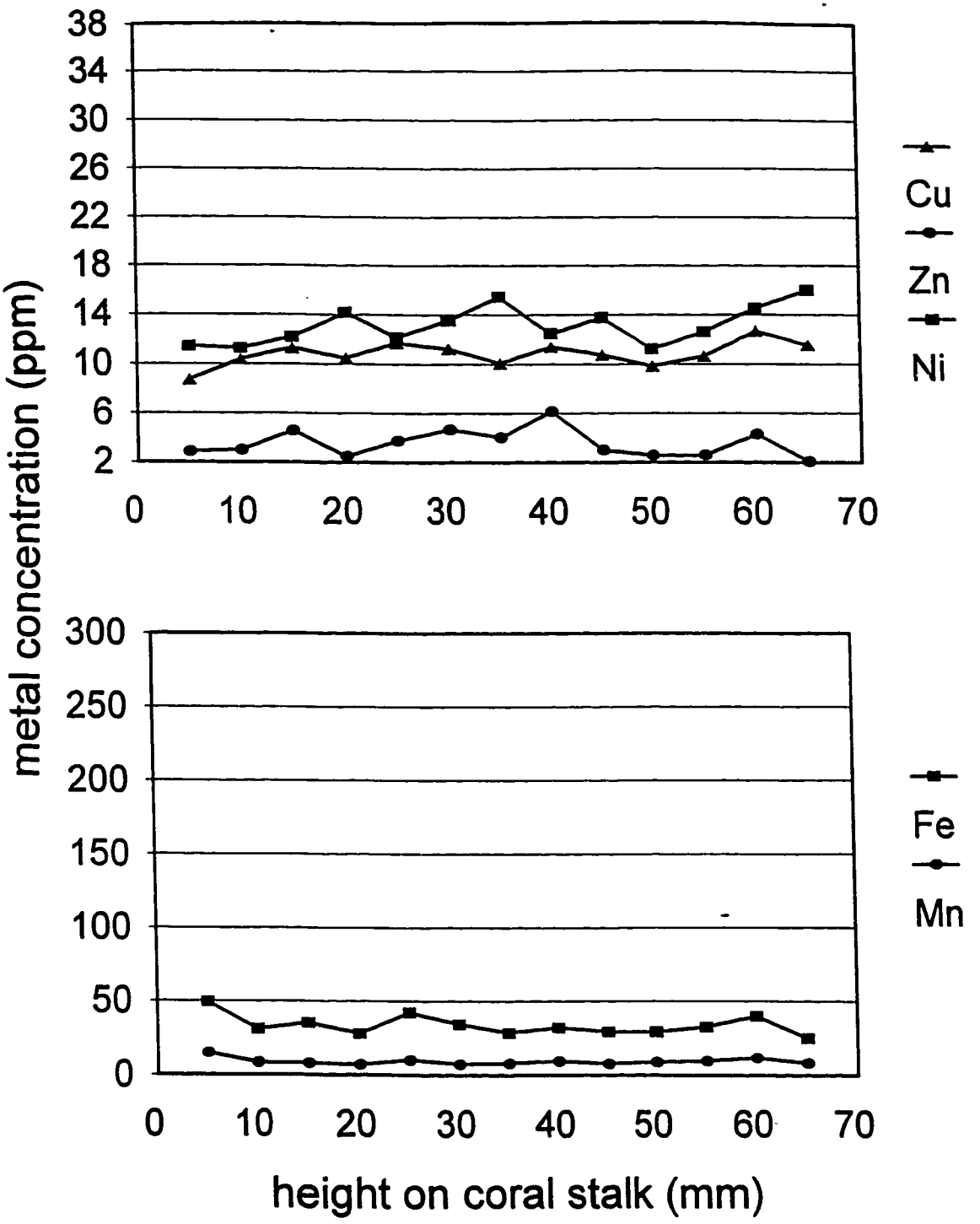

Figure 9: Cu, Zn, Ni (top) and Fe, Mn (bottom) concentrations in OK2 plotted against height on coral stalk

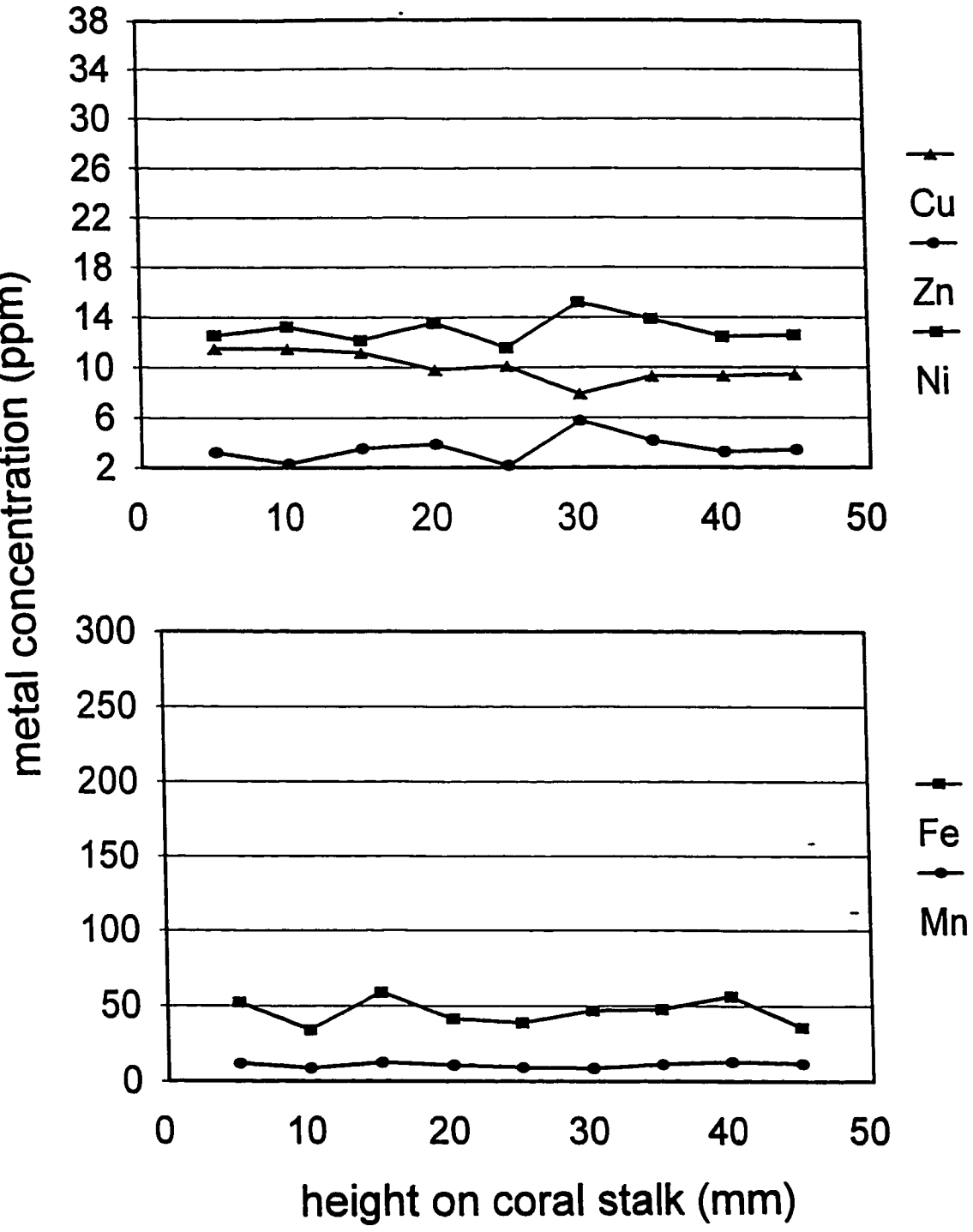

Figure 10: Cu, Zn, Ni (top) and Fe, Mn (bottom) concentrations for OK3 plotted against height on coral stalk

Table 7: Statistical Summary		Mid-Atlantic Ridge	Orphan Knoll	Significantly different?
		n = 43	n = 41	
Copper	Average	13.99 ppm	11.58	
	Std. dev.	4.11	1.99	yes
Zinc	Average	6.87	3.48	
	Std. dev.	5.74	1.03	yes
Manganese	Average	24.51	10.19	
	Std. dev.	24.24	2.52	yes
Nickel	Average	15.63	13.45	
	Std. dev.	3.40	1.62	yes
Iron	Average	78.11	38.09	
	Std. dev.	60.86	9.42	yes

Table 7: Statistical summary for MAR vs OK corals for each metal

6.5 Discussion

6.5.1 Origin of Metals

Figures 5-10 show that there are episodically-elevated amounts of metals in the mid-Atlantic-ridge coral skeletons compared to the Orphan Knoll population. Ordinary seawater, such as that in which the Orphan Knoll corals grew, contains minute quantities of many metals which may become incorporated into precipitated skeletal material. The elevated values in the mid-Atlantic-ridge corals requires additional explanation. Analyses of metabasalts dredged from the mid-Atlantic ridge suggest that the rocks were originally olivine tholeiitic basalts, of which heavy metals comprise a significant number of the elements present (Bonatti *et al.*, 1976). It is possible that weathering of these relatively-fresh basalts resulted in elevated amounts heavy metal ions in the overlying seawater which were eventually incorporated into the coral skeletons.

This explanation, however, does not account for the episodic nature of metal inclusion in the corals: almost certainly basalt weathering and subsequent metal ion release would be a continuous process. It also does not explain why some of the metal spikes represent excursions of Fe and Mn only, while others only include Cu, Ni and Zn.

Bischoff and Dickson (1975) set up laboratory experiments to simulate an active hydrothermal system. They knew that seawater circulates through fresh, hot basaltic rocks at depths of about 1/2 to 1 kilometre - in the Reykjanes area of the Mid-Atlantic Ridge, this corresponds to temperatures of about 200° and 500 bars of pressure. After establishing these conditions in the test vessel, they then proceeded to react seawater with basalt over the course of almost 5000 hours. They

found that the pH of the seawater dropped substantially in the first few hours and attributed this to reactions, such as the precipitation of Fe^{2+} and Mn^{2+} ions, which liberate hydrogen ions Bischoff and Dickson (1975) also found that the reacted seawater was significantly enriched in some heavy elements. Iron and manganese displayed almost identical patterns (as in this study): the concentrations of both rose very quickly, reaching a maximum at 1000 hours, then slowly decreased throughout the rest of the experiment. Copper and nickel were also found in significant quantities, each rising in concentration further into the experiment. The altered seawater in this experiment did not contain detectable amounts of zinc, cadmium or lead.

Because of the similarity of the metal profiles in the mid-Atlantic-ridge corals and Bischoff and Dickson's (1975) experimental results, and because of the proximity of the corals to the hydrothermal system, we believe the heavy metals in the coral skeletons had their provenance at the spreading centre. After rising into the mid-Atlantic rift valley, magma solidifies and cools slowly from its initial temperature of about 1,200°C. Seawater permeates fissures in the solid basalt, is heated to several hundred degrees Celsius and becomes transformed from an oxygenated electrolyte solution into a progressively more reduced state. In the early stages of hydrothermal activity fissures are abundant and open, giving a high water / rock ratio. While this ratio is approximately 42:1, the fresh basalt reacts with seawater Mg^{2+}, H_2O and O_2 to produce smectite, various ions (Ca^{2+}, Na^{2+}, Fe^{2+}, Mn^{2+}, H^+) and H_4SiO_4 (Lydon, 1988). As minerals precipitate, the fissures become progressively filled, lowering the water / rock ratio. When the ratio is about 20:1, the basalt begins to react with Na^{2+} and H^+, as well as seawater Mg^{2+}, H_2O and O_2 to produce

smectite, albite, Ca^{2+}, Fe^{2+}, Mn^{2+} and H_4SiO_4. A coral growing in the region, therefore, could incorporate Fe and Mn into its skeleton during the early stages of hydrothermal activity. With continued generation of H^+ and H_4SiO_4, the pH of the seawater solution is progressively lowered (Edmond *et al.*, 1982). Minerals in the basalt undergo reactions in which H^+ ions displace metal cations into the solution. The metal concentration of the hydrothermal solution (e.g., Cu, Ni, Zn, Pb) in equilibrium with the mineral assemblages increases with higher temperature and lower pH. The metals may then form complex ions in which the metal ion is linked to one of several possible ligands, rendering them mobile (Edmond *et al.*, 1982). Corals growing in the region at the time of significant metal generation may incorporate increased amounts of Cu, Ni, and Zn into their skeletons.

At both early and later stages of hydrothermal activity, a hot, acidic and metaliferous solution rises to the seafloor and comes in contact with cold, oxygenated seawater. Sulphides and sulphates are precipitated, creating 'chimneys'. These chimneys are zoned, i.e., composed of different minerals from the inside to the outside, reflecting the changing chemistry of the effluent (Lydon, 1988). Some of the particulate iron sulphide is carried upwards as a 'black smoke'; Mn^{2+} plus some Fe^{2+} and other metallic cations remain in solution. The exact proportions of the different metals in a hydrothermal solution varies not only with time, but also location (e.g., Von Damm et al., 1985; Lydon, 1988), but exist in the same general ratios as seen in this study. The differences presumably reflect variations in the composition of the basalt. The solutions are disharged from black smokers at fast rates (> 1m/s), and "behave like a jet at the vent orifice because of their momentum" (Rona, 1989). The

plume rises by free convection to attain density equilibrium in the water column between 300 and 470 m above the seafloor (Rona, 1989). Ocean currents disperse the plumes laterally from the smoker's vent; eventually the metals oxidize and precipitate, forming a metalliferous sediment. Metaliferous components from the hydrothermal fluid have been detected in the water column at distances of more than 750 km from its source (Rona, 1984)

All three mid-Atlantic-ridge corals seem to have recorded a hydrothermal event, or a portion of one. Specimen MAR 1 began to grow after the period of high Fe and Mn discharges, but records Cu, Zn and Ni spikes during the first portion of its life. MAR 2 first shows an iron and manganese enrichment followed by Cu, Zn and Ni maxima. MAR 3 records the beginning of a hydrothermal event, with late-life Fe and Mn anomolies.

6.5.2 Timing of Hydrothermal Events

Sea-floor spreading is continuous over geological time, but is actually the integration of many individual small-scale events. The average duration of an individual hydrothermal occurrence is one to three decades (Trefry *et al.*, 1985) after which the rocks have cooled substantially and once-abundant fractures are plugged with minerals precipitated from the circulating seawater. Cores taken from the rift valley floor at a hydrothermal field from the mid-Atlantic ridge show discrete layers up to several centimeters thick of sediment anomalously enriched in copper, iron, zinc and other metals interposed within predominently carbonate material (Trefry *et al.*, 1985). These layers record fallout from

episodic hydrothermal plumes, but because of bioturbation, sediment transport and fluctuating sedimentation rates, the duration of each event often cannot be ascertained with a resolution better than a few centuries (CLIMAP, 1984). The deep-sea corals are free from those confounding effects, however, and offer independent evidence that the duration of a particular hydrothermal event is from less than a decade up to 30 years or so.

Currently we can only estimate the period of a particular hydrothermal event: attempts so far to acquire absolute ages for these coral specimens using both radiocarbon and $^{234}U/^{230}Th$ dating have been unsuccessful. We assume that 'dead' carbon from the mantle and uranium and thorium liberated from the fresh basalt have confounded the isotopic ratios. The corals, however, all seem to be late Pleistocene in age.

6.5.3 Stable Isotopes

Azooxanthellate corals do not precipitate their skeleton in equilibrium with seawater. Furthermore, the isotopic ratios vary widely and can be several per mil away from aragonite-seawater equilibrium for the conditions of deposition (Smith et al., in manuscript). The $\delta^{13}C$ vs $\delta^{18}O$ regression lines, however, can be used to reconstruct aspects of a coral's environment during its lifetime (Smith et al., in revision). All of the regression lines showed high r^2 values, i.e., with little scatter of the individual points, which generally implies that the corals grew under uniform conditions. This suggests that the episodic metal pulses in the

mid-Atlantic-ridge corals were not accompanied by changes in the temperature or isotopic composition of the ambient seawater.

6.5.4 Concentration of Trace Metals in Seawater

We also cannot, as of yet, use the metal concentrations in the corals' skeletons to reconstruct unequivocally the elements' abundance in the seawater. To assess changes in the trace-element compostion of seawater quantitively requires the isolation of metals which are incorporated directly into coral aragonite with a known distribution coefficient (Brand, 1994). To achieve this, trace metals associated with components other than the aragonite matrix must be removed (Shen and Boyle, 1988). To do so, however, results in the loss of significant amounts of skeletal material. This is acceptable when investigating abundant colonial reef corals, which may have a mass of several kilograms: in contrast, the 'supply' of mid-Atlantic ridge corals is limited and, more importantly, each specimen weighs only a few grams. The benefits of acquiring more precise data on hydrothermal events in the deep sea must be weighed against loss of material that can provide other types of data.

An additional complication is that some mechanisms of incorporation of metals into coral skeletons are as yet unclear. There may be uptake from zooplankton specimens captured by the coral - the chitinous exoskeletons of these organisms are known to incorporate metals. There may also be direct uptake across the epithelium: since these metals are presumably toxic to the corals, the organism may 'push' them into precipitating skeletal material in order to avoid tissue contact

(Brand, 1994).

6.6 Conclusions

Our results are best viewed as allowing relative comparisons between regions of contrasting tectonic style: there are episodically-elevated amounts of metals in the mid-Atlantic-ridge coral skeletons compared to the Orphan Knoll population. If the metal 'spikes' seen episodically in the mid-Atlantic-Ridge corals did originate in a hydrothermal discharge zone associated with the mid-Atlantic spreading centre, then we have some evidence for the duration of these hydrothermal events at this section of the ridge.

With sufficient specimens of known age it should be possible to reconstruct the history of a particular segment of a spreading centre by establishing times of magmatic intrusions, metalogenic pulses, and hydrothermal activity. The deep-sea corals offer the potential of decadal or even annual resolution in the timing of these events.

6.7 Acknowledgements

We thank Martin Knyf and Ian Campbell for held with analyses and Mark Epp for advice and useful information. The Orphan Knoll corals were donated by the Atlantic Geoscience Centre (Geological Survey of Canada), Darmouth, N.S.: the mid-Atlantic-ridge corals were donated by the Canadian Museum of Nature, Ottawa. This study was funded by a

Natural Sciences and Engineering Research Council (NSERC) grant to UB, an NSERC collaborative grant to HPS and MJR and NSERC graduate student support to JES.

6.8 References

Bischoff, J.L. and Dickson, F.W. (1975) Seawater-basalt interaction at 200°C and 500 bars: Implications for origin of seafloor heavy-metal deposits and regulation of seawater chemistry. *Earth and Planetary Science Letters* **25** , pp. 385 - 397.

Bonatti, E., Guerstein-Honnorez, B.M. and Honnorez, J. (1976) Copper-iron sulfide mineralizations from the equatorial Mid-Atlantic Ridge. *Econ. Geology* **71**, pp. 1515 - 1525.

Brand, U. (1994) Morphochemical and replacement diagenesis of biogenic carbonates. *In*: Wolf, K.H. and Chilingarian, G.V. (eds.) *Diagenesis, IV. Developments in Sedimentology 51*. Elsevier Science, Amsterdam, pp. 217 - 282.

CLIMAP (1984) The last interglacial ocean. *Quaternary Research* **21**, pp. 123 - 224.

Edmond, J.M., Von Damm, K.L., McDuff, R.E. and Measures, C.I. (1982) Chemistry of hot springs on the East Pacific Rise and their effluent dispersal. *Nature* **297**, pp. 187 - 191.

Lydon, J.W. (1988) Ore deposit models #14. Volcanogenic massive sulphide deposits. Part 2: Genetic models. *Geoscience Canada* **15**, pp. 43 - 65.

Rona, P.A. (1984) Hydrothermal mineralization at seafloor spreading centres. *Earth-Science Reviews* **20**, pp 1 - 104.

Rona, P.A. and Speer, K.G. (1989) An Atlantic hydrothermal plume: Trans-Atlantic Geotraverse (TAB) area, Mid-Atlantic Ridge crest near 26°N. *Journal of Geophysical Reseach* **94**, pp.13,879-13,893.

Shen, G.T. and Boyle, E.A. (1988) Determination of lead, cadmium and other trace metals in annually-banded corals. *Chemical Geology* **67**, pp. 47 - 62.

Shen, G.T., Boyle, E.A. and Lea, D.W. (1987) Cadmium in corals as a tracer of historical upwelling and industrial fallout. *Nature* **328**, pp. 794 - 796.

Smith, J.E. (1993) Late Quaternary Climatic Reconstruction Using the Deep-Water Coral *Desmophyllum cristagalli*. *Geological Survey of Canada Open File*, **2950**. 100 pp.

Smith. J.E., Schwarcz, H.P., Risk, M.J., McConnaughey, T.A. and Keller, N.B. (1995) Isotopic analyses of deep-sea corals yield climatic information after compensating for kinetic isotope effects. Spring Meeting, American Geophysical Union, *EOS* **77**, April 23, 1996

Supplement, S160. (abstract)

Smith, J.E., Risk, M.J., Schwarcz, H.P. and McConnaughey, T.A. (1997) Rapid climate change in the North Atlantic as recorded by deep-sea corals. *Nature* **386**, pp. 818-820.

Smith, J.E., Schwarcz, H.P., Risk, M.J. and McConnaughey, T.A. (in manuscript) Patterns of disequilibria in azooxanthellate coral skeletons. For submission to Palaeogeography, Palaeoclimatology, Palaeoecology

Smith, J.E., Schwarcz, H.P., Risk, M.J., McConnaughey, T.A. and Keller, N.B. (in revision) Deep-sea corals as paleotemperature indicators: Overcoming 'vital effects'. *Geochimica et Cosmochimica Acta.*

Stanley, G.D. and Cairns, S.D. (1988) Constructional azooxanthellate coral communities: An overview with implications to the fossil record. *Palaios* **3**, pp. 233 - 242.

Trefry, J.H., Trocine, R.P., Klinkhammer, G.P. and Rona, P.A. (1985) Iron and copper enrichment of suspended particles in dispersed hydrothermal plumes along the Mid-Atlantic Ridge. *Geophysical Reseach Letters* **12**, pp. 506-509.

Von Damm, K.L., Edmond, J.M., Grant, B. and Measures, C.I. (1985) Chemistry of submarine hydrothermal solutions at 21N, East Pacific Rise. *Geochim. et Cosmochim. Acta* **49**, pp. 2197-2220.

CHAPTER 7

CONCLUSION

In our understanding of the coupled forces and processes that shape our world, perhaps no aspect is more critical than the mechanisms by which the atmosphere, shallow oceans, and deep oceans are linked. It is the rate at which processes are transferred, and the specific triggers of change, that control the climate of the globe.

Until recently, the great unknown in this scheme has been processes acting in the deep sea. Some general trends have been described, but deep-sea core data are inherently too imprecise to allow coupling rates to be estimated. Now, deepwater corals (dubbed 'The New Archive' by Dr. Wally Broecker) offer a mechanism by which precise oceanographic data, with a potential yearly time resolution, may be obtained. This is the first time in the history of oceanographic investigations that this has been possible. The answers to fundamentally important questions, such as the rate of climate change, mechanisms of stopping and starting the Gulf Stream, and the rate of downward advection of dissolved carbon dioxide, are now within our reach.

In order to translate the data contained with azooxanthellate corals, the 'New Archive', we need a Rosetta Stone. In this thesis, I have outlined some of the ways in which we may access the data encoded in the skeletons of deepwater corals. The problem of the 'vital effects' remains unsolved, but temperature records may still be recovered via the

use of the graphical technique outlined in Chapter 4. For more detailed work, it will be necessary to work inside the coral skeletons, on (ideally) the central plane of the septa. The growth recessions described in Chapter 2 certainly complicate interpretations, and may in many cases make precise year-to-year correlations impossible.

The means of preservation of these data bears further discussion. Most of the specimens analysed for this thesis grew below the lysocline, that depth at which calcium carbonate skeletons begin to dissolve due to pressure increase. All of the corals collected alive and many of the fossil corals are in excellent states of preservation. In many cases, there is a large activation energy requirement: the carbonates may be unstable, but they persist for thousands of years. Some of the corals may also have fallen from the rock faces on which they usually live, and been buried in sediments.

There is evidence, however, that some of the Orphan Knoll corals were exposed on the sea floor for long periods of time, perhaps the entire time span between death and dredge. Careful examination of these corals shows the interseptal spaces frequently packed with planktonic foraminifera and sponge spicules. Occasionally, icerafted fragments also may be found in the coralla. Both these pieces of evidence dictate that the corals were exposed for extremely long periods of time.

The reasons for the existence and persistence of these corals becomes even more enigmatic when we consider that they are sometimes intensely bioeroded, and sometimes relatively untouched (described by C. Boerboom, J. Smith and M. Risk in "Bioerosion and Micritization in the Deep-Sea", in press, Historical Biology). Clionid sponge borings are common, as are borings made by spionid polychaetes. Microboring fungi

are virtually ubiquitous in the corals, sometimes creating areas of micrite (these are the deepest biological micrites ever found.) The pattern of bioerosion usually consists of internal "mining" of both the septa and the septathecal wall. One pattern that has never been observed is what could be predicted from the growth recessions described in Chapter 2. As the coral grows upwards and the tissue elevates, the stalk of the coral becomes exposed: but these bases are never preferentially attacked. In shallow-water corals, the bases are often attacked: it was this characteristic of shallow, solitary Rugose corals that allowed workers (M.J. Risk, S.E. Pagani and R.J. Elias in "Another Internal Clock: Preliminary Estimates of Growth Rates Based on Cycles of Algal Boring Activity", 1987, Palaios 2, pp. 323-331) to obtain growth estimates for Paleozoic corals. The reasons for the pristine preservation of many entire epitheca are unclear. These deepwater corals may be chemically defended, similar to the process that protects the bases of shallow-water soft corals (Risk, pers. comm. 1997). These soft corals, despite their name, secret hard bases made of fused calcite spicules. To protect themselves from fouling and bioerosion, the animals secret a variety of bioactive substances, with the result that the bases are relatively untouched. Given the importance of the "stalk" to deepwater corals - without it they would die - it would be reasonable to suggest that the animals defend it chemically. At any rate, the result is an archive of data encoded in coral skeletons whose specific preservation histories remain unknown to us.

In summary, the deep-sea coral have the potential to offer decadal or even annually-resoved stable-isotope and trace-element paleonoceanographic data, if subjected to suitable sampling schemes. In

particular:

- *Desmophyllum cristagalli* grows by secreting growth bands in lamellae in successive layers between the tissue layer and the skeleton, over a central trabecular framework.
- The central trablcular plane in the protected septa and inner theca provide the most complete record of the life of the coral, as the epitheca may be subject to chemical dissolution by the surrounding waters of the ocean.
- The timing and causes of banding in deep-water corals remain unknown.
- The small thickness of the bands and their often-erratic patterns makes sampling this deep-water coral for year-by-year paleoclimatic information a difficult, if not impossible, task.
- Oxygen isotope ratios of multiple samples from coeval surfaces vary widely and may be several per mil from the calculated oxygen isotope aragonite-seawater equilbrium point.
- The extent of disequilibrium does not vary in any systematic, significant manner on the coral skeleton. Portions of the skeleton which do approach oxygen isotope equilibrium cannot readily be identified beforehand.
- Large isotopic disequilibria documented on coeval surfaces suggest it will be difficult to develop a sampling strategy whereby environmental reconstruction over the course of the coral's life can be made.
- From the $\delta^{13}C$ vs $\delta^{18}O$ regression line for an individual coral, the $\delta^{18}O_{arag}$ value corresponding with $\delta^{13}C_{arag}$ equal to $\delta^{13}C_{water}$, corrected by $\delta^{18}O_{water}$ is a function of temperature.

- Isotopic analyses of subsamples removed randomly from modern azooxanthellate corals can be used to give the temperature at which the coral grew; for pre-Holocene corals, an estimate of the paleo-isotopic equilibrium point can be obtained.
- With sufficient specimens of known age it should be possible to reconstruct the history of a particular segment of a spreading centre by establishing times of magmatic intrusions, metalogenic pulses, and hydrothermal activity.